UNIVERSITY OF CALIFORNIA

Santa Barbara

The isolation and post-assembly modification of acyl peptidic siderophores

A dissertation submitted in partial satisfaction of the

requirements for the degree Doctor of Philosophy

in Chemistry

by

Michelle Peov Kem

Committee in charge:

Professor Alison Butler, Chair

Professor Peter Ford

Professor Trevor Hayton

Professor Stanley Parsons

December 2014

The dissertation of Michelle Peov Kem is approved.

_____

Peter Ford

_____

Trevor Hayton

_____

Stanley Parsons

_____

Alison Butler, Committee Chair

December 2014

The isolation and post-assembly modification of acyl peptidic siderophores

by

Michelle Peov Kem

ACKNOWLEDGEMENTS

I first want to thank my advisor, Professor Alison Butler, for her mentorship and friendship throughout my graduate career. Her constant encouragement, enthusiasm and support has allowed me to learn more than I thought was possible over the past five years.

I also want to thank my fellow Butler lab members for their friendship and support throughout the years and for making the lab a great place to be everyday. I especially want to thank Dr. Moriah Sandy, Dr. Hannah Zane and soon-to-be Dr. Stephen Springer for their friendship, both professionally and personally. They have taught me so much about life, friendship, hard work and laughter, and I'm so grateful to have them in my life. I also want to thank Dr. James Pavlovich for his assistance with mass spectrometry and my committee members for their support and advice throughout the years.

Finally, I want to thank my family who are the most loving and supportive group of people anyone can ask for. Without them I would not be the person I am today. I also want to thank Dr. Adam Pollak who has been incredibly supportive during our graduate careers and has shown me that anything can be accomplished with hard work, positive thinking and perseverance.

VITA OF MICHELLE PEOV KEM

December 2014

EDUCATION

Doctor of Philosophy in Chemistry, 2014 (expected)
University of California, Santa Barbara

Bachelor of Science in Chemistry, 2008
The University of Arizona

PROFESSIONAL EXPERIENCE

Teaching Assistant, Advanced physical chemistry laboratory 2013, 2014
The University of California, Santa Barbara, CA

Teaching Assistant, Introductory general chemistry laboratory 2009-2011
The University of California, Santa Barbara, CA

Research aide; Advisor: Dr. William Montfort, 2008-2009
The University of Arizona Department of Biochemistry, Tucson, AZ

PUBLICATIONS

Kem, M.P.; Butler, A. Acyl peptidic siderophores: Structures, biosynthesis and post-assembly modifications. Biometals, *submitted*.

Kem, M.P.; Naka, H.; Iinishi, H.; Haygood, M.G.; Butler, A., Fatty acid hydrolysis of acyl-marinobactin siderophores by *Marinobacter* acylases, *submitted*.

Kem, M.P.; Zane, H.K.; Springer, S.D.; Gauglitz, J.M.; Butler, A., Amphiphilic siderophore production by oil-associating microbes. Metallomics 2014, 6, 1150-1155.

Weichsel, A.; Kem, M.; Montfort, W.R., Crystal Structures of Human Thioredoxin Revealing Unraveled Helix and Exposed S-Nitrosation Site, Protein Science 2010, 19, 1801-1806.

CONFERENCE PRESENTATIONS

Kem, M; Butler, A., Investigating the microbial modification of an amphiphilic siderophore. 16th International Conference of Bioinorganic Chemistry (ICBIC). Poster Presentation, July 22-26, 2013. Grenoble, France.

Kem, M.; Springer, S.; Sandy, M.; Vraspir, J.; Zane, H.; Butler, A. Microbial Siderophores: Structure and Reactivity. 241st American Chemical Society Meeting (ACS). Poster presentation, March 27th-31st, 2011. Anaheim, CA.

Kem. M.; Springer, S.; Vraspir, J.; Zane, H.; Butler, A. Amphiphilic Siderophores from Marine Pathogenic Bacteria. Gordon Research Seminar: Bioinorganic Chemistry. Poster Presentation, February 3-6th, 2011. Ventura, CA.

AWARDS

Robert H. DeWolfe Graduate Teaching Award, The University of California, Santa Barbara

ABSTRACT

The isolation and post-assembly modification of acyl peptidic siderophores

by

Michelle Peov Kem

Acyl peptidic siderophores are produced by a variety of bacteria and are often produced in a suite where the iron(III)-binding headgroup remains constant while the fatty acid appendage varies by length and functionality. The inclusion of a fatty acid tail is clearly advantageous for some siderophores, such as the mycobactins, whose amphiphilic properties allow the siderophore to freely diffuse between membranes and media for iron acquisition from macrophages; however, for the majority of acyl siderophores, the biological significance of the fatty acid tail has yet to be determined. This work is focused on the production and post-assembly modification of acyl siderophores.

The ubiquitous marine hydrocarbon-degrading bacterium, *Alcanivorax borkumensis* SK2, was determined to produce the amphibactins, which have been isolated from multiple oil-associating marine bacteria. Only longer tailed amphibactins (C16 and C18) were isolated from the cell pellet of *A. borkumensis* SK2 following centrifugation, as identified by tandem mass spectrometry. Putative biosynthetic genes for amphibactin biosynthesis were also evaluated in the genome of *A. borkumensis* SK2.

The marine bacteria *Marinobacter* sp. DS40M6 and *Marinobacter nanhaiticus* D15-8W produce a suite of acyl peptidic marinobactin siderophores to acquire iron under iron-limiting

conditions. During late-log phase growth, the marinobactins are hydrolyzed to form the marinobactin headgroup with release of the corresponding fatty acid tail. The *bntA* gene, a homologue of the *Pseudomonas aeruginosa* pyoverdine acylase gene, *pvdQ,* was identified from *Marinobacter* sp. DS40M6. A *bntA* knockout mutant of *Marinobacter* sp. DS40M6 produced the suite of acyl marinobactins A-E, without the usual formation of the marinobactin headgroup. Another marinobactin-producing species, *Marinobacter nanhaiticus* D15-8W, is predicted to have two *pvdQ* homologues, *mhtA* and *mhtB*. MhtA catalyzes hydrolysis of the apo-marinobactin siderophores, as well as, the quorum sensing signaling molecule, dodecanoyl-homoserine lactone. In contrast to hydrolysis of the suite of apo-marinobactins by MhtA, hydrolysis of the iron(III)-bound marinobactins was not observed.

The post-assembly modification of another acyl siderophore is seen with the amphi-enterobactins produced by *Vibrio harveyi* BAA-1116. A dimer of 2,3-dihydroxybenzoyl-L-Ser is found in the cell-free supernatant of *V. harveyi* BAA-1116 following centrifugation. *V. harveyi* BAA-1116 does not possess biosynthetic genes for 2,3-dihydroxybenzoyl-L-Ser, suggesting the dimer is formed as a hydrolysis product of the amphi-enterobactins. Adding Fe(III)-amphi-enterobactins to crude cell-free extracts of *V. harveyi* BAA-1116 results in dimer formation; however, dimer formation is not seen when the apo-amphi-enterobactins are incubated with cell-free extracts, suggesting this could be a mechanism for iron release and siderophore recycling.

TABLE OF CONTENTS

LIST OF FIGURES

LIST OF TABLES

LIST OF ABBREVIATIONS

Amp	ampicillin
Bp	base pair
DANSYL	5-dimethylamino-1-naphthalenesulphonyl
DHBA	dihydroxybenzoic acid
FA	Fatty acid
IPTG	Isopropyl β-D-thiogalactopyranoside
Kan	kanamycin
kDa	Kilodalton
MWCO	molecular weight cut-off
O.D.	Optical density
PAGE	Polyacrylamide gel electrophoresis
RP-HPLC	Reverse phase high performance liquid chromatography
SDS	Sodium dodecyl sulfate
Sp	spectinomycin

I. Introduction: The structure and post-assembly modification of acyl peptidic siderophores

1.1 Low solubility of iron

Iron is necessary for the growth of almost all bacteria as it is required for important physiological functions, such as, oxygen transport, DNA synthesis, respiration and nitrogen fixation. However, the low solubility of iron in aerobic environments at physiological pH (K_{sp} of $Fe(OH)_3 = 10^{-39}$) limits the availability of this essential nutrient.[1] Bacteria require a micromolar range of iron for adequate growth, but the sequestering of iron by iron transport and binding proteins (transferrin, lactoferrin, hemoglobin, etc.) lead to a free iron concentration in human serum of 10^{-24} M.[2,3] Aerobically growing marine bacteria are also faced with a scarcity of iron due to free iron concentrations in the range of 0.01-2 nM in high-nutrient low-chlorophyll zones of surface ocean waters.[4] To acquire iron in iron-limited environments bacteria have developed biological systems to scavenge, solubilize, transport, and store this important nutrient. One method bacteria have evolved to acquire iron is through the synthesis and secretion of siderophores, low molecular weight iron (III) chelators.

1.2 Siderophore binding groups

Siderophores typically chelate ferric iron in a hexadentate fashion with catecholate, hydroxamate or α-hydroxycarboxylate functional groups (Figure 1.1). Siderophores can be comprised of three of the same bidentate ligand, as seen with the tris-catecholate siderophore enterobactin and the tris-hydroxamate siderophore desferrioxamine, or a combination of ligands as seen with the siderophores petrobactin and aerobactin (Figure 1.2).

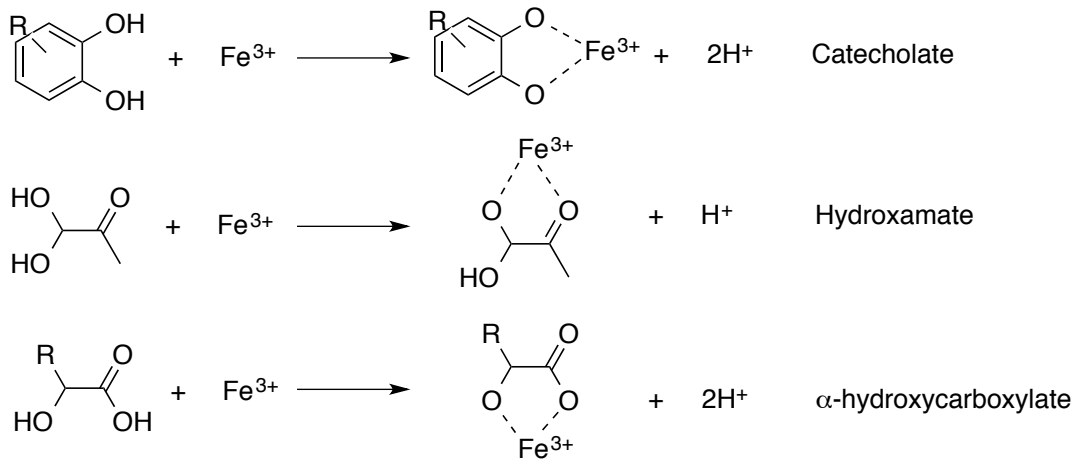

Figure 1.1. Common iron-chelating functional groups found in siderophores.

1.2.1 Catecholate siderophores

Enterobactin, isolated in 1970 by Pollak and Neilands,[5] is the prototypic siderophore comprised of three L-serine-2,3-dihydroxybenzoic acid moieties (Figure 1.2). Since then, many different enteric bacteria have been shown to produce enterobactin. Ferric iron binds to enterobactin in a hexadentate geometry with three catecholate OO' donor in a Δ configuration at the metal center.[6] The high spin $[Fe\text{-}Ent]^{3-}$ complex has a proton independent stability constant of 10^{49} making it exceptionally thermodynamically stable.[7]

Tris-catecholate siderophores structurally similar to enterobactin have been isolated from various bacterial species. Bacillibactin, produced by many *Bacillus* species, has a trithreonine, rather than triserine, lactone scaffold and a glycine spacer between the serine and 2,3-dihydroxybenzoic acid.[8] Like enterobactin, bacillibactin coordinates ferric iron with an exceptionally high proton-independent stability constant (10^{48}) through three catecholate moieties.[9] The salmochelins are a modified form of enterobactin where one or more of the catechol groups are β-C-glucosylated (Figure 1.2).[10] Unlike enterobactin, the salmochelins are able to evade host immune defenses due to the inability of the of the mammalian protein, siderocalin, to bind and sequester the salmochelins.[11] Trichrysobactin, turnerbactin, and streptobactin, are each triscatecholate siderophores with spacer lysine, ornithine and arginine residues between the serine (or threonine in the case of streptobactin) and the 2,3-dihydroxybenzoic acid moieties, respectively.[12,13,14]

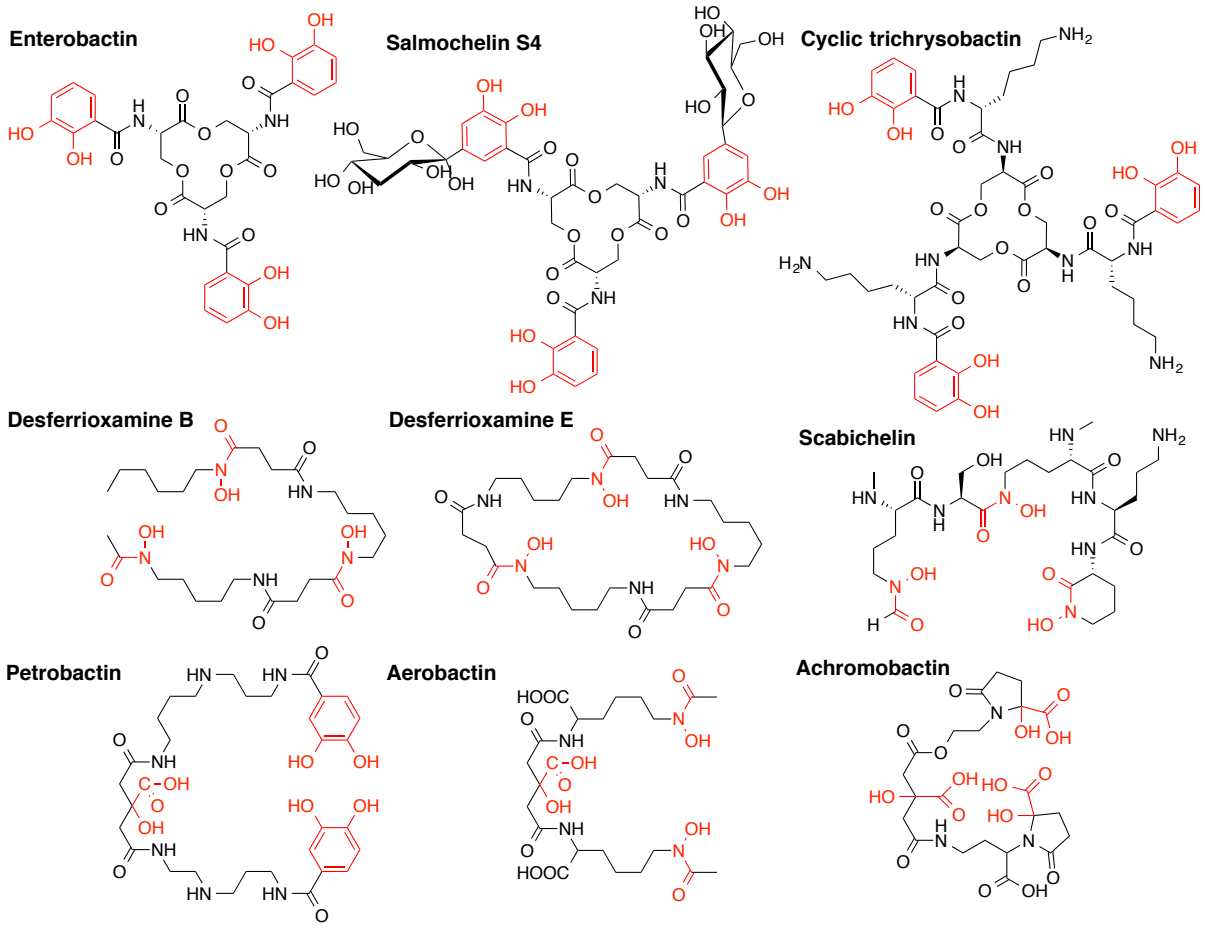

Figure 1.2. Enterobactin,[5] salmochelin S4[10] and cyclic trichrysobactin[12] are examples of tris-catecholate siderophores. Desferrioxamine B,[15] desferrioxamine E[16] and scabichelin[17] are examples of tris-hydroxamate siderophores. Examples of mixed ligand siderophores containing α-hydroxycarboxylates are represented by petrobactin,[18] aerobactin,[19] and achromobactin.[20] Fe(III)-binding groups are highlighted in red.

1.2.2 Tris-hydroxamate siderophores

Tris-hydroxamate siderophores are commonly represented by the family of desferrioxamines produced by many *streptomyces* species.[21] The desferioxamine siderophores (Figure 1.2) are comprised of varying groups of α-amino-ω-hydroxyaminoalkane and succinic or acetic acid and form both linear (A, B, C, D_1, F, and G) and cyclic (D_2 and E) complexes. The desferrioxamine siderophores bind iron through three

hydroxmate OO' donors in an octahedral high spin fashion. Desferrioxamine B, the most studied siderophore of the family, is used clinically for iron overload disease as the drug Desferal.[15] The plant pathogen, *Streptomyces scabies*, also produces a tris-hydroxymate siderophore termed scabichelin. Scabichelin is comprised, from N-terminus to C-terminus, of N^2-methyl-N^5-formyl-N^5-hydroxyornithine, serine, N^2-methyl-N^5-hydroxyornithine, ornithine and a cyclic N^5-hydroxyornithine (Figure 1.2). A relatled species, *Streptomyces turgidiscabies*, produces another trishydroxamte siderophore similar in structure to scabichelin termed turgichelin. Turgichelin differs from scabichelin through the substitution of ornithine for a serine.[17]

1.2.3 Mixed ligand siderophores

The α-hydroxycarboxylate moiety is found in the structure of mixed ligand siderophores such as petrobactin, aerobactin, and achromobactin (Figure 1.2).[18,22] The α-hydroxycarboxylate group is another OO' donor ligand and has unique photochemical properties. Photolysis of the α-hydroxycarboxylate-to-Fe(III) charge-transfer band falls in the near UV wavelength range. The photo-induced ligand oxidation results in the release of CO_2 and the reduction of ferric iron to ferrous iron.[23] Siderophores containing an α-hydroxycarboxylate group often contain hydroxamate and catecholate moieties as their other ferric iron chelating groups.

1.3 Fur Regulation of siderophore transport and production

Bacteria need iron for growth, however, too high of intracellular iron levels can produce toxic effects through the production of reactive oxygen species. As a result, the tight regulation of bacterial iron levels, including siderophore production, is crucial for survival. In

1981, Hantke discovered that a *fur* (ferric uptake regulator) mutation in *Escherichia coli* caused the bacteria to behave as if it was iron-starved under iron-rich conditions by expressing previously determined siderophore biosynthesis and transport genes.[24] This greatly contributed to the understanding that siderophore-mediated iron transport and uptake processes were controlled through the repression of *fur* by Fe^{2+}.[25] When Fe^{2+} is present, Fur binds to its target sequence, GATAATGATAATCATTATC, known as the Fur box blocking transcription of target genes (Figure 1.3).[26,27]

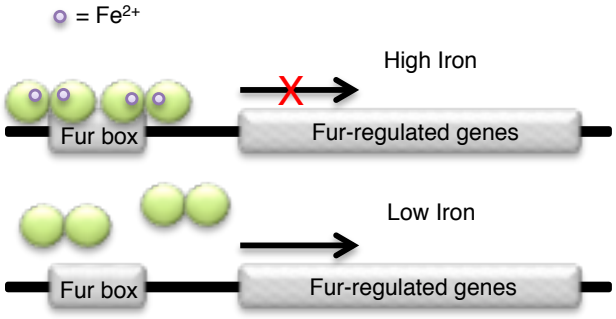

Figure 1.3. The regulation of siderophore biosynthesis by *fur*. Under iron-rich conditions, Fur binds to the Fur box repressing siderophore biosynthesis. Under low-iron conditions Fur is released from the Fur box allowing transcription to occur.

The *E. coli* Fur protein is a 17 kDa homodimeric, DNA binding protein with two metal binding sites per monomer: one for zinc and one for Fe^{2+}. The N-terminal domain of Fur is responsible for binding DNA and the C-terminal domain is involved in dimerization. Under low-iron conditions, Fur releases bound iron resulting in the dissociation of Fur from DNA.[28] Fur represses transcription of over 90 iron-regulated genes.[29] Interestingly, however, *fur* is not only involved in the regulation of genes directly related to iron metabolism. Fur has been shown to repress genes involved in metabolism, oxidative stress, and virulence factors.[29]

1.4 Amphiphilic siderophores

One structural feature commonly found in marine siderophores, is the inclusion of a fatty acid appendage attached to the Fe(III)-binding headgroup (Figure 1.4), which results in an amphiphilic compound.[30] Acyl peptidic siderophores span a wide-range across the amphiphilic spectrum, from those that are hydrophobic and remain cell associated to those that are hydrophilic. Acyl siderophores with short peptides (4 amino acids) and longer fatty acid tails (≥ C16), such as the amphibactins, have been isolated from multiple marine bacteria,[30,31] including the well-studied hydrocarbon degrader, *Alcanivorax borkumensis* SK2.[32]

On the other hand, acyl siderophores with longer peptidic headgroups, such as the loihichelins (8 amino acids) and aquachelins (7 amino acids) (Figure 1.4), are quite hydrophilic and are isolated from the supernatant of harvested cultures.[30,33] The marinobactins produced by *Marinobacter sp*. DS40M6 have a six amino acid headgroup connected to fatty acids ranging from 12-18 carbons.[30, 34] The hydrophobicity of the marinobactins varies among the suite based on the length of the fatty acid. As a result, marinobactins with shorter fatty acid appendages are released into the extracellular milieu while the longer tailed derivatives remain associated with the bacterial membrane.[34]

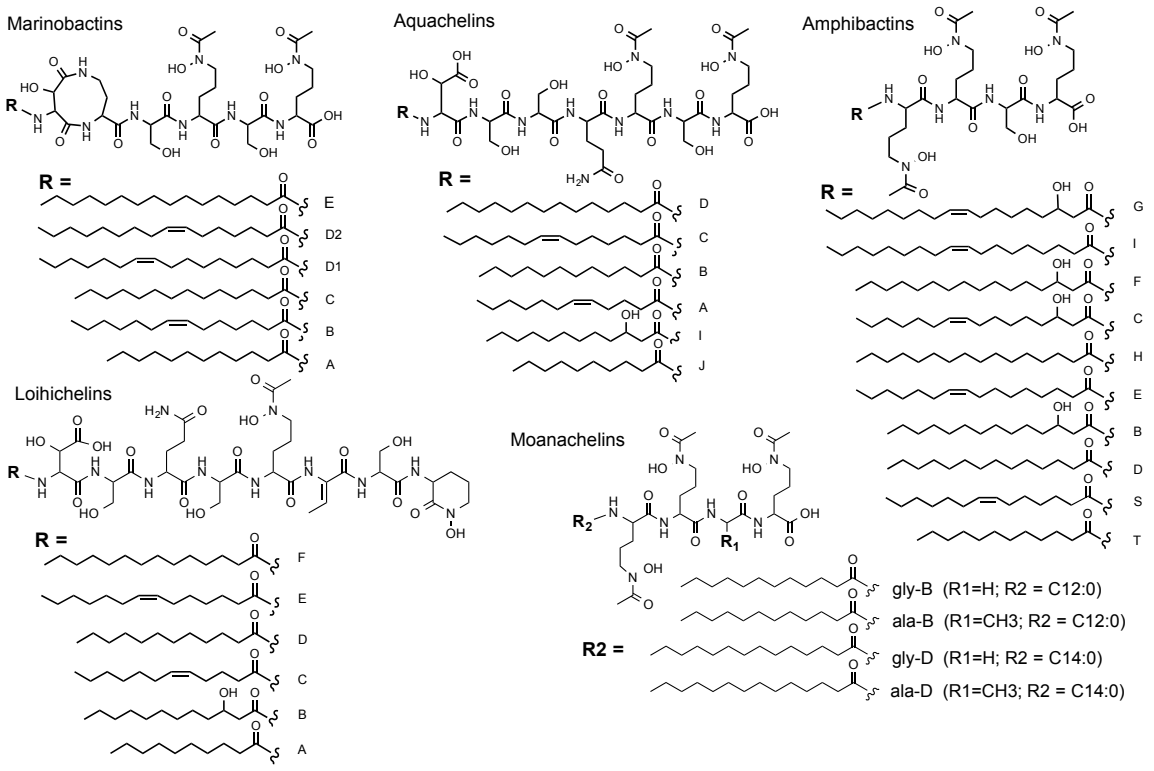

Figure 1.4. Structures of peptidic acyl siderophores produced by different marine bacteria isolated from ocean surface waters. Moanachelins gly-C (R1=H; R2=C14:1) and gly-E (R1=H; R2=C16:1) were also isolated, however, the location of the double bond has not been determined.

Recently, the amphi-enterobactins, which are fatty acid derivatives of the well-known siderophore enterobactin (Figure 1.5), were isolated from the marine bioluminescent bacterium, *Vibrio harveyi* BAA-1116 (reclassified as *Vibrio campbellii*).[35] Unlike enterobactin, the amphi-enterobactins have a fourth serine incorporated into the tri-lactone backbone forming a tetra-lactone ring. This additional serine is used as the attachment point for a fatty acid appendage in place of a 2,3-dihydroxybenzoic acid moiety. Due to the already hydrophobic nature of enterobactin,[36] the addition of the acyl moiety to the amphi-enterobactins greatly increases their hydrophobicity and causes the siderophores to associate with the cell membrane.[35]

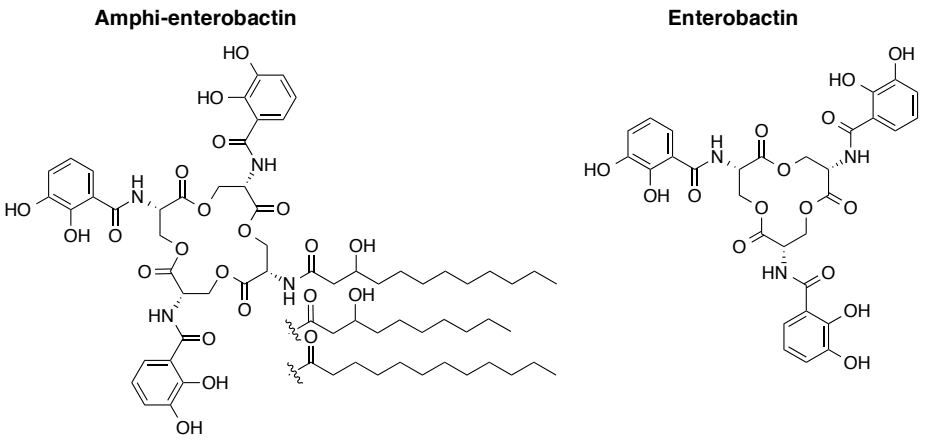

Figure 1.5. The amphi-enterobactins produced by *Vibrio harveyi* BAA-1116 are acylated derivatives of the prototypic siderophore, enterobactin. Amphi-enterobactins with a C12:1, C12:1-OH, C14:1, and C14:1-OH fatty acid were also isolated, however, the location of the double bond was not determined.

1.5 Non-marine amphiphilic siderophores from pathogens and marine isolates

Amphiphilic siderophores are not limited to the marine environment. The mycobactins are acyl peptidic siderophores produced by *Mycobacteria* species and differ slightly in the peptidic core structure depending on the producing species.[37, 38] The human pathogenic bacterium, *Mycobacterium tuberculosis*, produces Mycobactin T and the more hydrophilic mycobactin derivative, carboxymycobactin T. Unlike the acyl siderophores previously discussed, the internal lysine of the mycobactin core is acylated with a C18-C23 fatty acid rather than the N-terminal residue.[37]

The carboxymycobactins are mainly produced by pathogenic species of *Mycobacteria* and differ slightly in structure from the mycobactins due to a shorter fatty acid appendage, which is also functionalized with a terminal carboxylic acid or methyl ester (Figure 1.6).[39,40] The shorter, functionalized tail of the carboxymycobactins, however, allows them to be excreted into the extracellular milieu. It has been hypothesized that the carboxymycobactins

transfer iron to the mycobactins in the bacterial membrane, which act as short-term storage molecules for Fe(III).[41]

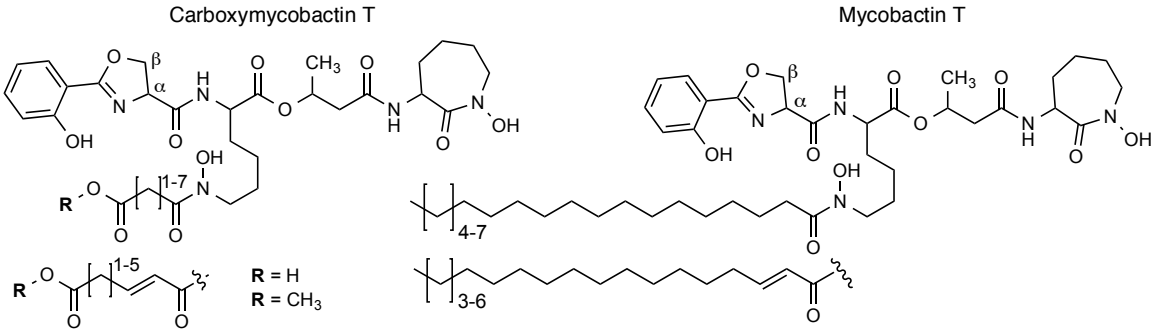

Figure 1.6. Siderophores produced by *Mycobacterium tuberculosis*. The α- and β- labeled carbons on the oxazoline ring of mycobactin T and carboxymycobactin T may be methylated.

Cupriachelin and taiwachelin are structurally similar amphiphilic siderophores isolated from different *Cupriavidus* species, which are often found in soil and freshwater environments (Figure 1.7).[42, 43] Both siderophores have β-hydroxyaspartic acid residues in their headgroup providing unique photochemical properties, which will be discussed later in this review. The serobactins, isolated from the plant endophytic bacterium, *Herbaspirillum seropedicae* Z67, are structurally similar to cupriachelin and taiwachelin (Figure 1.7).[44] All three siderophores are quite hydrophilic and were isolated from culture supernatants.

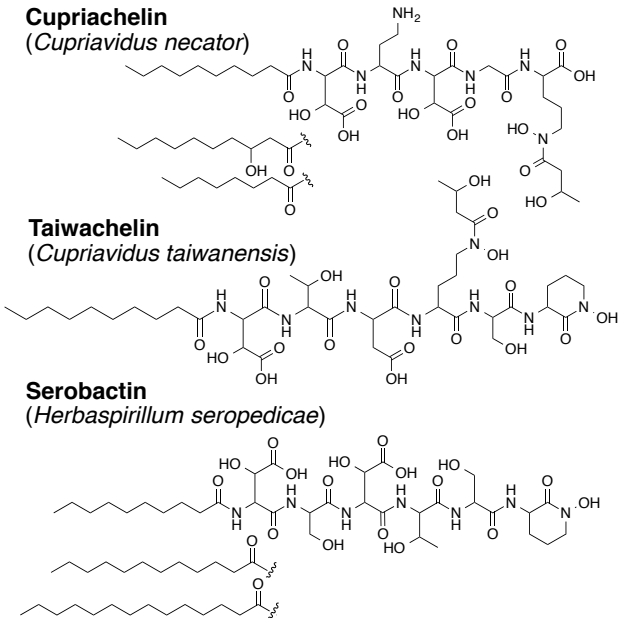

Figure 1.7. Non-marine acyl siderophores containing β-hydroxyaspartic acid residues.

1.6 Membrane partitioning of the marinobactins

The marinobactin siderophores produced by *Marinobacter* sp. DS40M6 were used to investigate how the amphiphilic properties of a siderophore might aid in membrane partitioning and iron uptake. The partition coefficient of the longest chain marinobactin, apo-M_E (6387 M^{-1}), into phospholipid vesicles was determined to be about 50-fold greater than the partitioning of the iron-bound form, Fe(III)-M_E (174 M^{-1}).[45] It is hypothesized that the change in geometry of the marinobactin headgroup upon binding Fe(III) results in a more hydrophilic surface as the oxygen and nitrogen atoms orient to face the aqueous environment. The partition coefficient into model membranes also shows an order of magnitude decrease when moving from apo-M_E (C16:0) to apo-M_C (C14:0) *and* apo-M_C (C14:0) to apo-M_A (C12:0). These observed changes in partition coefficients with respect to fatty acid length suggests the suite of siderophores are making a gradient out of the cell membrane.[45]

1.7 Self-assembly of the marinobactins

The marinobactins are characterized by having an unusually low critical micelle concentrations (CMC) ranging from 25 μM for apo-M_E (C16:0) to 150 μM for apo-M_A (C12:0).[30] The iron-bound marinobactins are characterized by having slightly higher CMC values than the apo-marinobactins. When iron (III) is added in a 1:1 equivalent to apo-marinobactin micelles the diameter of the micelles decrease (i.e. 4.0 nm for apo-M_E to 2.8 nm for Fe(III)-M_E).[46] This is likely due to a change in molecular geometry of the headgroup into a more conical shape upon binding ferric iron. In the presence of a small excess of iron (III), the micelles rearrange into unilamellar vesicles, while a large excess of iron (III) initiates another rearrangement into multilamellar vesicles and stacked bilayers (Figure 1.8).[46]

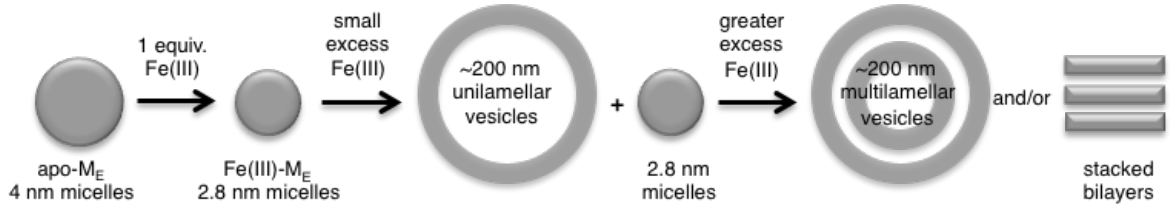

Figure 1.8. Self-assembly of marinobactin E in the presence of Fe(III). Adapted with permission from Owen, T.; Pynn, R.; Martinez, J.S.; Butler, A. *Langmuir* 2005, 21(26), 12109-12114. Copyright 2005 American Chemical Society.

1.8 Membrane partitioning and self-assembly of the mycobactins

The permeability of the mycobactins into membrane systems is an important aspect contributing to the virulence of *Mycobacterium tuberculosis*. *M. tuberculosis* can evade host immune defenses and reside in the phagosomes of host macrophages.[47] The amphiphilic properties of the mycobactins allow the siderophores to freely diffuse out of the phagosomes to acquire iron from intracellular iron pools within the macrophages. The ferric-mycobactins

can then freely diffuse into lipid droplets within the macrophages for transport and iron delivery back to the mycobacterium.[48] This is an example of how the amphiphilic properties of the mycobactins increase the bacterium's ability to acquire iron.

1.9 Biosynthesis of amphiphilic siderophores

1.9.1 General NRPS mediated biosynthesis

Siderophores can be comprised of a combination of proteogenic and non-proteogenic amino acids as a result of being synthesized by large, assembly line-like proteins called non-ribosomal peptide synthetases (NRPS). A basic NRPS module consists of an adenylation, condensation and thiolation domain. The adenylation domain selects a specific amino acid from a pool of substrates and activates the amino acid to form the corresponding aminoacyl adenylate through the consumption of ATP (Figure 1.9A).[49] The aminoacyl adenylate is then loaded onto an adjacent thiolation domain (also referred to as the peptidyl carrier protein, PCP) where it is stabilized through the formation of a thioester bond with a phosphopantetheinyl (Ppant) prosthetic group (Figure 1.9B). Prior to binding the aminoacyl adenylate, the apo-PCP is converted to its holo form through the post-translational transfer of a 4'-phosphopantetheinyl (4'-PP) cofactor of coenzyme A onto a serine residue of the enzyme active site to generate the Ppant prosthetic group. NRPS can also include various modifying domains, such as, epimerization, N- or C-methylation, or cyclization domains to increase the diversity and biological activity of non-ribosomally synthesized natural products.[50] In type A NRPS, the peptidyl chain grows unilaterally as the condensation domain catalyzes peptide bond formation of two activated amino acids on adjacent thiolation

domains (Figure 1.9C).[51] Type B NRPSs work iteratively by utilizing the modules and domains more than once to generate small peptides of repeating sequences. Non-linear NRPSs (Type C) produce natural products whose structures do not correspond to the linear arrangement of the NRPS modules and domains.[51] Release and termination of peptide chain elongation is commonly performed through hydrolysis or cyclization at the thioesterase domain.

The adenylation domains of NRPS modules have high substrate specificity, which allows specific amino acids to be incorporated into growing peptide chains. Overall, adenylation domains have a low sequence similarity to one another but they do contain core motifs (A1-A10) of high homology. [49] The substrate specificity of adenylation domains is mediated by a signature sequence consisting of eight amino acids lining the substrate-binding pocket.[49, 52] These signature sequences form a degenerate NRPS code where one or more codes can be utilized for the same amino acid. The signature sequences can be used to predict which amino acid will be incorporated into a growing peptidyl chain.[49]

Polyketide synthetases (PKSs) are also important components of the biosynthesis of some siderophores. Type I PKSs, are arranged in a modular fashion, and each module adds a new carbon unit to the growing polyketide chain.[53, 54] Type I PKSs are commonly composed of ketosynthase (KS), acyltransferase (AT) and acyl carrier protein (ACP) domains.[53] Some siderophores, such as the mycobactins, are synthesized by hybrid NRPS-PKS systems as described below.

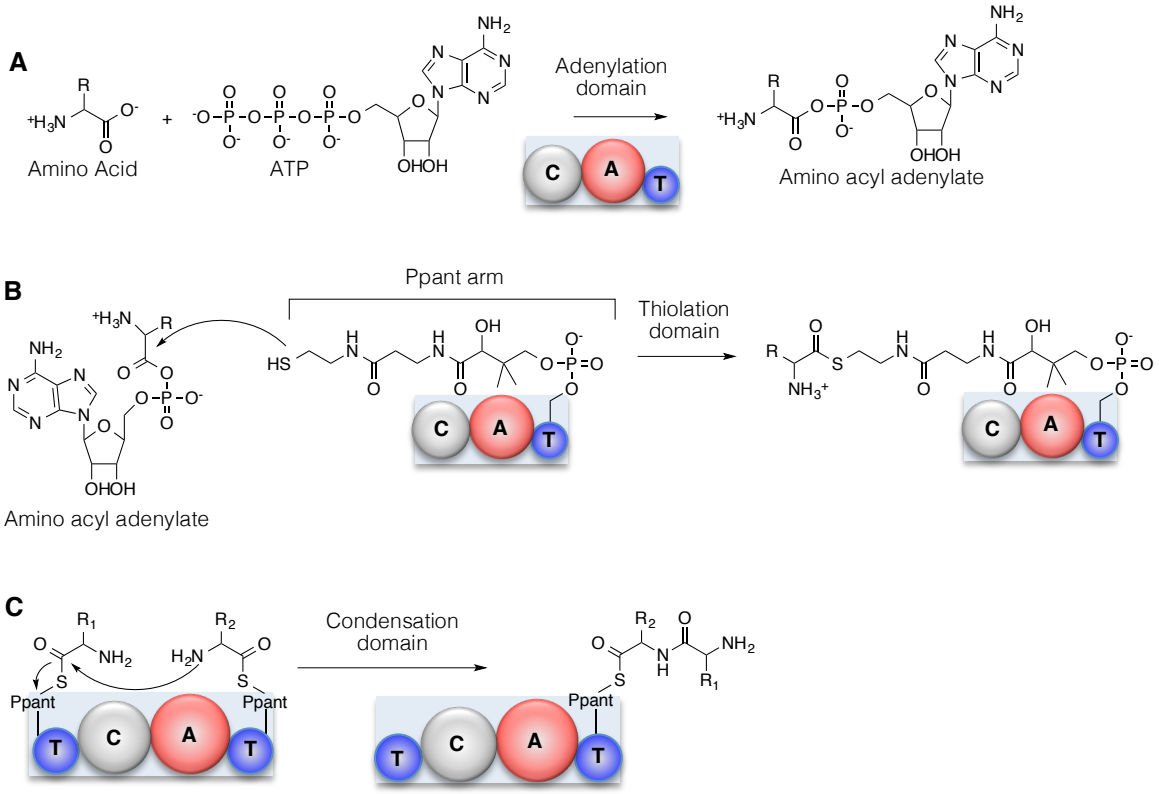

Figure 1.9. General NRPS biosynthetic scheme. (A) The adenylation domain selects a specific amino acid substrate and converts it to an aminoacyl adenylate under the consumption of ATP (B) The activated aminoacyl adenylate is then transferred to the Ppant arm of the thiolation domain (C) The condensation domain catalyzes amide bond formation of amino acids on adjacent thiolation domains. C = condensation domain; A = adenylation domain; T = thiolation domain; Ppant = phosphopantetheinyl.

1.9.2 Biosynthesis of the amphi-enterobactins

The amphi-enterobactins are comprised of three 2,3-dihydroxybenzoyl-L-serine units and one L-serine-fatty acid unit in a tetra-lactone ring. The proposed biosynthetic pathway of the amphi-enterobactins (Figure 1.10) contains six genes (AebA-F), which are predicted homologues of the well-studied enterobactin biosynthetic genes.[35] AebA, AebB (N-terminal domain) and AebC convert chorismate to 2,3-dihydroxybenzoic acid. AebB (C-terminal domain), AebE, AebD and AebF are NRPS enzymes, which polymerize and cyclize the L-

Ser-dihydroxybenzoic acid and Ser-fatty acid. Unlike EntF, which just catalyzes the condensation of L-serine and dihydroxybenzoic acid (DHBA),[55] the condensation domain of AebF displays unique dual activity by catalyzing amide bond formation between L-Ser and DHBA *and* the L-Ser and the fatty acid. To initiate biosynthesis, the incorporated fatty acid is activated by the protein product of *aebG*, a fatty acyl CoA ligase (FACL), which is in close proximity to *aebA-F*. A knockout mutant of *aebG* completely abolishes amphi-enterobactin production and no enterobactin is produced indicating that *aebG* is necessary for the acylation and initiation of amphi-enterobactin biosysnthesis.[35]

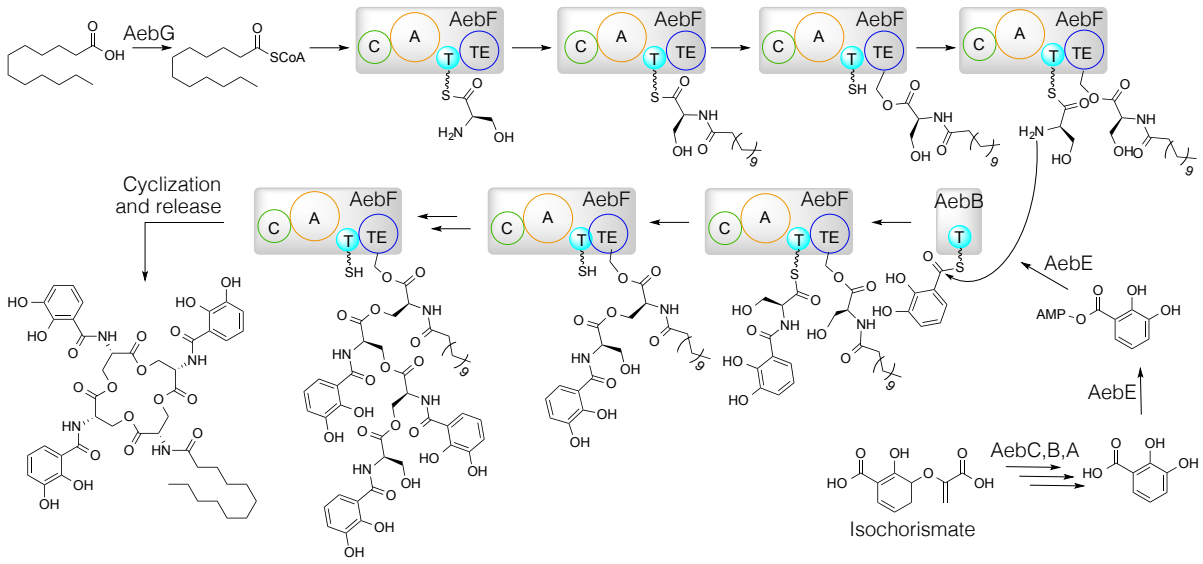

Figure 1.10. Proposed biosynthetic pathway for the amphi-enterobactins. Biosynthesis begins with the activation of a fatty acid by the fatty acyl CoA ligase, AebG. The fatty acid ranges from a C10-C14 and varies in degree of unsaturation and hydroxylation. Reprinted with permission from Zane, H.; Naka, H.; Rosconi, F.; Sandy, M.; Haygood, M.; Butler, A. *Journal of the American Chemical Society* 2014, 136 (15), 5615-5618. Copyright 2014 American Chemical Society.

1.9.3 Mixed NRPS/PKS biosynthesis: Mycobactins

The gene cluster encoding the biosynthetic enzymes for mycobactin assembly was discovered by the research group of Christopher Walsh following the sequencing of the *M. tuberculosis* genome in 1998;[56] however, until recently, the genes responsible for the acylation of the mycobactins was unknown. The mycobactins and carboxymycobactins are synthesized by hybrid NRPS-PKS proteins encoded by two gene clusters designated as *mbt-1* and *mbt-2* (Figure 1.11). The mycobactin core is assembled by *mbt-1*-encoded proteins, which are comprised of both NRPSs (MbtB, MbtE, MbtF) and PKSs (MbtC, MbtD).[56, 57] The adenylation domain of MbtB, which incorporates the serine or threonine to form the oxazoline ring, shows specificity for threonine; however, the majority of mycobactins are isolated without β-methylated oxazoline rings suggesting the methyl group is removed by an as yet to be determined mechanism. [57]

Gene cluster *mbt-2* consists of four open reading frames (*mbtL*, *mbtM*, *mbtN*, *mbtK*) that are necessary for mycobactin biosynthesis. The *mbt-2*-encoded proteins transfer an acyl substituent onto the side chain of a lysine residue for incorporation into the mycobactin core.[57-59] MbtM is homologous to fatty acyl-AMP ligases (FAAL) and activates fatty acids into their corresponding acyl adenylates under the consumption of ATP. The activated fatty acid is transferred to the Ppant arm of the carrier protein, MbtL, and MbtK transfers the fatty acid onto the ε-amino group of lysine (Figure 1.11). MbtM prefers long-chain fatty acids and does not bind to short acyl chains or dicarboxylic acid substrates suggesting that another protein is expressed to incorporate or functionalize the carboxymycobactin fatty acid tail.[59] A point of unsaturation is introduced at the α-β position of the fatty acid by the acyl-ACP dehydrogenase, MbtN, which catalyzes the dehydrogenation of the ACP-bound substrate.[58]

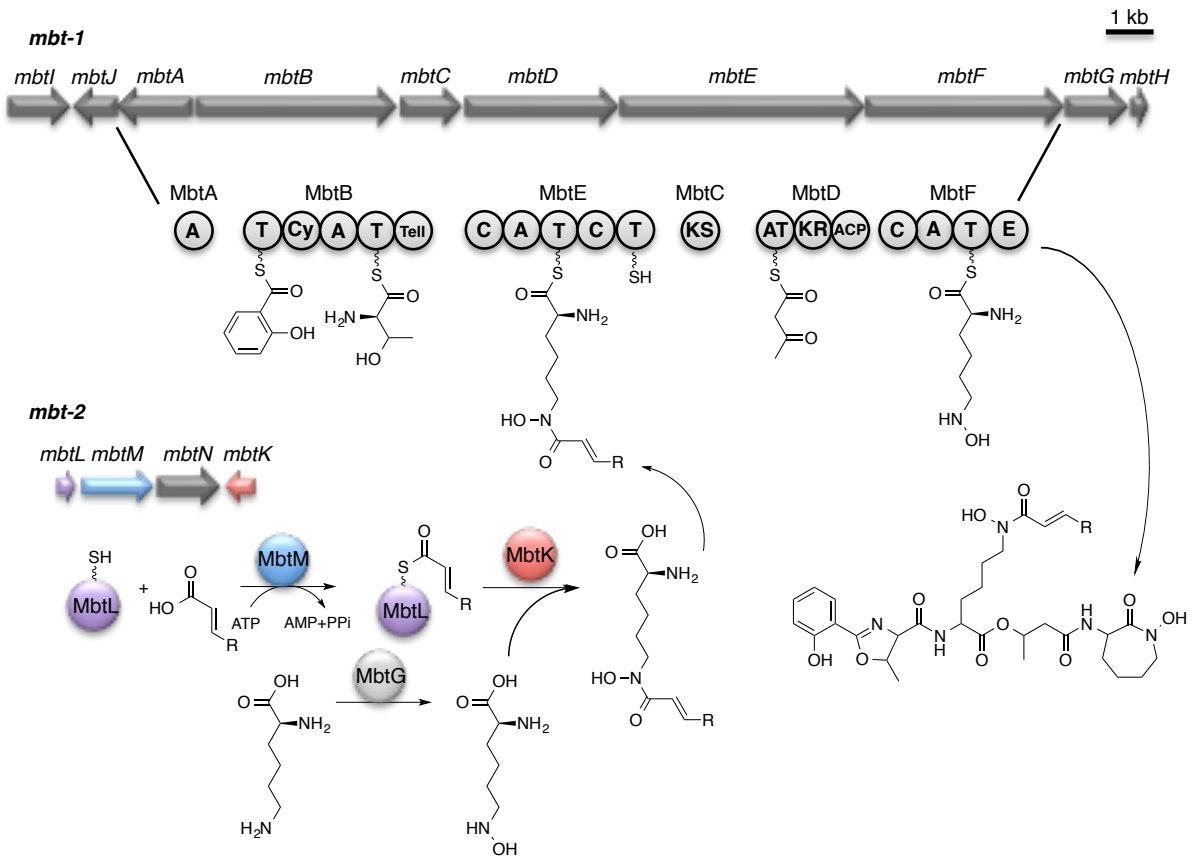

Figure 1.11. Proposed biosynthetic scheme for the mycobactins from *Mycobacterium tuberculosis*. The *mbt-2*-encoded proteins transfer an acyl substituent onto a lysine side chain for incorporation into the mycobactin core, which is assembled by *mbt-1*-encoded proteins. Only the α, β unsaturated fatty acids are shown (R = 15-18 carbons).

1.9.4 Pyoverdine

Pseudomonas species produce the fluorescent siderophore, pyoverdine, which differ in structure between species and even strains of the same species.[60] The peptide core of pyoverdine produced by *P. aeruginosa* PAO1 is synthesized by four different NRPS proteins: PvdI, PvdJ, PvdL, and PvdD (**Figure 1.12**).[61] The N-terminus of the peptide core begins with a chromophore moiety, which is formed from D-tyrosine and L-2,4-diaminobutyrate incorporated by module 3 (M3) and module 4 (M4) of PvdL,

respectively.[62,63] The first module of PvdL (M1, **Figure 1.12**) is homologous to fatty acyl AMP-ligases, which activate a fatty acid for peptide acylation.[60, 64] The activated fatty acid is then transferred to the carrier protein on M1 of PvdL where the condensation domain of module 2 (M2) from PvdL catalyzes amide bond formation between the activated fatty acid and the L-glutamic acid selected by M2. A pyrophosphate exchange assay of M1 from PvdL showed a preference for a C14 fatty acid.[65] The remaining PvdL modules, PvdJ, PvdI and PvdD complete the biosynthesis of the peptidic portion of the pyoverdine core. The maturation of the acylated, non-fluorescent pyoverdine precursor is proposed to occur in the periplasm by PvdP, PvdO, PvdN and PvdQ to form the final pyoverdine product.[66]

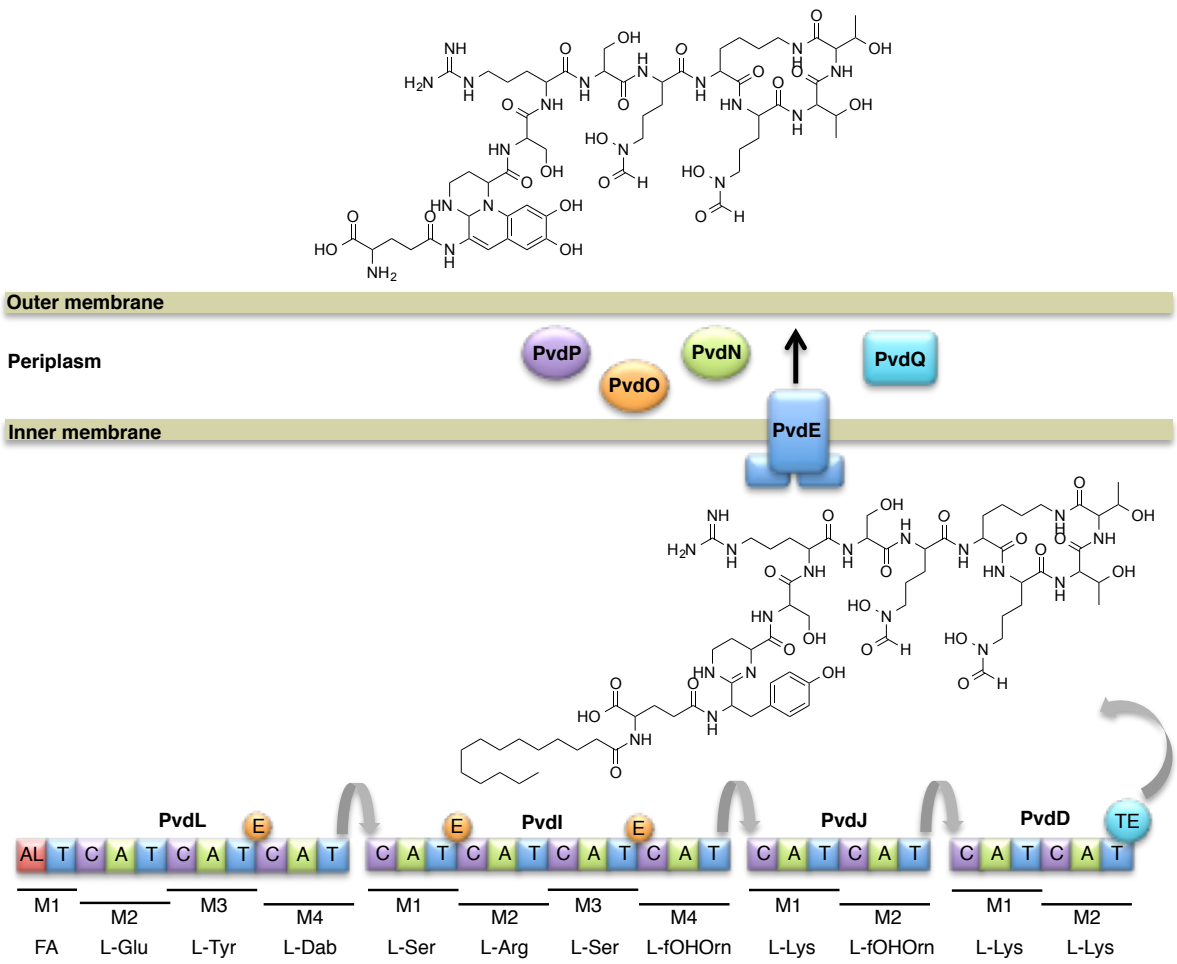

Figure 1.12. Proposed biosynthetic pathway of pyoverdine from *P. aeruginosa* PAO1. The starter unit of PvdL (AL) is a fatty acyl AMP-ligase, which activates a fatty acid for incorporation into the peptide chain. C = condensation domain, A = adenylation domain, T = thiolation domain, TE = thioesterase domain, E = epimerase. Periplasmic proteins PvdP, PvdO, PvdN and PvdQ are believed to be involved in siderophore maturation prior to excretion from the cell.

1.10 Genome derived biosynthesis of amphiphilic siderophores

Genome mining has been a useful tool for the discovery of peptide natural products, including siderophores. The wealth of information regarding the biosynthesis of natural products in conjunction with the modular logic of NRPSs has enabled the structural organization of non-ribosomally synthesized siderophores to be predicted. In particular for

siderophores, the sequences of proteins that synthesize common iron-binding groups (i.e. catecholates and hydroxamates) are well conserved, as are proteins involved in siderophore biosynthesis, tailoring and transport.

1.10.1 Fatty acid activation by an external ligase

Cupriachelin is synthesized through the concerted action of four NRPS proteins: CucF, CucG, CucJ, and CucH (Figure 1.13A).[42] CucF begins with an atypical N-terminal condensation domain suggesting it has an external ligase to activate a fatty acid for peptide acylation, similar to the biosynthesis of the amphi-enterobactins[35] (Figure 1.10) and surfactin.[67] Module 1 of CucF also contains an acyl carrier protein (ACP) domain, which tethers and transfers the activated fatty acid during biosynthesis. Module 2 of CucF ends with a TauD domain, which is predicted to catalyze the hydroxylation of the aspartate residues to form the α-hydroxycarboxylic acid moiety used in Fe(III) chelation. An analysis of the substrate specificity of the adenylation domain from CucG suggests L-Asp is hydroxylated following initiation of the adenylation step. CucH and CucJ finish the synthesis of the peptidic portion of the siderophore, as indicated in Figure 1.13A, however, CucH does not end in a terminal thioesterase domain. Instead, chain termination is proposed to occur by the hydrolase, CucC.[42]

The genome of *A. borkumensis* SK2 has two putative NRPSs predicted to be involved in amphibactin biosynthesis: ABO_2093 and ABO_2092, which are comprised of four classical NRPS modules (Figure 1.13B).[32] As seen with the biosynthesis of cupriachelin, module 1 of ABO_2093 begins with a N-terminal condensation domain, suggesting an external ligase activates a fatty acid for incorporation into the peptidic headgroup. Interestingly, however, no acyl carrier protein (ACP) domain is present in ABO_2093 to tether and transport the

activated fatty acid. An ACP domain is also omitted in the biosynthetic gene cluster of surfactin[67] and the amphi-enterobactins.[35] Biosynthesis then appears to occur in a linear fashion, as indicated in Figure 1.13B, ending with a thioestease domain, which is preceded by a domain of unknown function.

1.10.2 Fatty acid activation by a fatty acyl AMP-ligase domain

The marinobactin-producing bacterium, *M. nanhaiticus* D15-8W, has two putative NRPSs predicted to be involved in siderophore biosynthesis, ENO16763 and ENO16762 (Figure 1.13C). The first module of ENO16763 encodes a unique domain possessing high homology to fatty acyl AMP-ligases, as seen with the biosynthesis of pyoverdine from *P. aeruginosa* PAO1.[60] This module is predicted to activate a fatty acid for incorporation into the peptidic headgroup. Based on the structure of the marinobactins, the biosynthesis is proposed to occur in a linear fashion and terminates with a thioesterase domain as shown in Figure 1.13C. Similar to marinobactin biosynthesis, the predicted biosynthesis of the taiwachelins (Figure 1.13D)[43] and serobactins (Figure 1.13E)[44] begin with a N-terminal acyl AMP-ligase starter domain, which activates a fatty acid and initiates biosynthesis.

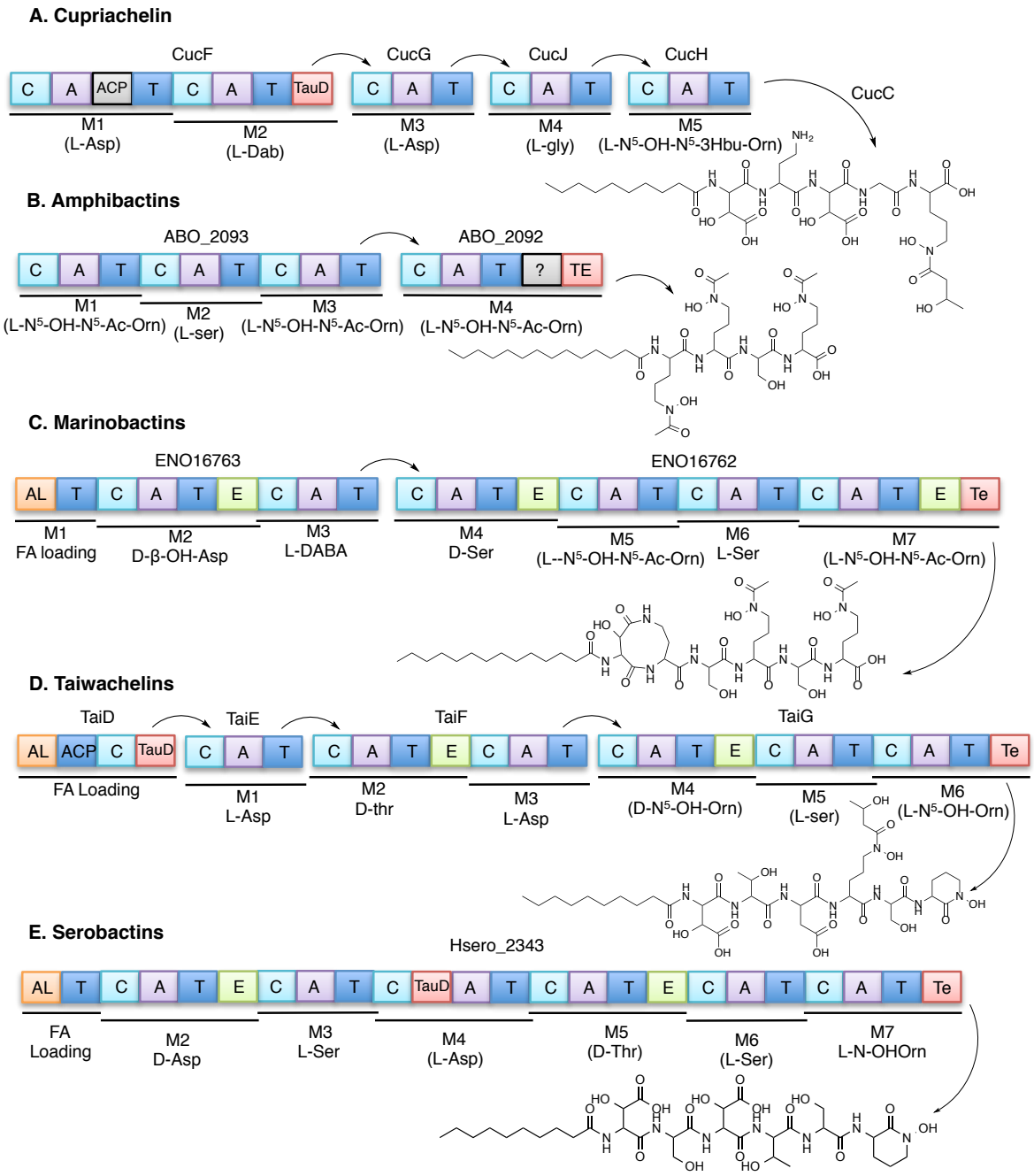

Figure 1.13. Proposed biosynthetic schemes for (A) cupriachelin from *C. necator* H16 (B) the amphibactins from *A. borkumensis* SK2 (C) the marinobactins from *M. nanhaiticus* D15-8W (D) taiwachelin from *C. taiwanensis* LMG19424 (E) serobactin from *H. seropedicae* Z67. C = condensation domain, A = adenylation domain, T = thiolation domain, TE = thioesterase domain, ACP = acyl carrier protein, TauD = hydroxylase, E = epimerase, AL = fatty acyl AMP-ligase

1.11 The post-assembly modification of siderophores

1.11.1 Pyoverdine maturation by PvdQ

Pyoverdine was discovered in 1892 and its involvement in bacterial iron uptake was established in the 1970s.[61] Not until recently, however, was it known that pyoverdine is partially synthesized in the cytoplasm as an acylated precursor prior to formation of the chromophore.[64, 66] The acylated pyoverdine precursor is then transported into the periplasm where it encounters the acylase, PvdQ. PvdQ removes the fatty acid from the pyoverdine precursor, followed by chromophore formation by PvdO, PvdP and PvdN (**Figure 1.12**).[66] A knockout mutant of PvdQ did not affect the growth of *P. aeruginosa*, however, it did abolish pyoverdine production and release. The PvdQ knockout mutant also resulted in the impairment of swarming motility and biofilm formation in *P. aeruginosa* and an overall reduced virulence in a *Caenorhabditis elegans* infection model.[68] As a result, finding small molecule inhibitors of PvdQ and altering its substrate specificity has been a topic of increasing interest to combat bacterial infection by pathogenic *Pseudomonas* species.[65,69,70,71]

Structural studies show PvdQ to be part of the Ntn-hydrolase superfamily of enzymes,[72] which are autoproteolytically activated by removing a N-terminal signal sequence and a 23 residue spacer peptide to form a 18 kDa α-chain and a 60 kDa β-chain.[73] Following self-activation, the serine nucleophile on the N-terminus of the β-chain is exposed. PvdQ was originally believed to be involved in quorum quenching due to the reactivity of PvdQ with acyl-homoserine lactones.[73-75] The location of *pvdQ* in the pyoverdine biosynthetic operon of *P. aeruginosa* PAO1, however, suggests PvdQ is involved with tailoring pyoverdine. The *pvdQ* gene is conserved among fluorescent *Pseudomonas* species although *pvdQ* is not

always contained in the pyoverdine biosynthetic operon. The *pvdQ* orthologues, however, are all iron-regulated and necessary for the production of pyoverdine.[76]

PvdQ prefers median chain fatty acids (C12, C14), which corresponds to the fatty acid preference of module 1 from PvdL.[65] It has been hypothesized that the acylated pyoverdine precursor prevents the siderophore from diffusing through the cytoplasm and periplasm. The acyl chain is thus proposed to hold the siderophore in the proper cellular location until biosynthesis is complete.[64, 77]

1.11.2 Enzymatic modification of the marinobactins

In addition to *M. nanhaiticus* D15-8W, the marinobactin siderophores are also synthesized by *Marinobacter* sp. DS40M6 under low-iron conditions. During mid to late log phase bacterial growth, deacylated marinobactins (M_{HG}) are detected in the culture supernatant of both *Marinobacter* species.[78] The PvdQ-like acylases, BntA, from *Marinobacter sp*. DS40M6 and MhtA from *M. nanhaiticus* D15-8W remove the fatty acid tail from the marinobactins to generate the marinobactin headgroup. MhtA does not, however, hydrolyze the Fe(III)-marinobactins suggesting a possible regulatory role in iron acquisition (Figure 1.14).

The fatty acid tail on the marinobactins allow for partitioning into membranes.[34] In membrane-rich environments, removal of the fatty acid would release M_{HG} from membrane association to scavenge for iron without changing its iron binding properties. *Marinobacter* species are also known for their hydrocarbon degrading abilities and could possibly utilize the fatty acid products as a carbon source, as seen with other bacteria expressing Ntn-hydrolases.[75, 79]

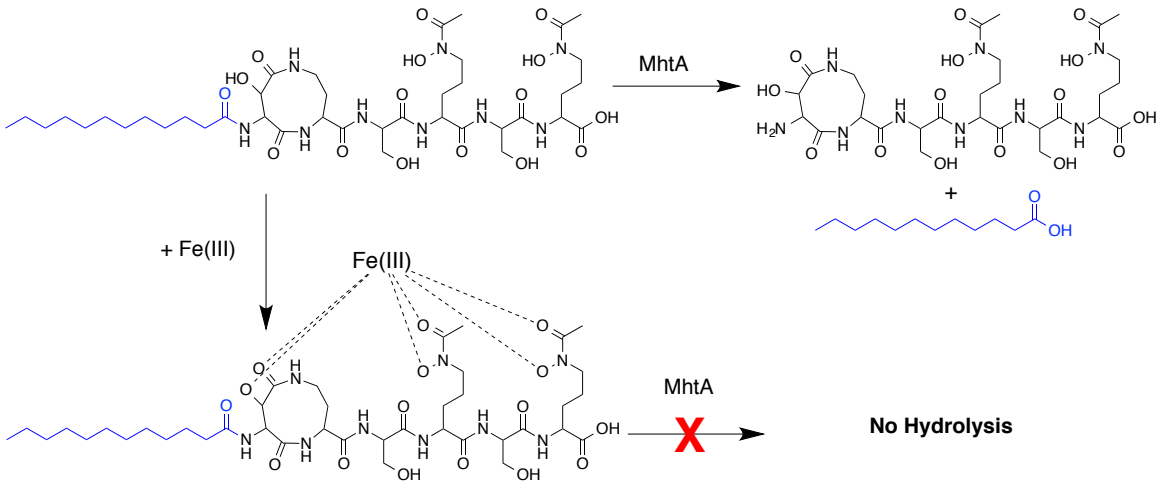

Figure 1.14. Hydrolysis of the marinobactins by MhtA.

1.11.3 Photochemistry of amphiphilic siderophores

Many marine siderophores possess α-hydroxycarboxylic acid functionalities to coordinate ferric iron. These α-hydroxycarboxylic acid moieties are part of β-hydroxyaspartic acid or citric acid, and are photoreactive when coordinated to Fe(III).[80] Photolysis induces ligand oxidation and the release of CO_2 in conjunction with the reduction of Fe(III) to Fe(II).[22, 81] During photolysis, the citrate ligand is converted to 3-ketoglutaric acid, which can undergo a keto-enol tautomerization to the enolate form. The enolate form is more prevalent in aqueous solutions and can chelate Fe(III).[22, 23] The photolysis of aerobactin has been studied most extensively and can be monitored by the disappearance of the α-hydroxycarboxylic acid-to-Fe(III) charge transfer band around 300 nm. UV-photolysis studies of the Fe(III)-ochrobactins and Fe(III)-snychobactins, which are acylated analogues of aerobactin, produced similar results.

Many structurally characterized amphiphilic siderophores also contain β-hydroxyaspartic acid residues, including the marinobactins, aquachelins, loihichelins, cupriachelin,

taiwachelin and serobactins.[30, 33, 42-44] The aquachelins produced by *Halomonas aquamarina* strain DS40M3 have a N-terminal β-hydroxyaspartic acid residue connected to the fatty acid. Photolysis of the ferric-aquachelins results in oxidative cleavage of the ligand, forming a hydrophilic peptide fragment without the fatty acid (**Figure 1.15**A). The hydrophilic peptide fragment is still able to chelate Fe(III), however, with a somewhat lower conditional stability constant ($K_{FeL,Fe'}^{cond} = 10^{11.5}$ M^{-1} vs. $10^{12.2}$ for the unmodified siderophore).[82] This decrease in the stability constant corresponds to the loss of the β-hydroxyaspartic acid residue, which is one of the Fe(III) chelating groups.

Cupriachelin has two β-hydroxyaspartic acid residues in its backbone; however, photo induced cleavage was only seen with the central β-hydroxyaspartic acid in the peptide backbone (**Figure 1.15**B).[42] Photo induced hydrolysis of the cupriachelin backbone results in the formation of Fe(II), a fatty acid containing peptide, and a small hydrophilic peptide.

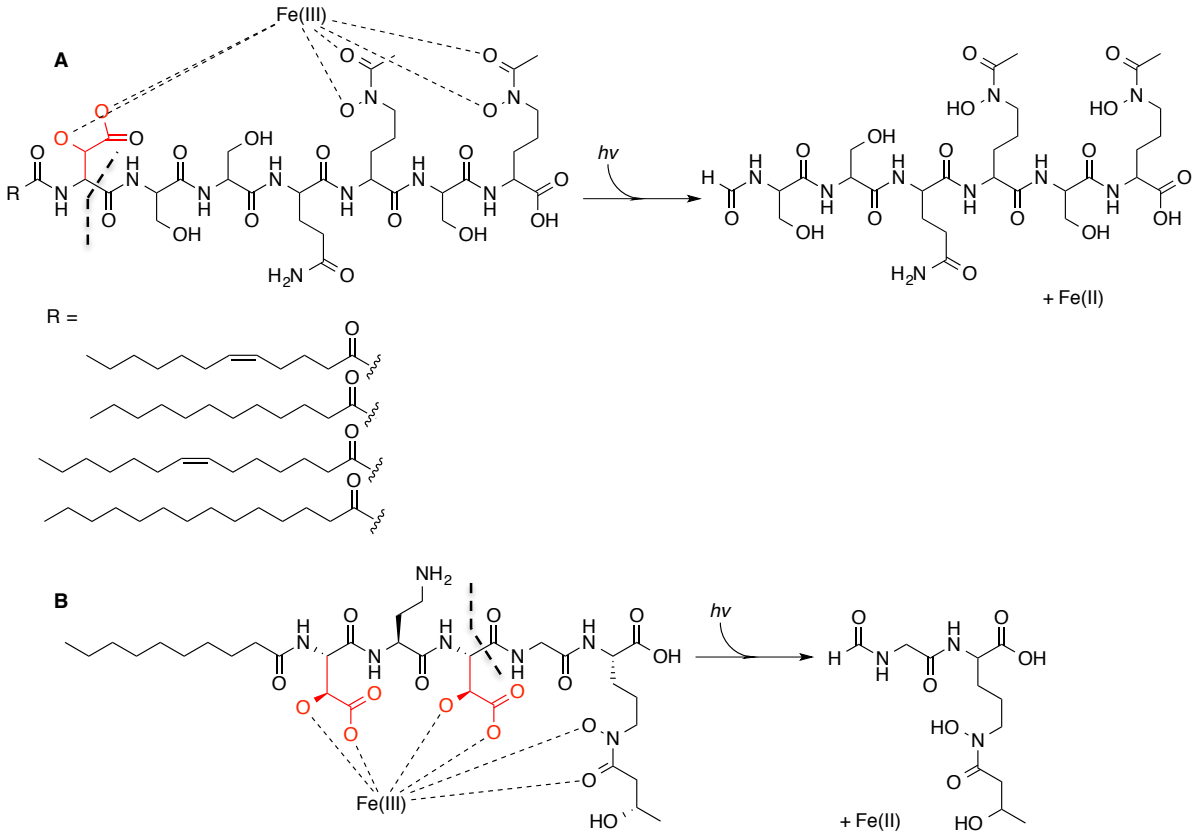

Figure 1.15. Photolysis of Fe(III)-bound siderophores (A) Cupriachelin has two β-hydroxyaspartic acid residues, however, only the center β-hydroxyaspartic acid results in peptide cleavage. (B) Photolysis of the aquachelins results in the loss of the fatty acid moiety producing a hydrophilic headgroup, which is still able to chelate Fe(III).

1.12 Conclusions

The wealth of microbial genomic information has clearly facilitated the discovery of new amphiphilic siderophores, not only in marine bacteria, but also in terrestrial microbes. Often fatty acid activation is required to initiate biosynthesis of the acyl-peptidic siderophores, through one of several different mechanisms. Fatty acyl-AMP ligases activate a fatty acid and initiate the biosyntheses of pyoverdine (**Figure 1.12**), marinobactins, taiwachelins and serobactins (Figure 1.13C-E). External ligases that reside outside the biosynthetic gene clusters for cupriachelins (Figure 1.13A), amphibactins (Figure 1.13B) and amphi-

enterobactins (Figure 1.10) are thought to initiate siderophore biosynthesis though initial fatty acid activation. The biosynthesis of the mycobactins is unique among the acyl siderophores described here in that acylation does not initiate biosynthesis of the siderophore, but rather is incorporated during peptide chain elongation through recognition of the L-N^6-OH-N^6-acyl-Lys unit by the A domain of MbtE (Figure 1.11).

These acyl peptidic siderophores may be further modified enzymatically through fatty acid hydrolysis to produce a more hydrophilic compound, which retains its ferric chelating abilities as occurs with the marinobactins (Figure 1.14) and pyoverdines (**Figure 1.12**). Acyl siderophore hydrophobicity can also be altered photochemically in the Fe(III) complexes of β-hydroxyaspartic acid-containing siderophores of the aquachelins and cupriachelin (**Figure 1.15**) through oxidative loss of the N-terminal β-hydroxyaspartic acid, as well as N-appended fatty acid. The ferric complexes of the taiwachelins, serobactins, and marinobactins are also photoreactive.

Clearly the amphiphilic nature of acylated siderophores is advantageous in the case of the mycobactins where amphiphilicity provides the siderophore with the ability to diffuse freely between membranes and media allowing the siderophore to acquire iron from macrophages. In the case of the acyl pyoverdine precursor, the fatty acid is proposed to anchor the growing chain in a membrane during biosynthesis, to prevent its diffusion. Fatty acid hydrolysis of the marinobactins during late log phase of growth by an Ntn-hydrolase, which also hydrolyzes acyl-homoserine lactones may provide a signaling function. Yet for the majority of the other siderophores described herein the biological function of siderophore acylation remains to be revealed.

Bioinformatics is clearly useful in identifying biosynthetic gene clusters for acyl peptidic siderophores, yet many question remain surrounding what controls the nature of the suite of acylated peptides. While the amphibactins are produced as a very large suite with fatty acid variation from C12 to C18 and with saturated, hydroxylated or desaturated fatty acids, other acyl peptidic siderophores such as cupriachelin or the serobactins are produced as a single acylated siderophore or as a small suite with only a couple of members. We look to future investigations to uncover the factors and the mechanisms governing the range of fatty acid incorporation into acyl peptidic siderophores.

1.13 References

1. Sandy, M.; Butler, A., Microbial Iron Acquisition: Marine and Terrestrial Siderophores. *Chemical Reviews* **2009,** *109* (10), 4580-4595.

2. Miethke, M.; Marahiel, M., Siderophore-based iron acquisition and pathogen control. *Microbiology and Molecular Biology Reviews* **2007,** *71* (3), 413-+.

3. Raymond, K.; Dertz, E.; Kim, S., Enterobactin: An archetype for microbial iron transport. *Proceedings of the National Academy of Sciences of the United States of America* **2003,** *100* (7), 3584-3588.

4. Martin, J.; Gordon, R., Northeast pacific iron distributions in relation to phytoplankton productivity. *Deep-Sea Research Part a-Oceanographic Research Papers* **1988,** *35* (2), 177-196.

5. Pollack, J.; Neilands, J., Enterobactin, an iron transport compound from *Salmonella typhimurium*. *Biochemical and Biophysical Research Communications* **1970,** *38* (5), 989-992.

6. Abergel, R.; Zawadzka, A.; Hoette, T.; Raymond, K., Enzymatic Hydrolysis of Trilactone Siderophores: Where Chiral Recognition Occurs in Enterobactin and Bacillibactin Iron Transport. *Journal of the American Chemical Society* **2009,** *131* (35), 12682-12692.

7. Loomis, L.; Raymond, K., Solution Equilibria of Enterobactin an Metal-Enterobactin Complexes. *Inorganic Chemistry* **1991,** *30* (5), 906-911.

8. May, J.; Wendrich, T.; Marahiel, M., The dhb operon of Bacillus subtilis encodes the biosynthetic template for the catecholic siderophore 2,3-dihydroxybenzoate-glycine-threonine trimeric ester bacillibactin. *Journal of Biological Chemistry* **2001,** *276* (10), 7209-7217.

9. Dertz, E.; Xu, J.; Stintzi, A.; Raymond, K., Bacillibactin-mediated iron transport in Bacillus subtilis. *Journal of the American Chemical Society* **2006,** *128* (1), 22-23.

10. Bister, B.; Bischoff, D.; Nicholson, G.; Valdebenito, M.; Schneider, K.; Winkelmann, G.; Hantke, K.; Sussmuth, R., The structure of salmochelins: C-glucosylated enterobactins of Salmonella enterica. *Biometals* **2004,** *17* (4), 471-481.

11. Fischbach, M.; Lin, H.; Liu, D.; Walsh, C., How pathogenic bacteria evade mammalian sabotage in the battle for iron. *Nature Chemical Biology* **2006,** *2* (3), 132-138.

12. Sandy, M.; Butler, A., Chrysobactin Siderophores Produced by Dickeya chrysanthemi EC16. *Journal of Natural Products* **2011,** *74* (5), 1207-1212.

13. Han, A.; Sandy, M.; Fishman, B.; Trindade-Silva, A.; Soares, C.; Distel, D.; Butler, A.; Haygood, M., Turnerbactin, a Novel Triscatecholate Siderophore from the Shipworm Endosymbiont Teredinibacter turnerae T7901. *Plos One* **2013,** *8* (10).

14. Matsuo, Y.; Kanoh, K.; Jang, J.; Adachi, K.; Matsuda, S.; Miki, O.; Kato, T.; Shizuri, Y., Streptobactin, a Tricatechol-Type Siderophore from Marine-Derived Streptomyces sp YM5-799. *Journal of Natural Products* **2011,** *74* (11), 2371-2376.

15. Dhungana, S.; White, P.; Crumbliss, A., Crystal structure of ferrioxamine B: a comparative analysis and implications for molecular recognition. *Journal of Biological Inorganic Chemistry* **2001,** *6* (8), 810-818.

16. Hossain, M.; Van Der Helm, D.; Poling, M., The Structure of Deferriferrioxamine E (Nocardamin), a Cyclic Trihydroxamate. *Acta Crystallographica Section B-Structural Science* **1983,** *39* (APR), 258-263.

17. Kodani, S.; Bicz, J.; Song, L.; Deeth, R.; Ohnishi-Kameyama, M.; Yoshida, M.; Ochi, K.; Challis, G., Structure and biosynthesis of scabichelin, a novel tris-hydroxamate siderophore produced by the plant pathogen Streptomyces scabies 87.22. *Organic & Biomolecular Chemistry* **2013,** *11* (28), 4686-4694.

18. Barbeau, K.; Zhang, G.; Live, D.; Butler, A., Petrobactin, a photoreactive siderophore produced by the oil-degrading marine bacterium Marinobacter hydrocarbonoclasticus. *Journal of the American Chemical Society* **2002,** *124* (3), 378-379.

19. Haygood, M.; Holt, P.; Butler, A., Aerobactin Production by a Planktonic Marine *Vibrio* sp. *Limnology and Oceanography* **1993,** *38* (5), 1091-1097.

20. Munzinger, M.; Budzikiewicz, H.; Expert, D.; Enard, C.; Meyer, J., Achromobactin, a new citrate siderophore of Erwinia chrysanthemi. *Zeitschrift Fur Naturforschung C-a Journal of Biosciences* **2000,** *55* (5-6), 328-332.

21. Imbert, M.; Bechet, M.; Blondeau, R., Comparison of the main siderophores produced by some species of *Streptomyces*. *Current Microbiology* **1995,** *31* (2), 129-133.

22. Kupper, F.; Carrano, C.; Kuhn, J.; Butler, A., Photoreactivity of iron(III) - Aerobactin: Photoproduct structure and iron(III) coordination. *Inorganic Chemistry* **2006,** *45* (15), 6028-6033.

23. Butler, A.; Theisen, R., Iron(III)-siderophore coordination chemistry: Reactivity of marine siderophores. *Coordination Chemistry Reviews* **2010,** *254* (3-4), 288-296.

24. Hantke, K., Regulation of Ferric Iron Transport in *Escherichia coli* K12: Isolation of a Constitutive Mutant. *Molecular & General Genetics* **1981,** *182* (2), 288-292.

25. Bagg, A.; Neilands, J., Mapping of a mutation affecting regulation of iron uptake systems in *Escherichia coli* K-12 *Journal of Bacteriology* **1985,** *161* (1), 450-453.

26. Braun, V.; Hantke, K.; Koster, W., Bacterial iron transport: Mechanisms, genetics, and regulation. *Metal Ions in Biological Systems, Vol 35* **1998,** *35*, 67-145.

27. Bagg, A.; Neilands, J., Ferric uptake regulation protein acts as a repressor, employing iron(II) as a cofactor to bind the operator of an iron transport operon in *Escherichia coli*. *Biochemistry* **1987,** *26* (17), 5471-5477.

28. Escolar, L.; Perez-Martin, J.; De Lorenzo, V., Opening the iron box: Transcriptional metalloregulation by the fur protein. *Journal of Bacteriology* **1999,** *181* (20), 6223-6229.

29. Hantke, K., Iron and metal regulation in bacteria. *Current Opinion in Microbiology* **2001,** *4* (2), 172-177.

30. Martinez, J.; Zhang, G.; Holt, P.; Jung, H.; Carrano, C.; Haygood, M.; Butler, A., Self-assembling amphiphilic siderophores from marine bacteria. *Science* **2000,** *287* (5456), 1245-1247.

31. Vraspir, J.; Holt, P.; Butler, A., Identification of new members within suites of amphiphilic marine siderophores. *Biometals* **2011,** *24* (1), 85-92.

32. Kem, M.; Zane, H.; Springer, S.; Gauglitz, J.; Butler, A., Amphiphilic siderophore production by oil-associating microbes. *Metallomics* **2014,** *6* (6), 1150-1155.

33. Homann, V.; Sandy, M.; Tincu, J.; Templeton, A.; Tebo, B.; Butler, A., Loihichelins A-F, a Suite of Amphiphilic Siderophores Produced by the Marine Bacterium Halomonas LOB-5. *Journal of Natural Products* **2009,** *72* (5), 884-888.

34. Martinez, J.; Butler, A., Marine amphiphilic siderophores: Marinobactin structure, uptake, and microbial partitioning. *Journal of Inorganic Biochemistry* **2007,** *101* (11-12), 1692-1698.

35. Zane, H.; Naka, H.; Rosconi, F.; Sandy, M.; Haygood, M.; Butler, A., Biosynthesis of Amphi-enterobactin Siderophores by Vibrio harveyi BAA-1116: Identifi*cation of a Bi*functional Nonribosomal Peptide Synthetase Condensation Domain. *Journal of the American Chemical Society* **2014,** *136* (15), 5615-5618.

36. Luo, M.; Lin, H.; Fischbach, M.; Liu, D.; Walsh, C.; Groves, J., Enzymatic tailoring of enterobactin alters membrane partitioning and iron acquisition. *Acs Chemical Biology* **2006,** *1* (1), 29-32.

37. Ratledge, C., Iron, mycobacteria and tuberculosis. *Tuberculosis* **2004,** *84* (1-2), 110-130.

38. Snow, G., Isolation and structure of mycobactin T, a growth factor from *Mycobacterium tuberculosis*. *Biochemical Journal* **1965,** *97* (1), 166-175.

39. Lane, S.; Marshall, P.; Upton, R.; Ratledge, C.; Ewing, M., Novel Extracellular Mycobactins, The Carboxymycobactins from *Mycobacterium avium*. *Tetrahedron Letters* **1995,** *36* (23), 4129-4132.

40. Gobin, J.; Moore, C.; Reeve, J.; Wong, D.; Gibson, B.; Horwitz, M., Iron acquisition by *Mycobacterium tuberculosis*: Isolation and characterization of a family of iron-binding exochelins. *Proceedings of the National Academy of Sciences of the United States of America* **1995,** *92* (11), 5189-5193.

41. Gobin, J.; Horwitz, M., Exochelins of Mycobacterium tuberculosis remove iron from human iron-binding proteins and donate iron to mycobactins in the M-tuberculosis cell wall. *Journal of Experimental Medicine* **1996,** *183* (4), 1527-1532.

42. Kreutzer, M.; Kage, H.; Nett, M., Structure and Biosynthetic Assembly of Cupriachelin, a Photoreactive Siderophore from the Bioplastic Producer Cupriavidus necator H16. *Journal of the American Chemical Society* **2012,** *134* (11), 5415-5422.

43. Kreutzer, M.; Nett, M., Genomics-driven discovery of taiwachelin, a lipopeptide siderophore from Cupriavidus taiwanensis. *Organic & Biomolecular Chemistry* **2012,** *10* (47), 9338-9343.

44. Rosconi, F.; Davyt, D.; Martinez, V.; Martinez, M.; Abin-Carriquiry, J.; Zane, H.; Butler, A.; de Souza, E.; Fabiano, E., Identification and structural characterization of serobactins, a suite of lipopeptide siderophores produced by the grass endophyte *Herbaspirillum seropedicae*. *Environmental Microbiology* **2013,** *15* (3), 916-927.

45. Xu, G.; Martinez, J.; Groves, J.; Butler, A., Membrane affinity of the amphiphilic marinobactin siderophores. *Journal of the American Chemical Society* **2002,** *124* (45), 13408-13415.

46. Owen, T.; Pynn, R.; Martinez, J.; Butler, A., Micelle-to-vesicle transition of an iron-chelating microbial surfactant, marinobactin E. *Langmuir* **2005,** *21* (26), 12109-12114.

47. De Voss, J.; Rutter, K.; Schroeder, B.; Su, H.; Zhu, Y.; Barry, C., The salicylate-derived mycobactin siderophores of Mycobacterium tuberculosis are essential for growth in macrophages. *Proceedings of the National Academy of Sciences of the United States of America* **2000,** *97* (3), 1252-1257.

48. Luo, M.; Fadeev, E.; Groves, J., Mycobactin-mediated iron acquisition within macrophages. *Nature Chemical Biology* **2005,** *1* (3), 149-153.

49. Stachelhaus, T.; Mootz, H.; Marahiel, M., The specificity-conferring code of adenylation domains in nonribosomal peptide synthetases. *Chemistry & Biology* **1999,** *6* (8), 493-505.

50. Marahiel, M.; Stachelhaus, T.; Mootz, H., Modular peptide synthetases involved in nonribosomal peptide synthesis. *Chemical Reviews* **1997,** *97* (7), 2651-2673.

51. Grunewald, J.; Marahiel, M., Chemoenzymatic and template-directed synthesis of bioactive macrocyclic peptides. *Microbiology and Molecular Biology Reviews* **2006,** *70* (1), 121-146.

52. Challis, G.; Ravel, J.; Townsend, C., Predictive, structure-based model of amino acid recognition by nonribosomal peptide synthetase adenylation domains. *Chemistry & Biology* **2000,** *7* (3), 211-224.

53. Shen, B., Polyketide biosynthesis beyond the type I, II and III polyketide synthase paradigms. *Current Opinion in Chemical Biology* **2003,** *7* (2), 285-295.

54. Staunton, J.; Weissman, K., Polyketide biosynthesis: a millennium review. *Natural Product Reports* **2001,** *18* (4), 380-416.

55. Gehring, A.; Mori, I.; Walsh, C., Reconstitution and characterization of the Escherichia coli enterobactin synthetase from EntB, EntE, and EntF. *Biochemistry* **1998,** *37* (8), 2648-2659.

56. Quadri, L.; Sello, J.; Keating, T.; Weinreb, P.; Walsh, C., Identification of a Mycobacterium tuberculosis gene cluster encoding the biosynthetic enzymes for assembly of the virulence-conferring siderophore mycobactin. *Chemistry & Biology* **1998,** *5* (11), 631-645.

57. McMahon, M.; Rush, J.; Thomas, M., Analyses of MbtB, MbtE, and MbtF Suggest Revisions to the Mycobactin Biosynthesis Pathway in Mycobacterium tuberculosis. *Journal of Bacteriology* **2012,** *194* (11), 2809-2818.

58. Krithika, R.; Marathe, U.; Saxena, P.; Ansari, M.; Mohanty, D.; Gokhale, R., A genetic locus required for iron acquisition in Mycobacterium tuberculosis. *Proceedings of the National Academy of Sciences of the United States of America* **2006,** *103* (7), 2069-2074.

59. Vergnolle, O.; Xu, H.; Blanchard, J., Mechanism and Regulation of Mycobactin Fatty Acyl-AMP Ligase FadD33. *Journal of Biological Chemistry* **2013,** *288* (39), 28116-28125.

60. Schalk, I.; Guillon, L., Pyoverdine biosynthesis and secretion in *Pseudomonas aeruginosa*: implications for metal homeostasis. *Environmental Microbiology* **2013,** *15* (6), 1661-1673.

61. Visca, P.; Imperi, F.; Lamont, I., Pyoverdine siderophores: from biogenesis to biosignificance. *Trends in Microbiology* **2007,** *15* (1), 22-30.

62. Ravel, J.; Cornelis, P., Genomics of pyoverdine-mediated iron uptake in pseudomonads. *Trends in Microbiology* **2003,** *11* (5), 195-200.

63. Mossialos, D.; Ochsner, U.; Baysse, C.; Chablain, P.; Pirnay, J.; Koedam, N.; Budzikiewicz, H.; Fernandez, D.; Schafer, M.; Ravel, J.; Cornelis, P., Identification of new, conserved, non-ribosomal peptide synthetases from fluorescent pseudomonads involved in the biosynthesis of the siderophore pyoverdine. *Molecular Microbiology* **2002,** *45* (6), 1673-1685.

64. Hannauer, M.; Schafer, M.; Hoegy, F.; Gizzi, P.; Wehrung, P.; Mislin, G.; Budzikiewicz, H.; Schalk, I., Biosynthesis of the pyoverdine siderophore of Pseudomonas aeruginosa involves precursors with a myristic or a myristoleic acid chain. *Febs Letters* **2012,** *586* (1), 96-101.

65. Drake, E.; Gulick, A., Structural Characterization and High-Throughput Screening of Inhibitors of PvdQ, an NTN Hydrolase Involved in Pyoverdine Synthesis. *Acs Chemical Biology* **2011,** *6* (11), 1277-1286.

66. Yeterian, E.; Martin, L.; Guillon, L.; Journet, L.; Lamont, I.; Schalk, I., Synthesis of the siderophore pyoverdine in Pseudomonas aeruginosa involves a periplasmic maturation. *Amino Acids* **2010,** *38* (5), 1447-1459.

67. Kraas, F.; Helmetag, V.; Wittmann, M.; Strieker, M.; Marahiel, M., Functional Dissection of Surfactin Synthetase Initiation Module Reveals Insights into the Mechanism of Lipoinitiation. *Chemistry & Biology* **2010,** *17* (8), 872-880.

68. Jimenez, P.; Koch, G.; Papaioannou, E.; Wahjudi, M.; Krzeslak, J.; Coenye, T.; Cool, R.; Quax, W., Role of PvdQ in Pseudomonas aeruginosa virulence under iron-limiting conditions. *Microbiology-Sgm* **2010,** *156*, 49-59.

69. Wurst, J.; Drake, E.; Theriault, J.; Jewett, I.; VerPlank, L.; Perez, J.; Dandapani, S.; Palmer, M.; Moskowitz, S.; Schreiber, S.; Munoz, B.; Gulick, A., Identification of Inhibitors of PvdQ, an Enzyme Involved in the Synthesis of the Siderophore Pyoverdine. *Acs Chemical Biology* **2014,** *9* (7), 1536-1544.

70. Koch, G.; Nadal-Jimenez, P.; Reis, C.; Muntendam, R.; Bokhove, M.; Melillo, E.; Dijkstra, B.; Cool, R.; Quax, W., Reducing virulence of the human pathogen Burkholderia by altering the substrate specificity of the quorum-quenching acylase PvdQ. *Proceedings of the National Academy of Sciences of the United States of America* **2014,** *111* (4), 1568-1573.

71. Clevenger, K.; Wu, R.; Er, J.; Liu, D.; Fast, W., Rational Design of a Transition State Analogue with Picomolar Affinity for *Pseudomonas aeruginosa* PvdQ, a Siderophore Biosynthetic Enzyme. *Acs Chemical Biology* **2013,** *8* (10), 2192-2200.

72. Bokhove, M.; Jimenez, P.; Quax, W.; Dijkstra, B., The quorum-quenching N-acyl homoserine lactone acylase PvdQ is an Ntn-hydrolase with an unusual substrate-binding pocket. *Proceedings of the National Academy of Sciences of the United States of America* **2010,** *107* (2), 686-691.

73. Sio, C.; Otten, L.; Cool, R.; Diggle, S.; Braun, P.; Bos, R.; Daykin, M.; Camara, M.; Williams, P.; Quax, W., Quorum quenching by an N-acyl-homoserine lactone acylase from Pseudomonas aeruginosa PAO1. *Infection and Immunity* **2006,** *74* (3), 1673-1682.

74. Wahjudi, M.; Papaioannou, E.; Hendrawati, O.; van Assen, A.; van Merkerk, R.; Cool, R.; Poelarends, G.; Ouax, W., PA0305 of Pseudomonas aeruginosa is a quorum quenching acylhomoserine lactone acylase belonging to the Ntn hydrolase superfamily. *Microbiology-Sgm* **2011,** *157*, 2042-2055.

75. Huang, J.; Han, J.; Zhang, L.; Leadbetter, J., Utilization of acyl-homoserine lactone quorum signals for growth by a soil pseudomonad and Pseudomonas aeruginosa PAO1. *Applied and Environmental Microbiology* **2003,** *69* (10), 5941-5949.

76. Koch, G.; Jimenez, P.; Muntendam, R.; Chen, Y.; Papaioannou, E.; Heeb, S.; Camara, M.; Williams, P.; Cool, R.; Quax, W., The acylase PvdQ has a conserved function among fluorescent Pseudomonas spp. *Environmental Microbiology Reports* **2010,** *2* (3), 433-439.

77. Guillon, L.; El Mecherki, M.; Altenburger, S.; Graumann, P.; Schalk, I., High cellular organization of pyoverdine biosynthesis in Pseudomonas aeruginosa: clustering of PvdA at the old cell pole. *Environmental Microbiology* **2012,** *14* (8), 1982-1994.

78. Gauglitz, J.; Inishi, A.; Ito, Y.; Butler, A., Microbial Tailoring of Acyl Peptidic Siderophores. *Biochemistry* **2014,** *53* (16), 2624-2631.

79. Lin, Y.; Xu, J.; Hu, J.; Wang, L.; Ong, S.; Leadbetter, J.; Zhang, L., Acyl-homoserine lactone acylase from Ralstonia strain XJ12B represents a novel and potent class of quorum-quenching enzymes. *Molecular Microbiology* **2003,** *47* (3), 849-860.

80. Barbeau, K.; Rue, E.; Bruland, K.; Butler, A., Photochemical cycling of iron in the surface ocean mediated by microbial iron(III)-binding ligands. *Nature* **2001,** *413* (6854), 409-413.

81. Martin, J.; Ito, Y.; Homann, V.; Haygood, M.; Butler, A., Structure and membrane affinity of new amphiphilic siderophores produced by Ochrobactrum sp SP18. *Journal of Biological Inorganic Chemistry* **2006,** *11* (5), 633-641; Ito, Y.; Butler, A., Structure of synechobactins, new siderophores of the marine cyanobacterium Synechococcus sp PCC 7002. *Limnology and Oceanography* **2005,** *50* (6), 1918-1923.

82. Barbeau, K.; Rue, E.; Trick, C.; Bruland, K.; Butler, A., Photochemical reactivity of siderophores produced by marine heterotrophic bacteria and cyanobacteria based on characteristic Fe(III) binding groups. *Limnology and Oceanography* **2003,** *48* (3), 1069-1078.

II. Siderophore production by the oil-associating microbe *Alcanivorax borkumensis* SK2

Parts or sections of this chapter were taken with permission from: Kem, M.P.; Zane, H.K.; Springer, S.D.; Gauglitz, J.M.; Butler, A. Amphiphilic siderophore production by oil-associating microbes. *Metallomics.* **2014**, *6*, 1150-1155.

Reproduced by permission of the Royal Society of Chemistry.

(http:// http://pubs.rsc.org/en/content/articlehtml/2014/mt/c4mt00047a)

2.1 Introduction

The primary fate of oil in the ocean is degradation by oil-associating marine microbes.[1] The bacterium, *Alcanivorax borkumensis*, is the most common of these oil-associating marine microbes and accounts for 80-90% of the bacterial community in oil-polluted waters.[2,3] Bioremediation of oil-contaminated waters, however, is greatly limited by the availability of necessary nutrients, including iron, which is highly restricted in surface ocean waters due to the insolubility of iron under aerobic conditions. The dependence of efficient hydrocarbon degradation on iron could be related to the iron-containing oxygenases required for initial hydrocarbon breakdown, such as, the alkane monooxygenase, AlkB2, and cytochrome P450 (CYP).[4] AlkB2 is a non-heme diiron alkane monooxygenase that is required for the first step of hydrocarbon degradation, hydroxylating the terminal position of

the alkane.[5,6] This pathway is found in the vast majority of medium to long chain alkane-oxidizing aerobic bacteria.[4]

Many marine bacteria produce siderophores to solubilize and transport iron; however, the mechanism of iron acquisition by the majority of oil-associating microbes, including *A. borkumensis*, has not been well characterized.[7,8] Marine bacteria commonly produce acylated siderophores, which are produced in a suite and can associate with the bacterial membrane (**Figure 2.1**). Previously, the Butler group has identified and characterized siderophore production from two oil-associated microbes. *Pseudoalteromonas* sp. S2B and *Vibrio* sp. S4BW were isolated from the Gulf of Mexico following the Deepwater Horizon oil spill and produce the lystabactins and ochrobactins-OH siderophores, respectively.[9,10] Here we report the production of the amphibactins by the well-studied hydrocarbon degrading bacterium, *A. borkumensis* SK2. The amphiphilic property of the amphibactins might aid in bacterial iron(III) solubilization in an oil-contaminated environment.

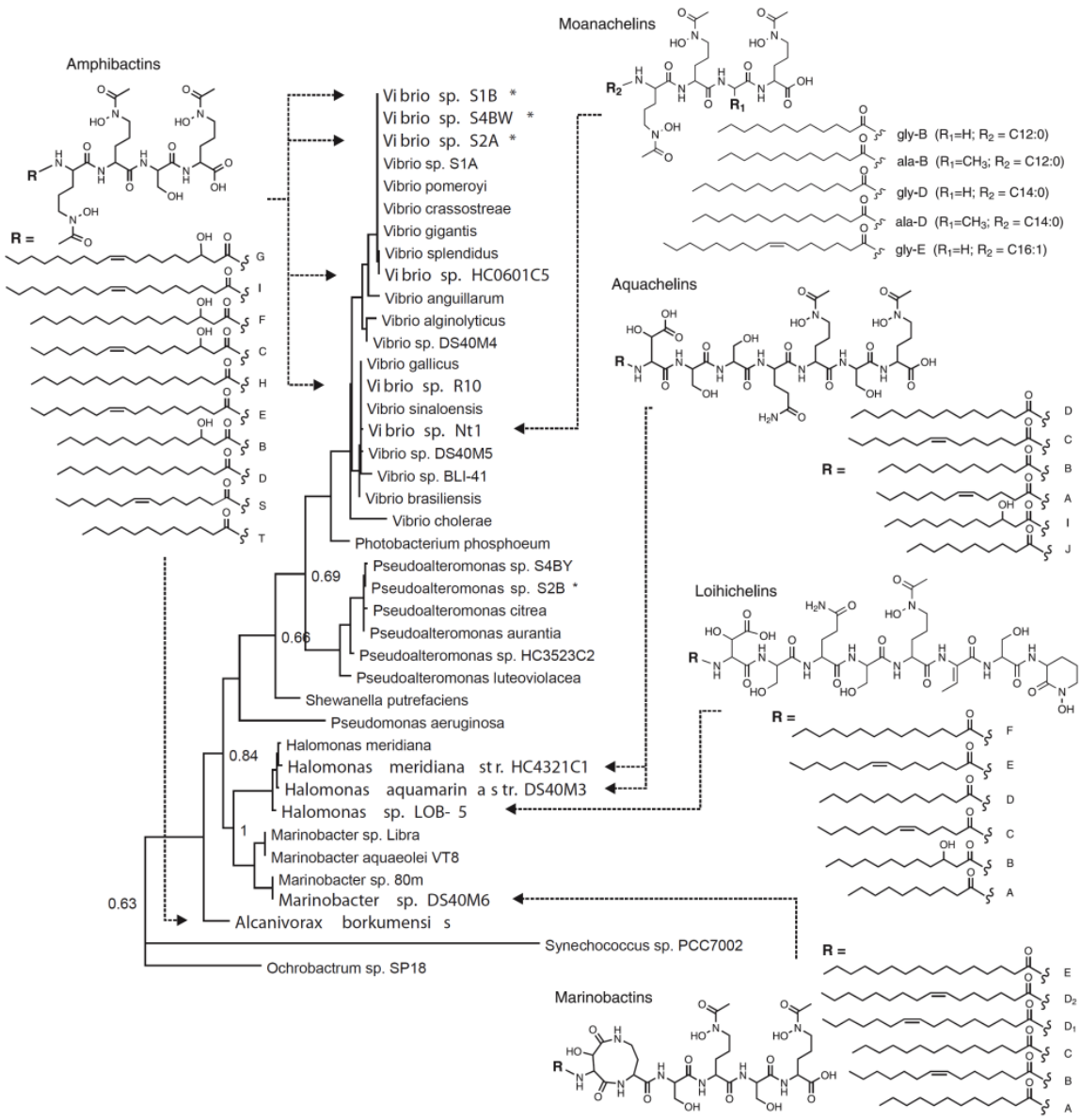

Figure 2.1. Phylogenetic tree of selected siderophore-producing bacteria and related species based on maximum likelihood analysis of SSU rDNA sequences.[11,12,13,14,15,16] Amphiphilic siderophore-producing bacteria are labeled in bold, with their corresponding structures. The asterisked (*) bacteria are oil-associated strains. Sequences of related bacteria and other known siderophore-producing bacteria were obtained from green genes[17] or GenBank.[18] (For moanachelin gly-C (R1 = H; R2 = C14:1) and marinobactin F (C18:1), not shown, the position and E/Z orientation of the double bond has not been determined).[19,20]

2.2 Experimental

2.2.1 Bacteria isolation and cultivation

Alcanivorax borkumensis SK2 was gifted to us from Professor David Valentine in the Department of Earth Sciences at UCSB. *A. borkumensis* SK2 was determined to produce siderophores by observing the appearance of orange halos surrounding bacterial colonies when grown on iron-limited CAS (chromazural S) agar plates.[21]

For bacterial cultivation, *A. borkumensis* SK2 was maintained on solid agar plates of marine broth 2216. Prior to inoculation into liquid cultures, the bacterium was streaked onto three consecutive Butler Plates (0.5 g yeast extract, 5.0 g peptone, 15 g agar in 1L of filtered natural seawater) to deplete the bacteria of iron. For siderophore isolation, a 5 mL aliquot of sterile NSW media (1g NH_4Cl/L, 2 g Casamino acids/L, 0.1g glycerol phosphate/L, 5 g sodium pyruvate/L, and 3 ml glycerol/L) was added to a Butler plate streaked with *A. borkumensis* SK2. The bacterium was resuspended using a sterile loop and all 5 mL were added to 2 L of sterile NSW media. The bacteria was cultured at 180 rpm on a rotary shaker at 30°C for about 3 days.

2.2.2 Siderophore isolation

Siderophores were isolated from cultures displaying a distinct color change from blue to pink following incubation with liquid CAS solution. The cultures were harvested at 6000 RPM for 30 minutes at 4^{O}C using a SLA-3000 rotor. The culture supernatants were decanted and siderophores were extracted from the cell pellet using 50 mL of 90% ethanol per 1 L of bacterial culture. The ethanol-extracted pellets were shaken at 120 RPM for 20-48 hours at

ambient temperature. The pellet extract was then filtered through a 0.22 μm filter and concentrated using a rotary evaporator until the solution just began to crash out. The concentrated extract was diluted 1:2 in water and loaded onto a 1 ml C-18 SepPack cartridge. The flow through was checked for the presence of siderophores using the liquid CAS assay. If siderophores were present, the flow through was diluted 1:2 with nanopoure water and reloaded onto the C-18 SepPack cartridge. This procedure was repeated until the flow through was no longer CAS active. The cartridge was rinsed with five column volumes of 50% methanol in water and siderophores were eluted with ten column volumes of 90% methanol.

The culture supernatant was also checked for siderophore production. The decanted supernatant was combined with 100 mL XAD-2 resin (pre-equilibrated with nanopure water) per liter of supernatant for 2 hours at ambient temperature, 120 rpm. The solution was filtered through a large pore filter to remove unabsorbed compounds and the resin was washed with 1 liter of nanopure water. The washed resin was loaded into a gravity column and eluted with 200 ml each of 20% methanol, 40% methanol, 60% methanol, 80% methanol and 100% methanol. Each fraction was concentrated by rotary evaporation to remove the methanol and the presence of siderophores was checked using the liquid CAS assay.

The foam produced by *A. borkumensis* SK2 was analyzed for the presence of siderophores. The foam, which associates with the glass flask, was separated from the bacterial culture and resuspended in methanol. The resuspended sample was diluted in water and purified using a 1 ml C-18 SepPack cartridge as previously described with the cell pellet extracts.

CAS positive fractions from the cell pellet, supernatant and foam were further purified using RP-HPLC with a Vydac C4 prep column. The compounds were eluted using a linear gradient of 50% methanol in nanopure water + 0.05% trifluoroacetic acid to 90% methanol in nanopure water + 0.05% trifluoroacetic acid over 35 minutes. The samples were detected at 215 nm for apo-peptidic siderophores and 400 nm for the iron-bound siderophores. Peaks obtained from RP-HPLC were collected and identified using ESI-MS and ESI-MS/MS on a Micromass QTOF2 Quadrupole/Time-of-Flight Tandem mass spectrometer using argon as the collision gas.

2.2.3 Analysis of amphibactin biosynthesis genes from *A. borkumensis* SK2

The genome of *A. borkumensis* SK2 is publicly available from the national center for biotechnology information (NCBI, http://www.ncbi.nlm.nih.gov) website. To identify the genes necessary for amphibactin biosynthesis, the genome of *A. borkumensis* SK2 was screened for genes enconding putative non-ribosomal peptide synthetases (NRPS) in close proximity to siderophore uptake and transport proteins. The Basic Local Alignment Tool (BLAST) was used to investigate the homology of unknown NRPS domains to known proteins. The publicly available NRPS/PKS analysis software (http://nrps.igs.umaryland.edu/nrps/) was used to predict the domain organization and amino acid specificity of the putative NRPS proteins.[22]

2.3 Results

2.3.1 Bacterial growth and siderophore detection

The ubiquitous oil-degrading microbe, *A. borkumensis* SK2, was screened for siderophore production. *A. borkumensis* SK2 was streaked onto CAS agar plates to initially determine if the bacterium produced siderophores. After a week of growing on CAS agar plates, orange halos appeared around bacterial colonies indicating that *A. borkumensis* SK2 does produce siderophores.

To isolate siderophores, *A. borkumensis* SK2 was grown in iron-limited NSW media. The bacteria reached stationary phase of growth after 20 hours at ambient temperature (Figure 2.2). When the culture was combined with liquid CAS solution after 26 hours of growth, a color change from blue to pink occurred indicating *A. borkumensis* SK2 was producing siderophores (Figure 2.3). The color change, however, occurred slowly and did not reach a bright pink color implying siderophore production was minimal. To increase siderophore production, cultures were grown for an additional 24 hours prior to harvesting and siderophore isolation.

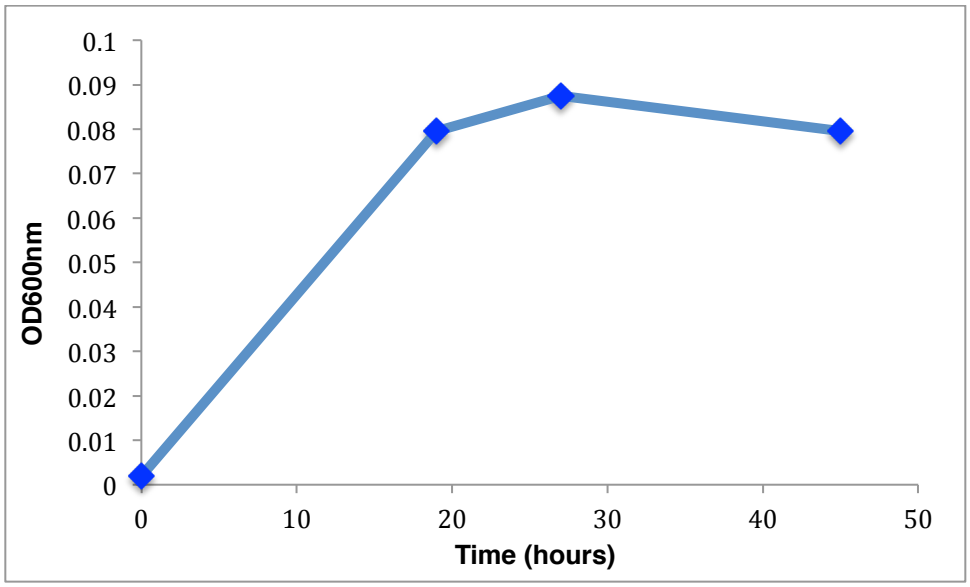

Figure 2.2. Growth curve of *A. borkumensis* SK2 when grown in iron-limited NSW media at ambient temperature.

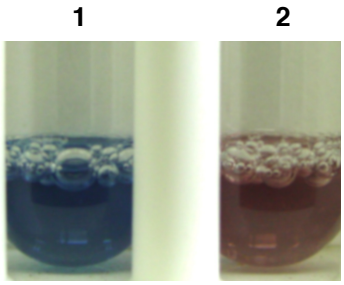

Figure 2.3. Analysis of siderophore production by *A. borkumensis* SK2 using the liquid CAS assay. Sample 1 is the NSW media + CAS control and sample two is the culture and CAS mixed 1:1.

2.3.2 Siderophore isolation

The bacterial pellet, supernatant, and foam from *A. borkumensis* SK2 was screened for siderophore production. Following centrifugation of the bacterial culture, the cell-free supernatant displayed very little CAS activity. Purification and concentration of compounds

released into the cell-free supernatant by adsorption onto XAD-2 resin did not increase the CAS activity. Likewise, RP-HPLC analysis of the cell-free supernatant extracts did not result in the isolation of any compounds with positive CAS activity. It is therefore hypothesized that *A. borkumensis* SK2 does not produce any siderophores that are released into the extracellular milieu, even following centrifugation.

The pellet extracts, however, did produce a strong color change from blue to pink when incubated with the liquid CAS assay, signifying the presence of siderophores. The pellet extracts also displayed low solubility in water suggesting the extracted compounds are hydrophobic in nature. A RP-HPLC trace of the bacterial pellet extract following Sep-Pack purification resulted in the appearance of four major peaks (Figure 2.4). Three out of the four peaks (labeled peaks 1-3) displayed a color change from blue to pink when incubated with the liquid CAS assay and were, therefore, analyzed further by ESI-MS and ESI-MS/MS.

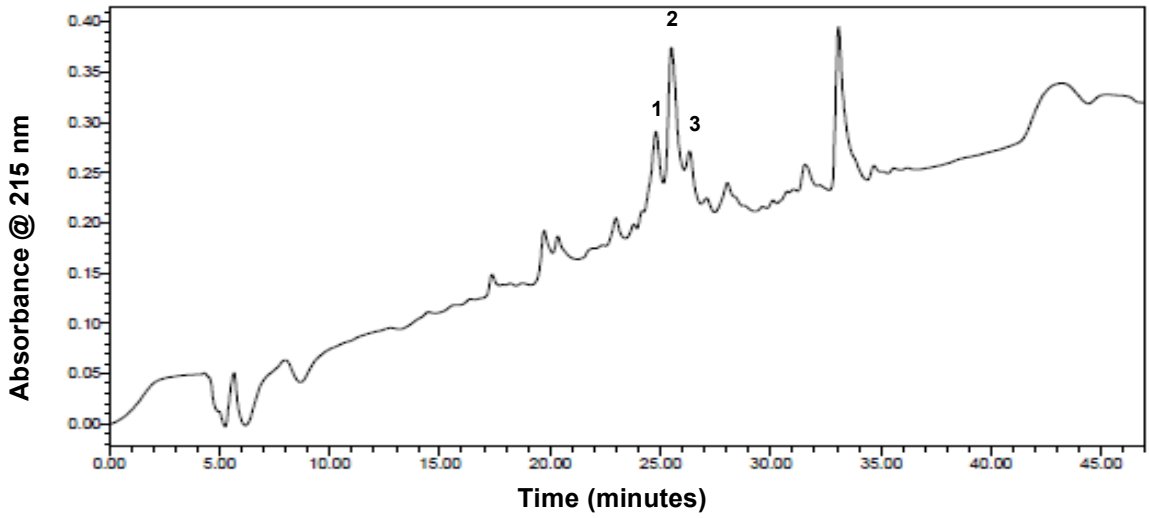

Figure 2.4. RP-HPLC analysis of the *A. borkumensis* SK2 pellet extract. Peaks 1-3 were determined to be CAS active and correspond to amphibactins E, H, and I, respectively.

2.3.3 Siderophore characterization

The identities of the compounds in peaks 1-3 were determined using electrospray ionization mass spectrometry (ESI-MS) and tandem mass spectrometry (ESI-MS/MS). Peptides commonly fragment at their amide bonds generating 'b' (starting at the N-terminus) and 'y' (starting at the C-terminus) ions.[23] This information can be used to determine the amino acids present in the peptide headgroup, as well as, how the amino acids might be connected (**Figure 2.5**B). ESI-MS/MS analysis indicated that all three siderophores have the same "y" ions with *m/z* values of 191, 278, and 450 corresponding to fragmentation of the peptide starting at the C-terminus. Therefore, a loss of 191 corresponds to the C-terminal N^5-acyl-N^5-hydroxyornithine. This is followed by a loss of 87 representing a serine attached to the C-terminal N^5-acyl-N^5-hydroxyornithine. This serine is attached to an internal N^5-acyl-N^5-hydroxyornithine on its N-terminus as seen with the loss of 172. The loss of the N-terminal N^5-acyl-N^5-hydroxyornithine is not readily detected, possibly due to its attachment to the fatty acid appendage. A similar peptide fingerprint pattern has been seen with amphibactins previously isolated from other marine species.[24]

The *m/z* value for the 'b' ions, however, differed between all three compounds, which is indicative of a suite of amphiphilic siderophores comprised of the same peptidic headgroup attached to varying fatty acid appendages.[24,25,19] The difference in the masses of the "b" ions can be used to predict the tail lengths and functionality of the isolated siderophores. The placement of these functionalities (unsaturation, hydroxylation), however, cannot be determined by this method.

Mass spectrometry analysis identified the compound from peak 1 as amphibactin E with a *m/z* of 858 for the $[M+H]^+$ (Figure 2.6). Amphibactin E has a C16 fatty acid with one

degree of unsaturation. The compound in peak 2 had an *m/z* value of 860 corresponding to the $[M+H]^+$ of amphibactin H (Figure 2.7). Like amphibactin E, amphibactin H also has a C16 fatty acid, but with no sites of unsaturation. The compound in peak 3 had an *m/z* of 886 corresponding to the $[M+H]^+$ of amphibactin I with a C18:1 fatty acid (Figure 2.8). Interestingly, only the non-hydroxylated forms of the longer chained amphibactins, previously isolated from other species, were produced by *A. borkumensis* SK2 (**Figure 2.5**A). The amphibactins were also isolated from other oil-associating *Vibrio* sp. isolated from the Gulf of Mexico following the Deepwater Horizon oil spill.[26] Likewise, these oil-associated *Vibrio* sp. only produced longer chain amphibactins (C14-C18) without any hydroxylated fatty acids.

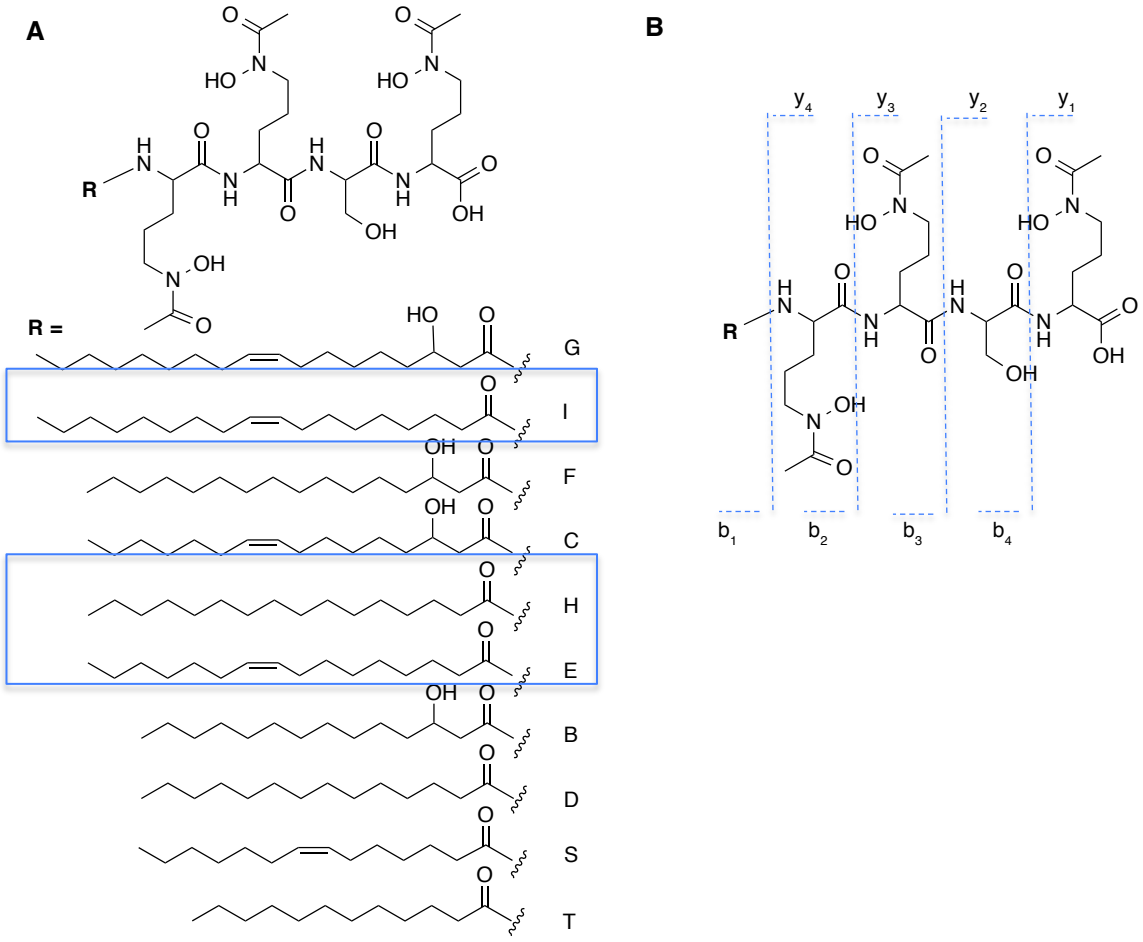

Figure 2.5. (A) Structures of the amphibactins that have been isolated and characterized from different marine species. The fatty acid tails highlighted in blue correspond to the amphibactins isolated from *A. borkumensis* SK2. (B) The major 'b' and 'y' ions expected from fragmentation of the amphibactin peptide backbone using ESI-MS/MS.

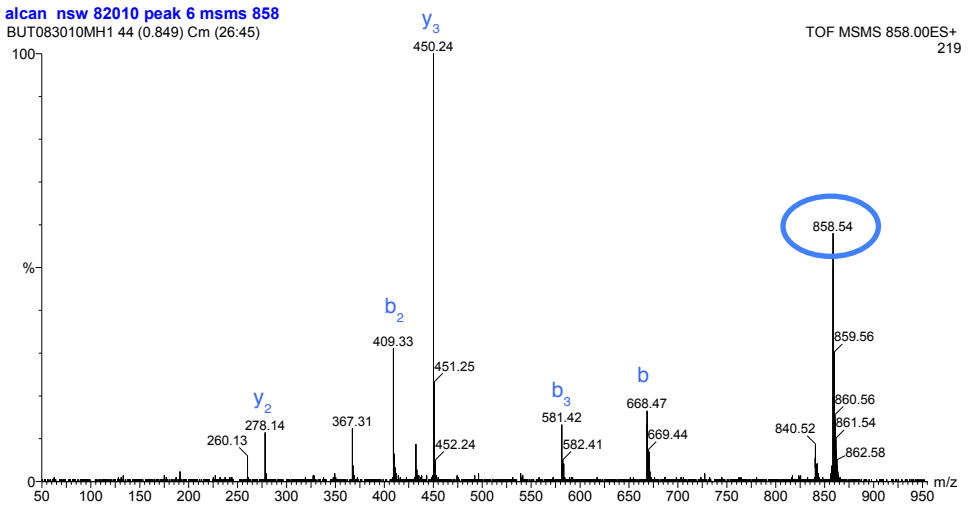

Figure 2.6. ESI-MS/MS analysis of peak 1 from RP-HPLC analysis of the ethanol extracted *A. borkumensis* SK2 pellet corresponding to amphibactin E.

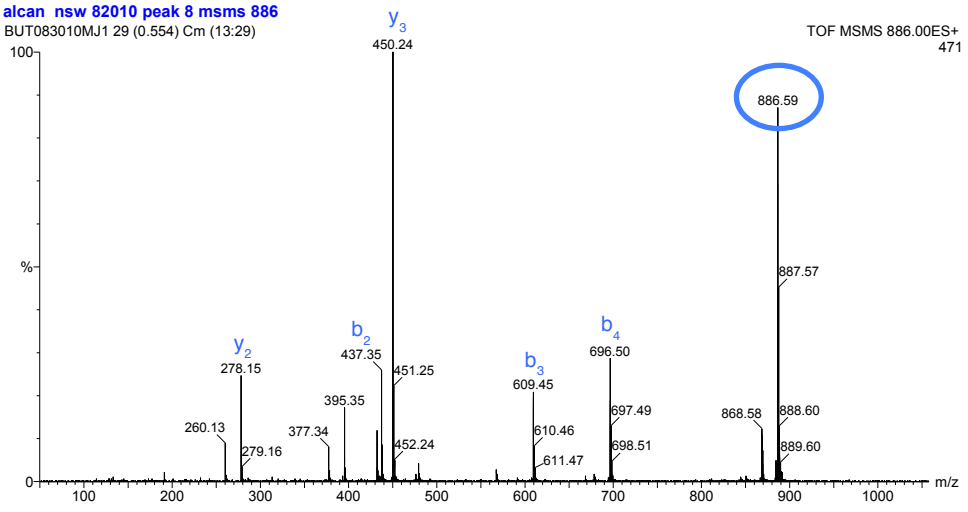

Figure 2.7. ESI-MS/MS analysis of peak 2 from RP-HPLC analysis of the ethanol extracted *A. borkumensis* SK2 pellet corresponding to amphibactin H.

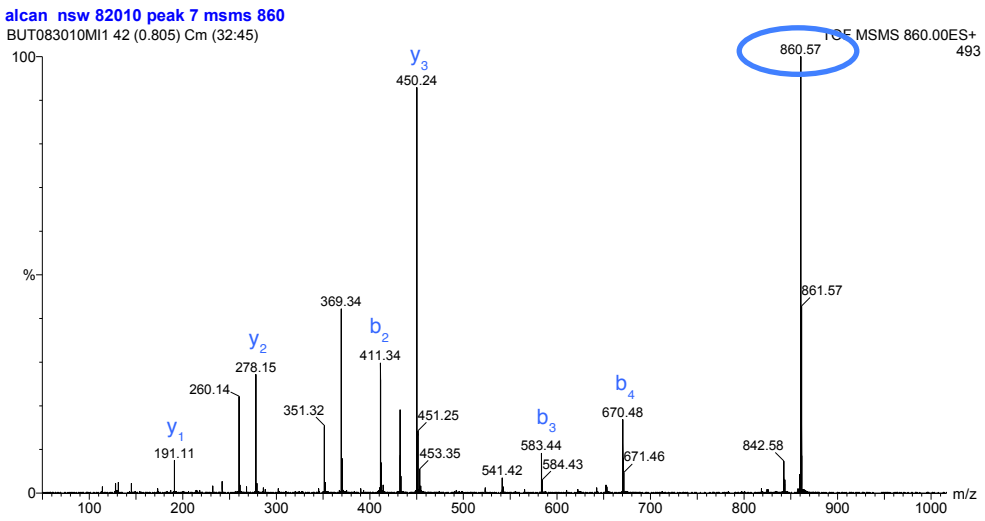

Figure 2.8. ESI-MS/MS analysis of peak 3 from the RP-HPLC analysis of the ethanol extracted *A. borkumensis* SK2 pellet corresponding to amphibactin I.

2.3.4 Siderophores isolated from the culture foam

Cultures of *A. borkumensis* SK2 release high volumes of biosurfactants, resulting in an accumulation of foam above the culture supernatant during growth. It is well-known that *A. borkumensis* SK2 produces biosurfactants to aid in the emulsification of hydrocarbons by decreasing oil droplet size and, therefore, increasing the surface area exposed to water.[27] Since no siderophores were detected in culture supernatants, it's possible that the amphiphilic nature of the amphibactins caused any siderophores released after centrifugation to associate with the foam.

The RP-HPLC analysis of compounds extracted from the foam shows the presence of five small peaks (Figure 2.9). ESI-MS/MS analysis of these peaks show peak 1 to be Fe(III)-amphibactin D (Figure 2.10) with an *m/z* of 885. Amphibactin D has a C14 fatty acid and was not isolated from the bacterial pellet; however, it is possible that only very small

amounts were produced and secreted into the culture supernatant due to the small size of peak 1. The compound in peak 2 was determined to be Fe(III)-amphibactin E with an *m/z* of 911 (Figure 2.11), and the compound in peak 3 was also determined to be Fe(III)-amphibactin E with an *m/z* of 911 (Figure 2.12). Peak 4 and peak 5 were determined to be Fe(III)-amphibactin H (*m/z* 913, Figure 2.13) and apo-amphibactin H (*m/z* 860, Figure 2.14), respectively. Fe(III)-amphibactins do not fragment well by ESI-MS/MS analysis so a peptide fingerprint pattern could not be obtained. Interestingly, the majority of the siderophores isolated from the biosurfactants are iron-bound. It is possible that the release of biosurfactants also aids in solubilizing the amphiphilic amphibactins for iron uptake in an aqueous environment.

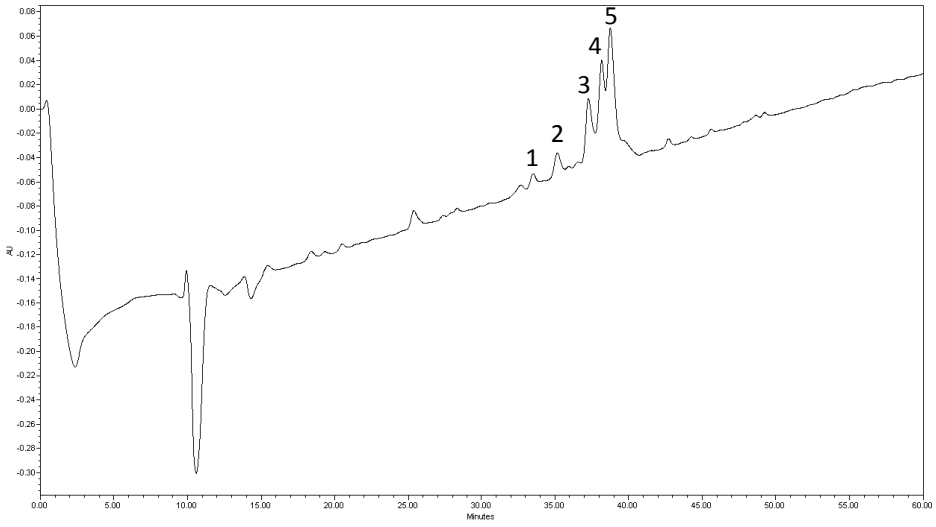

Figure 2.9. RP-HPLC chromatogram of siderophores isolated from the culture foam of *A. borkumensis* SK2 when grown in iron-limited media.

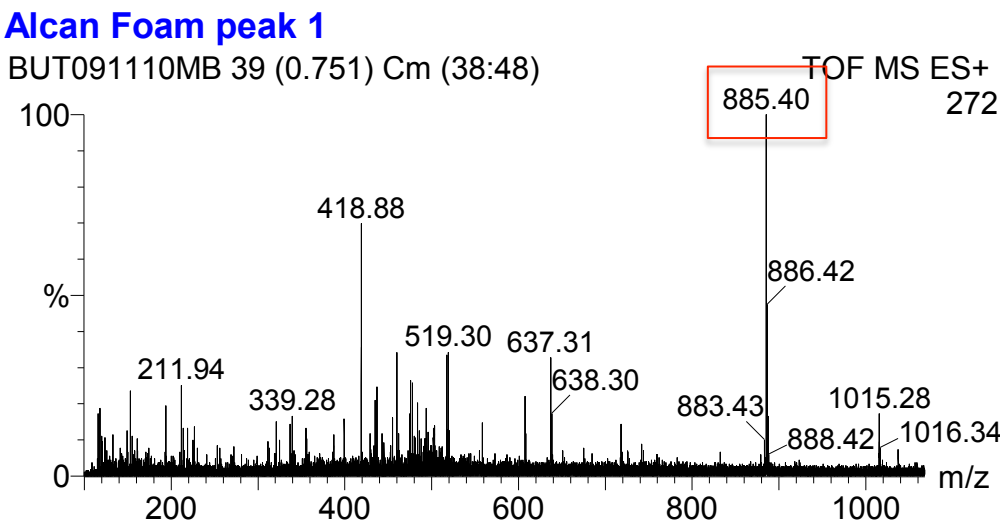

Figure 2.10. ESI-MS analysis of the compound in peak 1 isolated from foam produced by *A. borkumensis* SK2 during growth. The *m/z* of 885 corresponds to Fe(III)-amphibactin D.

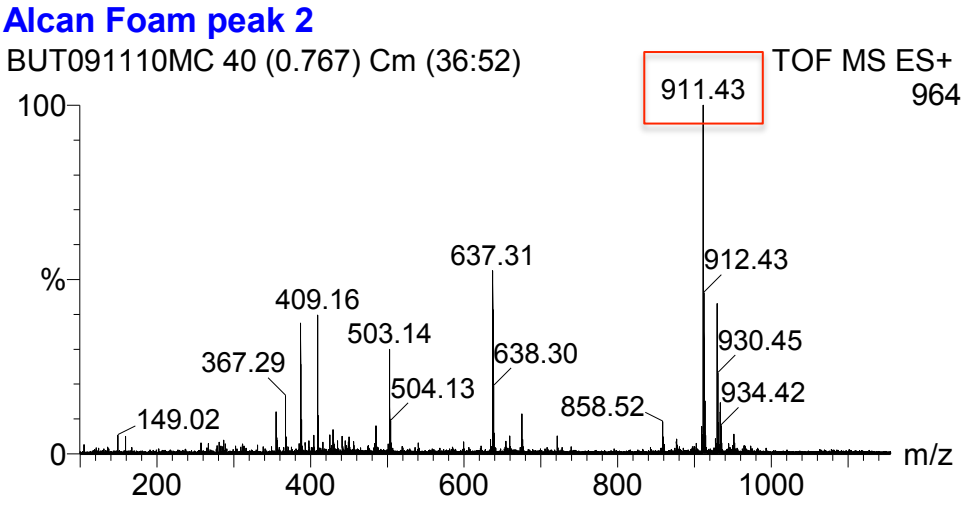

Figure 2.11. ESI-MS analysis of the compound in peak 2 isolated from foam produced by *A. borkumensis* SK2 during growth. The *m/z* of 911 corresponds to Fe(III)-amphibactin E.

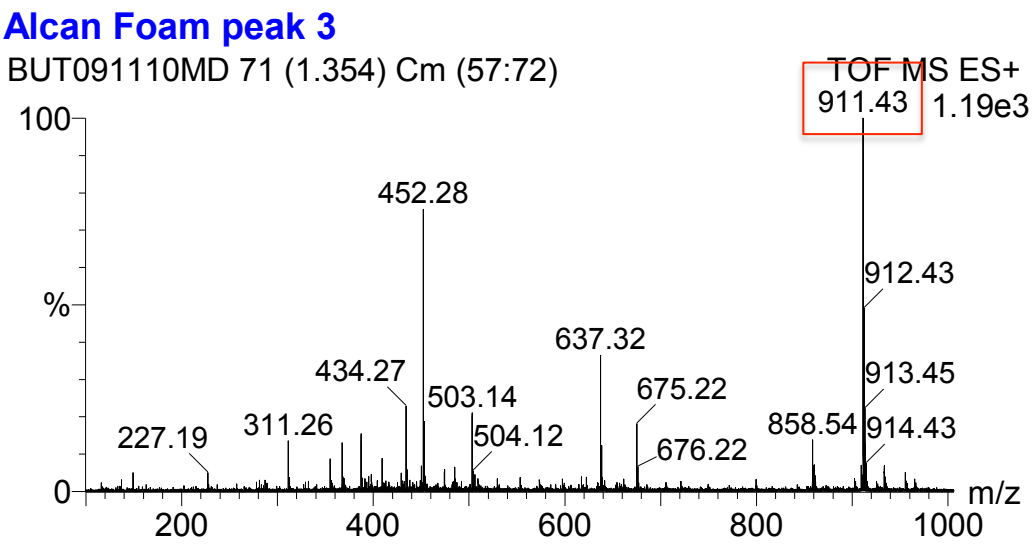

Figure 2.12. ESI-MS analysis of the compound in peak 3 isolated from foam produced by *A. borkumensis* SK2 during growth. The *m/z* of 911 corresponds to Fe(III)-amphibactin E.

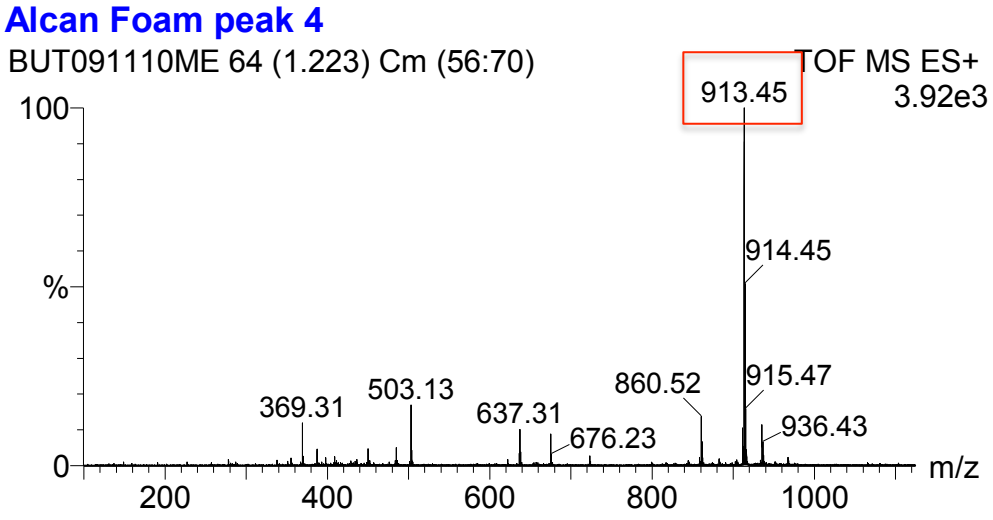

Figure 2.13. ESI-MS analysis of the compound in peak 4 isolated from foam produced by *A. borkumensis* SK2 during growth. The *m/z* of 913 corresponds to Fe(III)-amphibactin H.

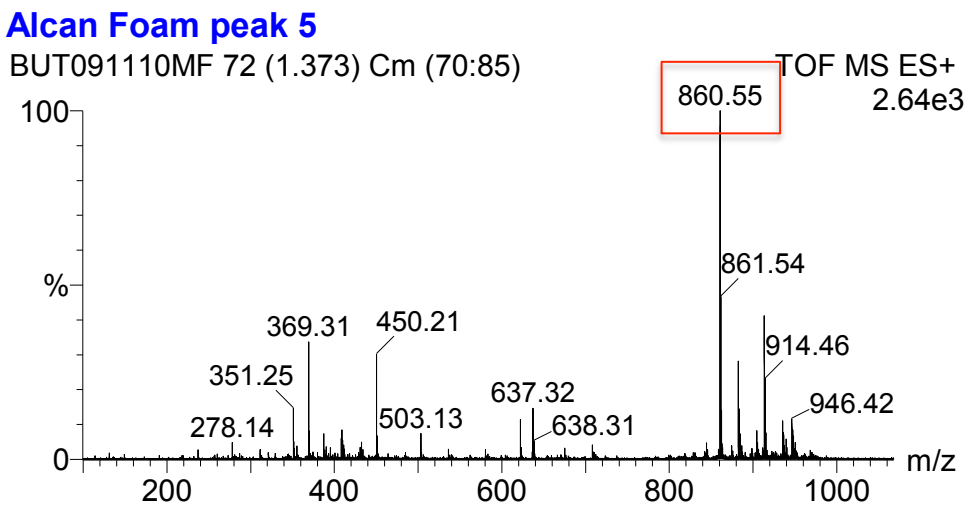

Figure 2.14. ESI-MS analysis of the compound in peak 5 isolated from foam produced by *A. borkumensis* SK2 during growth. The *m/z* of 885 corresponds to apo-amphibactin E.

2.3.5 Putative biosynthetic pathway for the amphibactin siderophores in *A. borkumensis* SK2

Due to the peptide-based structure of the amphibactins, it was predicted that the siderophores would be synthesized by non-ribosomal peptide synthetases (NRPSs). NRPSs are large multi-domain systems arranged in a modular fashion, which are responsible for the biosynthesis of both proteogenic and non-proteogenic amino acids into peptide based natural products. An evaluation of the *A. borkumensis* SK2 genome indicated the presence of a gene cluster comprised of eight ORF's involved in siderophore biosynthesis (Figure 2.15A, Table 2.1). BLASTp analysis suggests two of the genes are NRPS genes, ABO_2093 and ABO_2092. Together ABO_2093 and ABO_2092 are comprised of four classical NRPS modules and a unique termination domain (Figure 2.15B).

Traditionally, the first module in a NRPS domain consists of an adenylation domain and a thiolation domain to initiate biosynthesis; however, in the case of the amphibactins from *A. borkumensis* SK2, module 1 begins with a N-terminal condensation domain. This has been

seen previously with other lipopeptide natural products like surfactin, the amphi-enterobactins and cupriachelin.[28,29,30] Since no fatty acyl CoA ligase is present in the biosynthetic gene cluster, this suggests that an external fatty acyl CoA ligase is responsible for activation of a fatty acid to initiate biosynthesis of the amphibactins and incorporate an acyl moiety into the peptide chain. Like with surfactin and the amphi-enterobactins, no acyl carrier protein responsible for tethering the activated fatty acid appears to be incorporated into the biosynthetic gene cluster either.

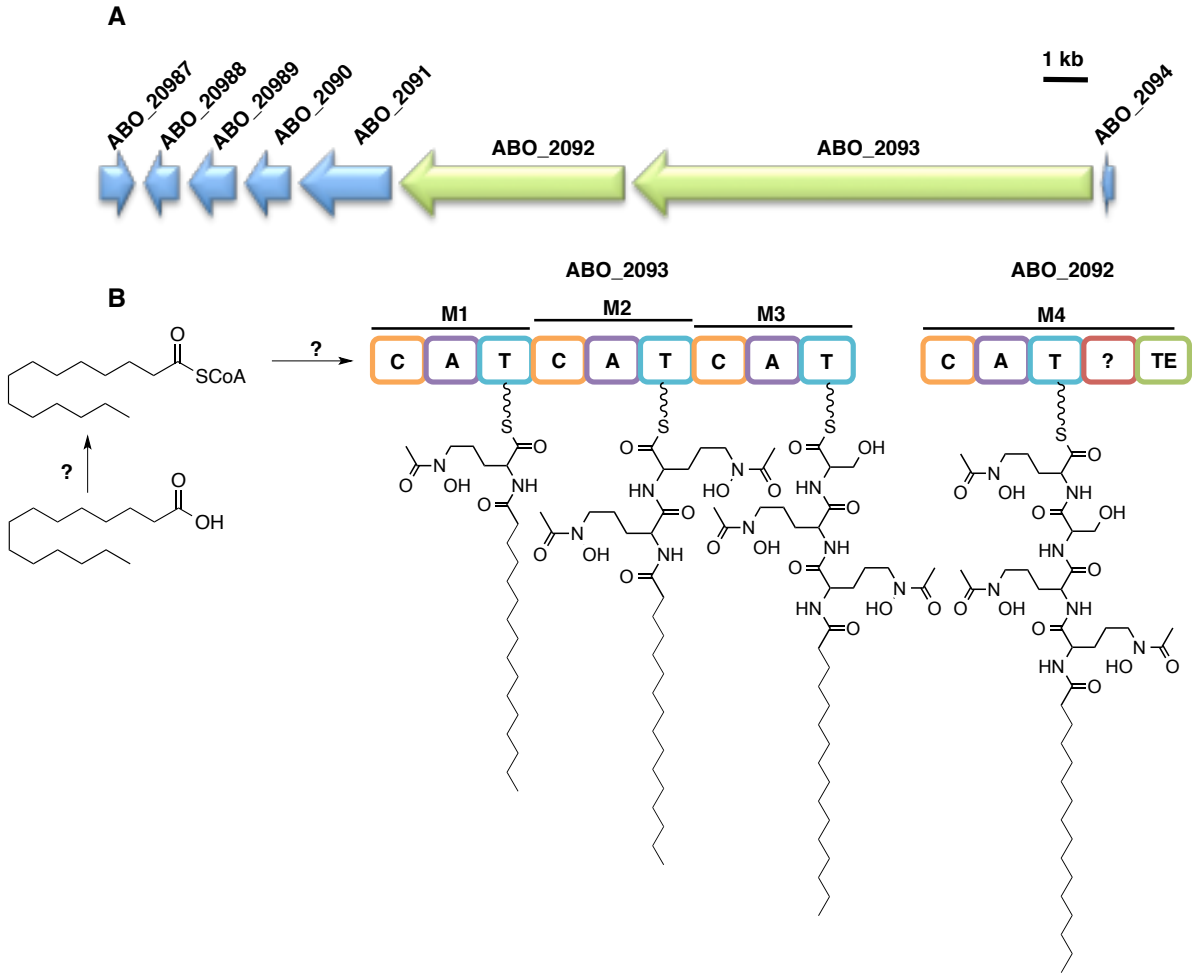

Figure 2.15. (A) Organization of the predicted open reading frames involved in amphibactin biosynthesis from *A. borkumensis* SK2. (B) The predicted NRPS modular assembly and adenylation domain specificity of the amphibactins.

The organization and amino acid specificity of the remaining NRPS modules predicted to synthesize the amphibactins were analyzed using the publicly available software, PKS/NRPS predictor (http://nrps.igs.umaryland.edu/nrps/).[22] The predicted organization of the amphibactin biosynthetic genes is shown in Figure 2.15. According to the modular organization of the NRPS, four adenylation domains are involved in the biosynthesis of the amphibactins consistent with the four amino acids present in the headgroup. Software predictions designate the third amino acid from the N-terminus to be a serine. The signature sequences of the remaining three adenylation domains are identical (DG-CTGGV), however, they do not have any catalytic residues that match those of known amino acids. Due to the presence of three N^5-acyl-N^5-hydroxyornithines seen in the structure of the amphibactins at the location of these adenylation domains, it can be postulated that these domains encode for N^5-acyl-N^5-hydroxyornithine. Also, genes ABO_2089 and ABO_2090 are predicted to be involved in the tailoring of ornithine to form N^5-acyl-N^5-hydroxyornithine. BLAST results predict ABO_2089 to be an L-ornithine N^5-monooxygenase, which hydroxylates ornithine. ABO_2090 is predicted to be an acyltransferase similar to lucB, which acetylates ornithine during aerobactin biosynthesis in *E. coli*. Genes ABO_2088 and ABO_2091 are involved in siderophore uptake and iron removal and genes ABO_2087 and ABO_2094 are necessary for siderophore biosynthesis. No epimerization domains were predicted in either NRPS protein suggesting that all amino acids are in the L-configuration.

The termination domain of ABO_2093 is atypical when compared to other NPRS termination domains. An unknown domain preceding the thioesterase domain is predicted to be homologous to reductases, which are sometimes used in chain termination in replace of thioesterase domains.[31] These domains, however, usually result in the cyclization of the final

product, which his not seen in the structure of the amphibactins. A thioesterase domain is also present in ABO_2092, which likely catalyzes chain termination and release suggesting the unknown domain has a different function.

Table 2.1. The predicted open reading frames involved in amphibactin biosynthesis by *A. borkumensis* SK2 and their putative functions.

Locus Tag	ORF Predicted Function	Gene Annotation	GenBank Accession
ABO_2087	Phosphopantetheinyl transferase	EntD	YP_693807
ABO_2088	Ferric iron reductase		YP_693808
ABO_2089	L-ornithine N^5-monooxygenase		YP_693809
ABO_2090	Acetyltransferase	lucb	YP_693810
ABO_2091	Ferrioxamine receptor	foxA	YP_693811
ABO_2092	Non-ribosomal peptide synthetase		YP_693812
ABO_2093	Non-ribosomal peptide synthetase		YP_693813
ABO_2094	Mbth-like protein		YP_693814

2.4 Discussion

While it is known that many alkane-degrading enzymes require iron as a cofactor, the siderophore-mediated iron uptake pathway for many oil-degrading microbes, including *Alcanivorax* spp., had not been investigated. In this work, we have determined the production of the amphibactin siderophores by *A. borkumensis* SK2. The production of membrane associated amphiphilic siderophores by oil-associated microbes is not surprising since iron uptake has to occur in an amphiphilic environment. Many oil-degrading bacteria have been shown to produce biosurfactants to lower the surface tension of water and emulsify hydrocarbons.[32,33] Studies have also shown that adding sophorose lipids as biosurfactants increases the percentage of hydrocarbon degradation by oil-degrading microbes.[34] The

amphiphilic nature of the amphibactins allows the siderophore to behave as a biosurfactant, aiding in iron uptake and hydrocarbon degradation by preventing siderophore diffusion and increasing the solubility of oil at the bacterial membrane. The isolation of siderophores from the culture foam also suggests that the acylated amphibactins could use the biosurfactants to travel further away from the cell membrane to acquire iron from a more diverse environment. Interestingly, no amphibactins with hydroxylated fatty acid tails were isolated as has been previously seen with other amphibactin-producing bacteria.[24,35]

2.5 References

1. Prince, R., Bioremediation of marine oil spills. *Trends in Biotechnology* **1997,** *15* (5), 158-160.

2. Harayama, S.; Kasai, Y.; Kishira, H.; Shutsubo, K., Petroleum biodegradation in marine environments. *Journal of Molecular Microbiology and Biotechnology* **1999,** *1* (1), 63-70.

3. Kasai, Y.; Kishira, H.; Syutsubo, K.; Harayama, S., Molecular detection of marine bacterial populations on beaches contaminated by the Nakhodka tanker oil-spill accident. *Environmental Microbiology* **2001,** *3* (4), 246-255.

4. Austin, R.; Groves, J., Alkane-oxidizing metalloenzymes in the carbon cycle. *Metallomics* **2011,** *3* (8), 775-787.

5. Kok, M.; Oldenhuis, R.; Vanderlinden, M.; Raatjes, P.; Kingma, J.; Vanlelyveld, P.; Witholt, B., The *Pseudomonas oleovorans* Alkane Hydroxylase Gene: sequence and expression. *Journal of Biological Chemistry* **1989,** *264* (10), 5435-5441.

6. Staijen, I.; van Beilen, J.; Witholt, B., Expression, stability and performance of the three-component alkane mono-oxygenase of *Pseudomonas oleovorans* in Escherichia coli. *European Journal of Biochemistry* **2000,** *267* (7), 1957-1965.

7. Dibble, J. T.; Bartha, R., Effect of iron on the biodegradation of petroleum in seawater. *Applied Environmental Microbiology* **1976,** *31* (4), 544-550.

8. Husain, S., Effect of ferric iron on siderophore production and pyrene degradation by Pseudomonas fluorescens 29L. *Current Microbiology* **2008,** *57* (4), 331-334.

9. Zane, H.; Butler, A., Isolation, Structure Elucidation, and Iron-Binding Properties of Lystabactins, Siderophores Isolated from a Marine Pseudoalteromonas sp. *Journal of Natural Products* **2013,** *76* (4), 648-654.

10. Gauglitz, J.; Zhou, H.; Butler, A., A suite of citrate-derived siderophores from a marine Vibrio species isolated following the Deepwater Horizon oil spill. *Journal of Inorganic Biochemistry* **2012,** *107* (1), 90-95.

11. Castresana, J., Selection of conserved blocks from multiple alignments for their use in phylogenetic analysis. *Molecular Biology and Evolution* **2000,** *17* (4), 540-552.

12. Chevenet, F.; Brun, C.; Banuls, A.; Jacq, B.; Christen, R., TreeDyn: towards dynamic graphics and annotations for analyses of trees. *Bmc Bioinformatics* **2006,** *7*.

13. Dereeper, A.; Guignon, V.; Blanc, G.; Audic, S.; Buffet, S.; Chevenet, F.; Dufayard, J.; Guindon, S.; Lefort, V.; Lescot, M.; Claverie, J.; Gascuel, O., Phylogeny.fr: robust phylogenetic analysis for the non-specialist. *Nucleic Acids Research* **2008,** *36*, W465-W469.

14. Haverty, P.; Hansen, U.; Weng, Z., Computational inference of transcriptional regulatory networks from expression profiling and transcription factor binding site identification. *Nucleic Acids Research* **2004,** *32* (1), 179-188.

15. Guindon, S.; Gascuel, O., A simple, fast, and accurate algorithm to estimate large phylogenies by maximum likelihood. *Systematic Biology* **2003,** *52* (5), 696-704.

16. Anisimova, M.; Gascuel, O., Approximate likelihood-ratio test for branches: A fast, accurate, and powerful alternative. *Systematic Biology* **2006,** *55* (4), 539-552.

17. DeSantis, T.; Hugenholtz, P.; Larsen, N.; Rojas, M.; Brodie, E.; Keller, K.; Huber, T.; Dalevi, D.; Hu, P.; Andersen, G., Greengenes, a chimera-checked 16S rRNA gene database and workbench compatible with ARB. *Applied and Environmental Microbiology* **2006,** *72* (7), 5069-5072.

18. Benson, D.; Karsch-Mizrachi, I.; Lipman, D.; Ostell, J.; Sayers, E., GenBank. *Nucleic Acids Research* **2011,** *39*, D32-D37.

19. Gauglitz, J.; Butler, A., Amino acid variability in the peptide composition of a suite of amphiphilic peptide siderophores from an open ocean *Vibrio* species. *Journal of Biological Inorganic Chemistry* **2013,** *18* (5), 489-497.

20. Martinez, J.; Butler, A., Marine amphiphilic siderophores: Marinobactin structure, uptake, and microbial partitioning. *Journal of Inorganic Biochemistry* **2007,** *101* (11-12), 1692-1698.

21. Schwyn, B.; Neilands, J., Universal chemical assay for the detection and determination of siderophores. *Analytical Biochemistry* **1987,** *160* (1), 47-56.

22. Bachmann, B.; Ravel, J.; Hopwood, D., Methods for In Silico Prediction of Microbial Polyketide and Nonribosomal Peptide Biosynthetic Pathways from DNA Sequence Data. *Complex Enzymes in Microbial Natural Product Biosynthesis, Part a: Overview Articles and Peptides* **2009,** *458*, 181-217.

23. Biemann, K., Sequencing of Peptides by Tandem Mass Spectrometry and High-Energy Collision-Induced dissociation. *Methods in Enzymology* **1990,** *193*, 455-479.

24. Martinez, J.; Zhang, G.; Holt, P.; Jung, H.; Carrano, C.; Haygood, M.; Butler, A., Self-assembling amphiphilic siderophores from marine bacteria. *Science* **2000,** *287* (5456), 1245-1247.

25. Homann, V.; Sandy, M.; Tincu, J.; Templeton, A.; Tebo, B.; Butler, A., Loihichelins A-F, a Suite of Amphiphilic Siderophores Produced by the Marine Bacterium *Halomonas* LOB-5. *Journal of Natural Products* **2009,** *72* (5), 884-888.

26. Kem, M.; Zane, H.; Springer, S.; Gauglitz, J.; Butler, A., Amphiphilic siderophore production by oil-associating microbes. *Metallomics* **2014,** *6* (6), 1150-1155.

27. Martins dos Santos, V.; Sabirova, J.; Timmis, K. N.; Yakimov, M. M.; Golyshin, P. N., *Alcanivorax borkumensis*. Springer Berlin Heidelberg: 2010.

28. Kraas, F.; Helmetag, V.; Wittmann, M.; Strieker, M.; Marahiel, M., Functional Dissection of Surfactin Synthetase Initiation Module Reveals Insights into the Mechanism of Lipoinitiation. *Chemistry & Biology* **2010,** *17* (8), 872-880.

29. Zane, H.; Naka, H.; Rosconi, F.; Sandy, M.; Haygood, M.; Butler, A., Biosynthesis of Amphi-enterobactin Siderophores by Vibrio harveyi BAA-1116: Identification of a Bifunctional Nonribosomal Peptide Synthetase Condensation Domain. *Journal of the American Chemical Society* **2014,** *136* (15), 5615-5618.

30. Kreutzer, M.; Kage, H.; Nett, M., Structure and Biosynthetic Assembly of Cupriachelin, a Photoreactive Siderophore from the Bioplastic Producer Cupriavidus necator H16. *Journal of the American Chemical Society* **2012,** *134* (11), 5415-5422.

31. Keating, T.; Ehmann, D.; Kohli, R.; Marshall, C.; Trauger, J.; Walsh, C., Chain termination steps in nonribosomal peptide synthetase assembly lines: Directed acyl-S-enzyme breakdown in antibiotic and siderophore biosynthesis. *Chembiochem* **2001,** *2* (2), 99-107.

32. Yakimov, M.; Golyshin, P.; Lang, S.; Moore, E.; Abraham, W.; Lunsdorf, H.; Timmis, K., Alcanivorax borkumensis gen. nov., sp. nov., a new, hydrocarbon-degrading and surfactant-producing marine bacterium. *International Journal of Systematic Bacteriology* **1998,** *48*, 339-348.

33. Bento, F.; Camargo, F.; Okeke, B.; Frankenberger, W., Diversity of biosurfactant producing microorganisms isolated from soils contaminated with diesel oil. *Microbiological Research* **2005,** *160* (3), 249-255.

34. Oberbremer, A.; Mullerhurtig, R.; Wagner, F., Effect of the Addition of Microbial Surfactants on Hydrocarbon Degradation in a Soil Population in a Stirred Reactor. *Applied Microbiology and Biotechnology* **1990,** *32* (4), 485-489.

35. Vraspir, J.; Holt, P.; Butler, A., Identification of new members within suites of amphiphilic marine siderophores. *Biometals* **2011,** *24* (1), 85-92.

III. Identification of a Ntn-hydrolase necessary for marinobactin fatty acid removal

3.1 Introduction

The marine bacterium, *Marinobacter* sp. DS40M6, produces a suite of amphiphilic siderophores termed the marinobactins.[1,2] The marinobactins are comprised of a hydrophilic peptide-based headgroup appended by a fatty acid at the amino terminus of the peptide. During mid-log phase of bacterial growth, the marinobactins are synthesized and secreted into the extracellular medium. As the bacterium approaches early stationary phase of growth, an enzyme is also expressed by the bacterium to remove the fatty acid appendage from the marinobactin headgroup (Figure 3.1).[3]

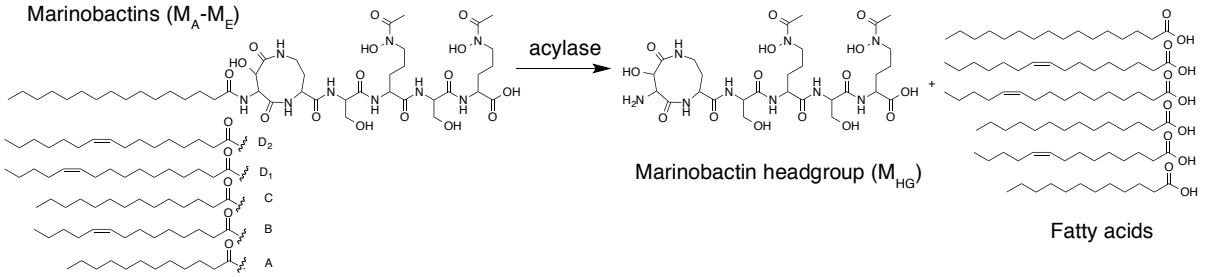

Figure 3.1. The marinobactin siderophores produced by *Marinobacter* sp. DS40M6, which also expresses an acylase to remove the fatty acid tail, producing the marinobactin headgroup.

Recently, a similar reaction has been reported with the gram-negative, pathogenic bacterium *Pseudomonas aeruginosa* PAO1. *P. aeruginosa* produces the siderophore pyoverdine, which is synthesized as an acylated precursor. Prior to excretion from the cell, the Ntn-hydrolase (N-terminal nucleophile), PvdQ, removes the fatty acid to form the mature form of pyoverdine (**Figure 3.2**).[4,5] PvdQ resides in the periplasm and can also hydrolyze long chain acyl homoserine lactones (HSL) used in quorum sensing; however, the location of the *pvdQ* gene in the pyoverdine biosynthetic operon suggests PvdQ is mainly associated with pyoverdine biosynthesis.[6,7] PvdQ is a proenzyme comprised of a signal peptide at the N-terminus followed by an α-subunit, a spacer peptide and the β-subunit. During self-activation, the enzyme loses the signal and spacer peptide to form a heterodimeric protein with a characteristic αββα-fold.[6]

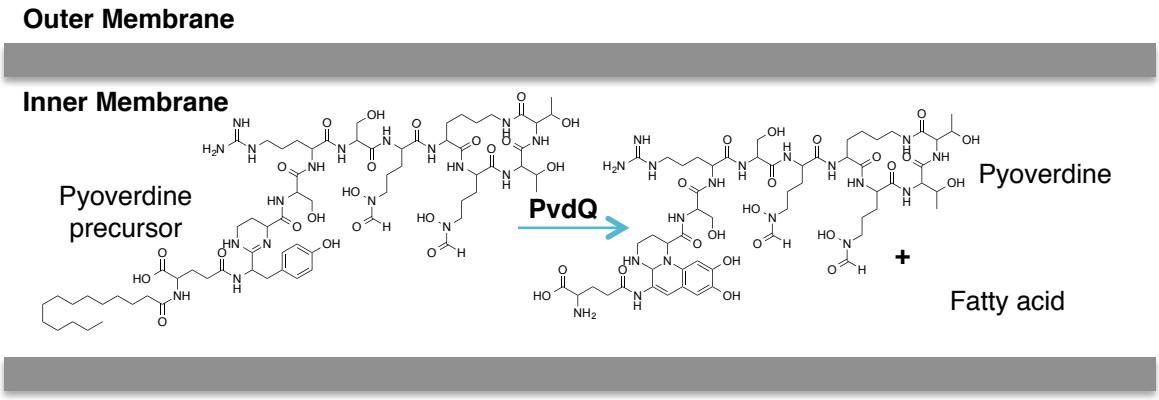

Figure 3.2. *P. aeruginosa* PAO1 produces the Ntn-hydrolase, PvdQ, which removes the fatty acid from an acyl pyoverdine precursor prior to excretion of the siderophore.

The genome of *Marinobacter* sp. DS40M6 is not sequenced; therefore, searching for a PvdQ-like marinobactin acylase involves great challenges. Using bioinformatic analysis we have designed degenerate primers based on the sequences of PvdQ and PvdQ-like hydrolases

from sequenced *Marinobacter* species to search for a gene necessary for M_{HG} production in *Marinobacter* sp. DS40M6.

3.2 Experimental

3.2.1 Bacterial strains, plasmids and culture conditions

Bacterial strains and plasmids used in this study are listed in **Table 3.1**. *Marinobacter* sp. DS40M6 was isolated off the coast of west Africa from open ocean water.[1] *Escherichia coli* strains were cultured in Luria Bertani (LB) broth or LB agar plates at 30°C or 37°C with shaking at 225 rpm. When required, the LB broth was supplemented with either 100 μg/mL ampicillin, 50 μg/mL kanamycin or 50 μg/mL spectinomycin.

Table 3.1. Bacterial Strains and Plasmids

Strain or Plasmid	Relevant characteristics	Source or reference
Marinobacter strain		
DS40M6	Wild-type, marine isolate	Ref. 1
HNMS1	*Marinobacter* sp. DS40M6Δ*bntA*	This study
E. coli strain		
Top10	F^- mcrA Δ(mrr-hsdRMS-mcrBC) φ80lacZΔM15 ΔlacX74 recA1 araD139 Δ(ara-leu) 7697 galU galK rpsL (StrR) endA1 nupG λ-	Invitrogen
XL-Blue MR	F^- Δ(mcrA)183 Δ(mcrCB-hsdSMR-mrr)173 endA1 supE44 thi-1 recA1 gyrA96 relA1 lac	Agilent
BL21-CodonPlus(DE3)-RIPL	B $F^–$ ompT hsdS($r_B^–m_B^–$) dcm^+Tet^r gal λ(DE3) endA Hte [argU proL Cam^r] [argU ileY leuW Strep/$Spec^r$]	Agilent
S17-1λ*pir*	λ-pir lysogen; thi pro hsdR hsdM+recA RP4 2-Tc::Mu-Km::Tn7(Tp^r Sm^r)	Ref. 8
Plasmid		
PCR.2.1 TOPO	3'-T overhangs for direct ligation of *Taq*-amplified PCR products	Invitrogen
pET24-b(+)	Expression vector with a T7 promoter, Amp	Novagen
pET32-a(+)	Expression vector with a T7 promoter, Amp	Novagen
SuperCos1	Cosmid vector for *M*. sp. DS40M6 cosmid library construction	Agilent
P2-3	Cosmid clone containing the bntA gene	This study
P2-3F	A 5 kb subclone of cosmid P2-3 in pET32-a(+) at the BamHI site	This study
pGEM-T easy	A vector for the cloning of PCR products with blue/white screening, Ap^r	Promega
pDM4	Suicide vector, *sacB* gene, R6k origin, Cm^r	Ref. 9
pIC156	Source of a spectinomycin cassette	Ref. 10
pHN26	pDM4 harboring Δ*bntA* and the Sp^r cassette from pIC156	This study
pMMB208	A broad-host-range expression vector; Cm^r IncQ lacIq Ptac; polylinker from M13mp19	Ref. 11
pHN27	pMMB208 harboring a Sp^r cassette	This study
pHN28	pHN28 harboring *bntA*	This study
p24-*bntA*-His_6	*bntA* cloned into the NdeI and XhoI sites of pET22a(+) with a C-terminal His-tag	This study
p32-Trx-*bntA*	*bntA* cloned into the NcoI and XhoI sites of pET32a(+) with a N-terminal Trx-tag and His-tag	This studdy

3.2.2 Identification of putative marinobactin acylases

The basic local alignment search tool (BLAST) was used to search for PvdQ-like proteins in sequenced *Marinobacter* species. The *pvdQ*-like genes were aligned with Cobalt alignment software and degenerate primers were designed using the CODEHOP (COnsensus-DEgenerate Hybrid Oligonucleotide Primer) PCR primer design strategy.[12]

3.2.3 PCR amplification of a putative marinobactin acylase gene fragment

To obtain genomic DNA, *Marinobacter* sp. DS40M6 was grown overnight in 5 mL of 2216 media at 30°C and 180 RPM. The cells were obtained by centrifugation and resuspended in 500 ul of TE buffer supplemented with 0.6% SDS and 0.12 mg/ml proteinase K. The mixture was incubated at 50-55°C for 1-3 hours with intermittent agitation. Protein was removed by extraction with phenol:chloroform:isoamyl alcohol (25:25:1) pH 8 with 1 mM EDTA. The aqueous phase was collected in a fresh tube and combined with 1/10 volume of 3 M sodium acetate pH 5.2. The DNA was precipitated with 2.5 volumes of ice cold ethanol and incubated at -80°C for 1 hr. The samples were centrifuged at 13,000 x g, 4°C for 20 minutes. The supernatant was decanted and the pellet was washed with 70% ethanol and dried. The resulting pellet was resuspened in 200-500 µL TE buffer and stored at 4°C for up to 1 week.

Touchdown PCR (TD-PCR) was used in conjunction with the CODEHOP designed primers for amplification of the pvdQ-like gene fragment.[13,12] Amplification from *Marinobacter* sp. DS40M6 genomic DNA was performed using the degenerate primers M6 acylase F1 (5'-CCACTACCGGATCGTGGGNCARTAYGC-3') and M6 acylase R1 (5'-CCAGGCCAGGTTCTCGTTRAARTTDAT-3'). PCR reactions were setup on ice using 1X

reaction buffer B, 1.5 mM $MgCl_2$, 86 ng of template genomic DNA, 200 μM DNTP mix, 200 nM M6 acylase F1 primer, 200 nM M6 acylase R1 primer and 0.025 units of Taq DNA polymerase in a 50 μl reaction volume. The thermocycler reaction was run under the conditions stated in Table 3.2. PCR products were analyzed on 2% agarose gels and visualized with ethidium bromide. The obtained amplified gene sequence was purified by band stab PCR and cloned into a TOPO TA PCR 2.1 vector using the TOPO TA cloning kit according to manufacturer protocol (Invitrogen #K4560-01) for sequencing at the UC Berkeley sequencing facility.

Table 3.2. TD-PCR conditions for amplification of a marinobactin acylase gene fragment from *Marinobacter* sp. DS40M6.

Phase 1	**Step**	**Temperature**	**Time**
1	Denature	95°C	3 min
2	Denature	95°C	30 sec
3	Anneal	T_M + 10°C	45 sec
4	Elongate	72°C	1 min
Repeat steps 2-4 15 times			
Phase 2	**Step**	**Temperature**	**Time**
5	Denature	95°C	30 sec
6	Anneal	T_M or (T_M-5°C)[a]	45 sec
7	Elongate	72°C	1 min
Repeat steps 5-7 20 times			
Termination	**Step**	**Temperature**	**Time**
8	Elongate	72°C	5 mins
9	Halt reaction	4°C	15 mins
10	Hold	23°C	Until removed

[a]anneal temperature should increase by 1°C/cycle each time step 2-4 are repeated.

3.2.4 Cosmid library construction and screening of *Marinobacter* sp. DS40M6 genome

The construction of the *Marinobacter* sp. DS40M6 cosmid library was performed using the SuperCos1 kit (Agilent). DNA fragments of *Marinobacter* sp. DS40M6 between 24 kb and 48 kb were obtained by partial digestion with the restriction enzyme Sau3A. This was performed by combining 65 ng of genomic DNA with 100 ug/ml BSA, 1X reaction buffer and 0.25 units of Sau3A at 37°C for 25 minutes. The reaction was quenched by the addition of 10 mM EDTA and protein was removed by phenol:chloroform extraction. The resulting pellet was resuspended in 150 μL water and slowly run (30 V) on a 0.5% low melting point agaorse gel at 4°C overnight. To isolate desired DNA fragments, the gel was cut across at the 24 kb λ DNA digest molecular weight marker, inverted and run backwards for 1-1.5 hours to compact the band of DNA fragments. The compacted band of DNA between the 24 kb λ DNA digest molecular weight marker and the 48 kb λ phage molecular weight marker was removed and placed in a fresh eppendorf tube. The DNA fragments were separated from the agarose using β-agarase and dephosphorylated with CIAP. This procedure was repeated until about 1.5 μg of DNA fragments between 24 kb and 48 kb were obtained. The fragments were then cloned into the SuperCos1 vector and packaged using the Gigapack III Gold Packaging kit (Invitrogen).

The unamplified cosmid library was screened for the gene of interest using the Digoxigenin-11-dUTP (DIG) High Prime DNA labeling kit (Roche). A probe was designed from a 238 bp fragment of the acquired 416 bp gene fragment using primers M6 probe F1 (5'-CTGAGGGCAAGAACAGGAG) and M6 probe R1 (5'CCGTTGGTGTTCAGATACCC). The hybridization was performed at 42°C and the

color substrate solution was incubated with the membranes for 3 hours in the dark. Cosmids with a positive hit were isolated and rescreened by colony PCR using the M6 probe F1/R1 primers.

3.2.5 Identification of the marinobactin acylase gene, *bntA*

The insert from cosmid P2-3 was excised at the NotI sites of the SuperCos1 vector then gel purified and digested with BamHI. The digested fragments were separated on an agarose gel and the fragment containing the gene of interest was identified using band stab PCR with the M6 probe F1/R1 primers. The gene fragment was gel purified and cloned into the TOPO TA 2.1 cloning vector according to manufacturers protocol for sequencing at the Berkeley DNA sequencing facility.

3.2.6 Cloning the *bntA* gene for protein expression

To clone *bntA* into the pET24a(+) vector with a C-terminal 6X His-tag, *bntA* was amplified from *Marinobacter* sp. DS40M6 genomic DNA using primers *bntA*_NdeI-F (5'-CGCGTACATATGATGAAATCGCTTCGCAAACCTTTCAG-3') and *bntA*_XhoI-R (5'-CCCCGGCTCGAGTTAATTGGTGATTGTTATTTCTCC-3', stop codon removed). The amplified gene product was digested sequentially with NdeI and XhoI and purified using a silica spin column. The pET24a(+) vector in TOP10 cells was grown in 5 mL of LB + amp overnight at 37°C. The vector was isolated using a silica spin column and digested sequentially with NdeI and XhoI followed by a final purification on a silica spin column. Ligation reactions were performed at a ratio of 1:2 (vector:insert) at 16°C overnight and transformed into *E. coli* TOP10 cells.

To clone *bntA* into the pET32a(+) vector with a N-terminal thioredoxin fusion tag, *bntA* was amplified from *Marinobacter* sp. DS40M6 genomic DNA using primers *bntA*_NcoI-F (5'-CGCGTACCATGGGCATGAAATCGCTTCGCAAACCTTTCAG-3') and *bntA*_XhoI_S-R (5'-CCCCGGCTCGAGTTAATTGGTGATTGTTATTTCTCC-3'). The amplified gene product was digested sequentially with NcoI and XhoI and purified using a silica spin colum. The vector digestion, ligation and transformation was performed as described above with the exception that NcoI was used instead of NdeI.

For expression analysis, the plasmids were transformed into *E. coli* BL21-CodonPlus(DE3)-RIPL cells. A starter culture (5 mL) was grown overnight at 30°C in LB + amp and used to inoculate 500 mL of LB + amp at 30°C, 225 RPM. When the O.D.600 reached 0.4-0.6, the cultures were cooled at 4°C for 30 minutes then induced with 0.4 mM IPTG. The induced cultures were grown at 16°C for 16-20 hrs at 225 RPM. Cells were harvested at 6,000 rpm (SLA-3000) for 10 minutes and either used immediately or flash frozen and stored at -80°C.

The cells were lysed by sonication (output control 2, amplitude at 40%, 10 seconds on/50 seconds off, X 3) in 20 mM sodium phosphate pH 7.8, 0.1 M NaCl, 5 mM imidazole, and 1% triton x-100. The crude lysate was centrifuged at 10,000 x g for 15 minutes and the resulting supernatant was filtered through a 0.45 μm sterile filter. The filtered supernatant was combined with Ni-NTA resin pre-rinsed with binding buffer (20 mM sodium phosphate pH 7.8, 0.1 M NaCl, 5 mM imidazole, 0.1% triton x-100) for 2 hours at 4°C with mild agitation. The resin was loaded onto a gravity column and washed with 5 column volumes of wash buffer (20 mM sodium phosphate pH 7.8, 0.1 M NaCl, 20 mM imidazole, 0.1% triton x-100). The His-tagged protein was eluted with 3 column volumes of elution buffer (20 mM sodium

phosphate pH 7.8, 0.1 M NaCl, 500 mM imidazole, 0.1% triton x-100) and the eluted fractions were concentrated and buffer exchanged into activity buffer (20 mM Tris pH 8, 50 mM NaCl, 2 mM $CaCl_2$) using a 50 MWCO spin column (2 mL, Millipore).

Following purification of Trx-tagged BntA, the thioredoxin tag was removed by incubating the purified protein with 1 ng of enterokinase for three hours at room temperature. The enterokinase was removed by gel filtration chromatography using a S200 HR10/30 column and an ATKA FPLC in 20 mM tris pH 9.0, 2 mM $CaCl_2$, 100 mM NaCl.

3.2.7 Siderophore production by Δ*bntA Marinobacter* sp. DS40M6

Our collaborators Dr. Hiroaki Naka and Dr. Margo Haygood constructed the deletion mutant strain, Δ*bntA Marinobacter* sp. DS40M6. Wild-type *Marinobacter* sp. DS40M6 and Δ*bntA Marinobacter* sp. DS40M6 were grown in 1 L of artificial seawater (ASW) media (15.5 g/L NaCl, 0.75 g/L KCl, 0.2 g/L $MgSO_4 \cdot 7H_2O$, 0.1 g/L $CaCl_2 \cdot 2H_2O$, 1.0 g/L NH_4Cl, 5 g/L succinic acid, 3 g/L Na_2HPO_4, pH 7.0) on a rotary shaker at 180 rpm and ambient temperature for 7 days. The cultures were harvested at 6,000 rpm for 30 minutes at 4°C and the supernatants were incubated with amberlite XAD-2 resin for 2 hours at ambient temperature with mild agitation. The siderophores were eluted from the resin with 100% methanol and concentrated by rotary evaporation. The extracts were analyzed by RP-HPLC on a C18 analytical column using water + 0.05% TFA (solvent A) and methanol + 0.05% TFA (solvent B) as the mobile solvents. The HPLC runs started at 100% solvent A for 3 minutes followed by conversion to 100% solvent B over 53 minutes. Peaks were identified by ESI-MS and ESI-MS/MS.

Siderophore production by the complement strain of Δ*bntA Marinobacter* sp. DS40M6 was analyzed by growing Δ*bntA Marinobacter* sp. DS40M6 + pMMB208-*bntA*, WT *Marinobacter* sp. DS40M6 + empty pMMB208 (positive control), and Δ*bntA Marinobacter* sp. DS40M6 + empty pMMB208 (negative control) in iron-limited ASW media and analyzing the culture supernatants for siderophore production as stated above.

3.2.8 Growth using M_{HG} compared to $M_{A\text{-}E}$

Marinobacter sp. DS40M6 was grown in 1 L of artificial seawater (ASW) media. During mid-log phase of bacterial growth, the culture was harvested at 6000 rpm, 4°C for 30 minutes. The pellet was rinsed and reconstituted in 40 mL of sterile ASW media. An aliquot (2 ml) of the reconstituted pellet was added to 250 mL of sterile ASW media with either (A) 1 μM Fe(III)-M_{HG} (B) 1 μM Fe(III)-$M_{A\text{-}E}$ (C) no added siderophores. Each of the samples was performed in triplicate and bacterial growth was monitored at an optical density of 600 nm daily.

3.3 Results and Discussion

3.3.1 Bioinformatic analysis of acylases in sequenced *Marinobacter* species

A BLASTp analysis of sequenced *Marinobacter* species using PvdQ as a query was performed to identify a potential marinobactin acylase. Seven *Marinobacter* species were found to contain PvdQ-like proteins and all were predicted to be part of the Ntn-hydrolase superfamily based on homology (Table 3.3). At the time of analysis, sequence information was only available for PvdQ-like hydrolases from *Marinobacter manganoxydans* Mn17-9,

Marinobacter adhaerens HP-15, and *Marinobacter algicola* DG893; therefore, these acylases were used as templates to design degenerate primers to amplify a *pvdQ*-like gene fragment from *Marinobacter* sp. DS40M6. The BLASTp results showed that these putative Ntn-hydrolases have 32-33% amino acid sequence similarity to PvdQ from *P. aeruginosa* PAO1.

Table 3.3. Putative PvdQ-like acylases in sequenced *Marinobacter* species and their percent identity to PvdQ from *P. aeruginosa* PAO1.

Accession #	Predicted function/species	Size (AA)	% identity to PvdQ
ADP96903	Acyl-homoserine lactone acylase (*Marinobacter adhaerens* HP15)	898	32%
EON91289	Aculeacin A acylase (*Marinobacter lipolyticus* SM19)	829	35%
EHJ0588	Penicillin amidase (*Marinobacter manganoxydans* MnI7-9)	890	33%
EDM49623	Peptidase S45 (*Marinobacter algicola* DG893)	882	32%
ERP91591	Peptidase S45 (*Marinobacter* sp. ES-1)	888	31%
ENO13542	Acyl-homoserine lactone acylase (*Marinobacter nanhaiticus* D15-8W)	894	30%
ENO13543	Acyl-homoserine lactone acylase (*Marinobacter nanhaiticus* D15-8W)	915	31%

3.3.2 Degenerate primer design and gene amplification

The CODEHOP strategy was used to design degenerate primers from the sequences of PvdQ-like acylases from *M. manganoxydans* Mn17-9, *M. adhaerens* HP-15, and *M. algicola* DG893 to see if a similar gene is present in the genome of *Marinobacter* sp. DS40M6. The CODEHOP strategy designs degenerate primers from an alignment of template amino acid sequences using conserved blocks of low degeneracy. Primers are designed from these conserved blocks consisting of a 5' consensus clamp and a 3' degenerate core to enhance primer to product annealing.[16] An amino acid alignment of the *M. manganoxydans* Mn17-9, *M. adhaerens* HP-15, and *M. algicola* DG893 sequences highlighting the conserved blocks of low degeneracy is shown in Figure 3.3. The conserved blocks chosen by the CODEHOP

software are highlighted in dark blue, and the specific blocks chosen for primer design and amplification in this study are highlighted in red.

Figure 3.3. Sequence alignment of *M. adhaerens* HP15 (top), *M. manganoxydans* MnI7-9 (middle), and *M. algicola* DG893 (bottom) for CODEHOP primer design. Conserved blocks of low degeneracy are shown in blue and the blocks chosen for forward (F➔) and reverse (➔R) primer design are shown in red.

Using degenerate primers designed from the sequences of PvdQ-like proteins in Table 3.3, a 416 bp gene fragment was amplified from *Marinobacter* sp. DS40M6 genomic DNA (**Figure 3.4**) indicating *Marinobacter* sp. DS40M6 also has an acylase related to PvdQ. The obtained fragment has greater than a 76% sequence identity to the putative Ntn-hydrolases from *M. manganoxydans* Mn17-9, *M. adhaerens* HP-15, and *M. algicola* DG893. Therefore, it appears that *Marinobacter* sp. DS40M6 also contains a PvdQ-like acylase.

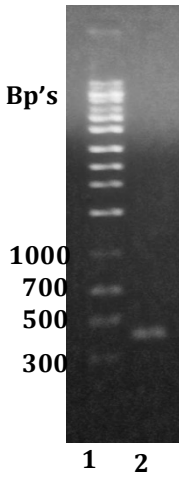

Figure 3.4. 1% agarose gel of PCR amplified gene fragment from *Marinobacter* sp. DS40M6 genomic DNA using sequences of predicted *pvdQ*-like acylases from *Marinobacter* species. Lane 1: Molecular weight marker. Lane 2: amplified 416 bp product.

3.3.3 Cosmid library construction and screening

The 416 bp gene fragment amplified from *Marinobacter* sp. DS40M6 genomic DNA was used to further determine the sequence of the entire acylase gene. A cosmid library of *Marinobacter* sp. DS40M6 was constructed using the SuperCos 1 kit from Agilent and resulted in the formation of 9300 colony forming units. A DIG labeled probe designed from the amplified 416 bp fragment was used to screen the unamplified cosmid library. Fourteen colonies gave a positive purple signal with one being especially bright (Figure 3.5). To

differentiate from false positives, the fourteen colonies were subjected to colony PCR using primers M6 probe F1 and M6 probe R1. Of the 14 colonies, 2 colonies resulted in the amplification of the expected 238 bp region when used as a template for PCR (Figure 3.6). These two colonies were grown in LB-ampicillin media overnight and the cosmids were isolated using a silica spin column. The purified cosmids were subjected to another round of PCR using primers M6 probe F1/R1. One colony named, P2-3, had a stronger amplification product and was subsequently used for further isolation.

Figure 3.5. The nitrocellulose membrane representing one plate of the cosmid library constructed from *Marinobacter* sp. DS40M6 genomic DNA. A bright, positive signal indicating hybridization of the probe to its complimentary DNA on a cosmid is circled in red.

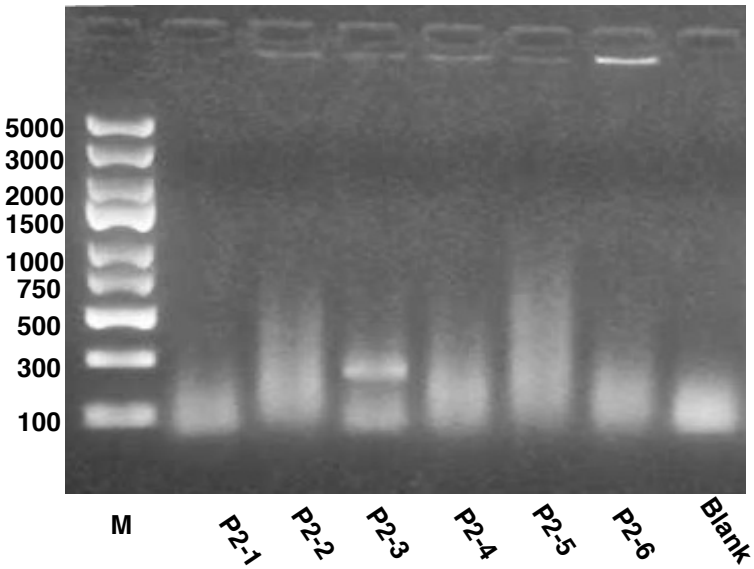

Figure 3.6. Agarose gel of a colony PCR analysis of 6 out of 14 colonies, which gave a positive signal indicating probe hybridization to a cosmid from the *Marinobacter* sp. DS40M6 cosmid library. One cosmid, P2-3, amplified the expected 238 bp region and was used for further analysis.

3.3.4 Subcloning to identify the *Marinobacter* acylase

The insert from cosmid P2-3 was excised using NotI, which has recognition sites flanking the insert in the SuperCos1 vector. The insert was gel purified and further digested with BamHI which does not have a recognition sequence in the known 416 bp fragment or in the acylase gene from *M. algicola* DG893, the closest related sequence as predicted from BLASTp results. Agarose gel analysis of the digest resulted in the appearance of 7 distinct bands with approximate lengths of 10,000 bp, 7,000 bp, 5,000 bp, 4,300 bp, 1,000 bp, 550 bp, and 400 bp (**Figure 3.7**). The predicted length of the acylase gene is around 2,700 bp, therefore, only the largest 4 digest products will be analyzed for the presence of the marinobactin acylase. The 4 bands were gel extracted and purified and each band was ligated into the pET-32a(+) vector. Each plasmid was screened using the same DIG-labeled probe as

above. The plasmids containing bands 1, 2, and 4 resulted in no positive hits. The transformation with band 3, however, showed a positive hybridization of the plasmid with the probe.

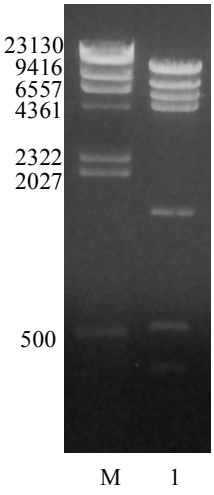

Figure 3.7. 0.8% agarose gel of the P2-3 insert digested with BamHI. Lane M: molecular weight marker, Lane 2: digested insert with BamHI.

3.3.5 *Marinobacter* sp. DS40M6 marinobactin acylase gene sequence

Cosmid library construction followed by hybridization screening resulted in the discovery of a 2646 bp ORF (named *bntA*), encoding a protein of 882 amino acids with a molecular weight of 94 kDa. The protein has a 96% amino acid identity to a protein annotated as a peptidase from *M. algicola* DG893 and 59-66% similarity to proteins annotated as acylases from other sequenced *Marinobacter* species. The protein has a 33% sequence identity to AaC, the quorum quencher from *Ralstonia solanacearum,* and 32% sequence identity to PvdQ from *P. aeruginosa* PAO1. The nucleotide sequence of *bntA* has been deposited in the GenBank database under accession number KM670457.

Ntn-hydrolases are characterized by a distinct αββα core structure following a post-translational processing of the propeptide into a heterodimeric form.[17] An amino acid alignment surrounding the active site region of PvdQ, BntA, and the other putative *Marinobacter* acylases, was performed to look for sequence conservation (**Figure 3.8**). The crystal structure of PvdQ from *P. aeruginosa* PAO1 was used to determine the nature of the highlighted residues.[6] A well-conserved glycine-serine-alanine sequence necessary for the post-translational processing of Ntn-hydrolases is closely conserved among PvdQ, BntA and the putative *Marinobacter* acylases.[18-20] Residues important for catalysis in PvdQ, including the N-terminal nucleophilic serine, and residues lining the substrate-binding site are conserved among all species. Conservation of amino acids, Val330 and Asn540, responsible for stabilization of the transient oxyanion transition state[6] are also present.

Figure 3.8. A sequence alignment surrounding the active site of PvdQ (top) and Ntn-hydrolases from sequenced *Marinobacter* species (middle 7 entries). The sequence of BntA from *Marinobacter* sp. DS40M6 is shown on the bottom line. Residues lining the substrate-binding site are labeled (**B**) while the residues important for proper catalytic function are highlighted in yellow. The serine nucleophile (•) is bolded and highlighted yellow and residues important for the stabilization of the oxyanion transition state are labeled as (O). The residues boxed in orange are closely conserved among Ntn-hydrolases and are believed to be important for self-activation.

3.3.6 Cloning and expression of *bntA* for protein production

The Ntn-hydrolase gene, *bntA*, from *Marinobacter* sp. DS40M6 was cloned into the pET24a(+) vector at the NdeI and XhoI sites resulting in a C-terminal 6X His-tagged construct, p24-*bntA*-His_6, for expression analysis in *E. coli* BL21-CodonPlus(DE3)-RIPL cells. An analysis of the crude lysate following induction shows a large band around 100 kDa that is not present in the uninduced samples (Figure 3.9). This mass corresponds to the inactive, non-processed pro-polypeptide. The presence of two subunits corresponding to the properly processed enzyme was not readily seen by SDS-page analysis. The crude lysate was centrifuged to separate the insoluble and soluble fractions of the cell and the majority of the expressed protein appears to stay in the insoluble fraction. To determine if small amounts of protein were active, the purified protein extracts were incubated with octanoyl *para*-nitroanaline (o-pNA), which produces a color change from colorless to bright yellow in the presence of an acylase, however, no color change was seen after incubation for several days. The enriched protein extracts were also incubated with apo-M_A and apo-M_E, however, no hydrolysis was seen with either substrate after two weeks of incubation. This suggests that the enzyme was being expressed in its non-active, insoluble form, which has been seen previously with the expression of other Ntn-hydrolases in *E. coli*.[21,20]

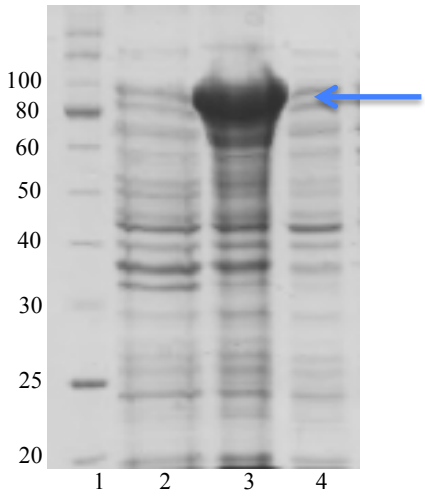

Figure 3.9. 12% SDS-page gel of p24-*bntA*-His_6 expressed in *E. coli*. Lane 1: Molecular weight marker, Lane 2: uninduced crude lysate control, Lane 3: Induced crude lysate, Lane 4: Induced soluble supernatant.

The *bntA* gene was also cloned into the pET32a(+) vector with a N-terminal thioredoxin fusion tag (Trx-tag). The Trx-tag can increase solubility of proteins by promoting proper disulfide bond formation during protein synthesis. Following expression, the Trx-tag can be removed from the protein using enterokinase. A 6X His-tag is also located between the thioredoxin fusion protein and the start of the *bntA* gene for purification purposes. Expression of Trx-His_6-*bntA* in *E. coli* BL21-CodonPlus(DE3)-RIPL cells resulted in the appearance of a band around 100 kDa (Figure 3.10) that appears to be mostly in the insoluble fraction as seen previously with the expression of p24-*bntA*-His_6. Following purification by Ni-NTA and removal of the trx-tag with enterokinase, the activity of His_6-BntA was evaluated with o-pNA. After five days of incubation with o-pNA, a small color change from colorless to yellow was seen indicating that small amounts of active His_6-BntA was being produced. The slow reaction rate due to small amounts of active BntA, however, was not compatible for activity studies with the marinobactins.

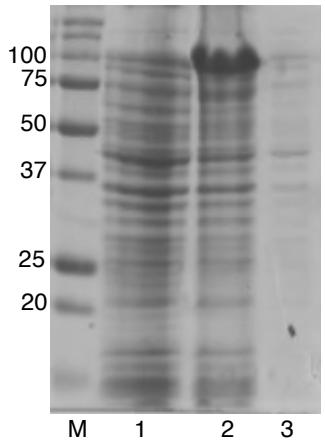

Figure 3.10. 12% SDS-page gel of p32-Trx- His_6-BntA expressed in *E. coli*. M: Molecular weight marker, Lane 1: uninduced crude lysate, Lane 2: Induced crude lysate, Lane 3: Induced soluble supernatant.

In hopes of obtaining a more soluble form of BntA, different constructs were cloned and analyzed for protein expression as shown in **Figure 3.11**. The pET24a(+) vector was used to clone a construct of *bntA* without any tags, however, no soluble, active protein was obtained. The gene was then cloned without the starter 24 amino acids representing the signal peptide and again no soluble, active protein was obtained. The pET44a(+) vector was used to add a N-terminal Nus-tag for solubility, but again, no activity was seen with o-pNA, M_A or M_E after a week of incubation.

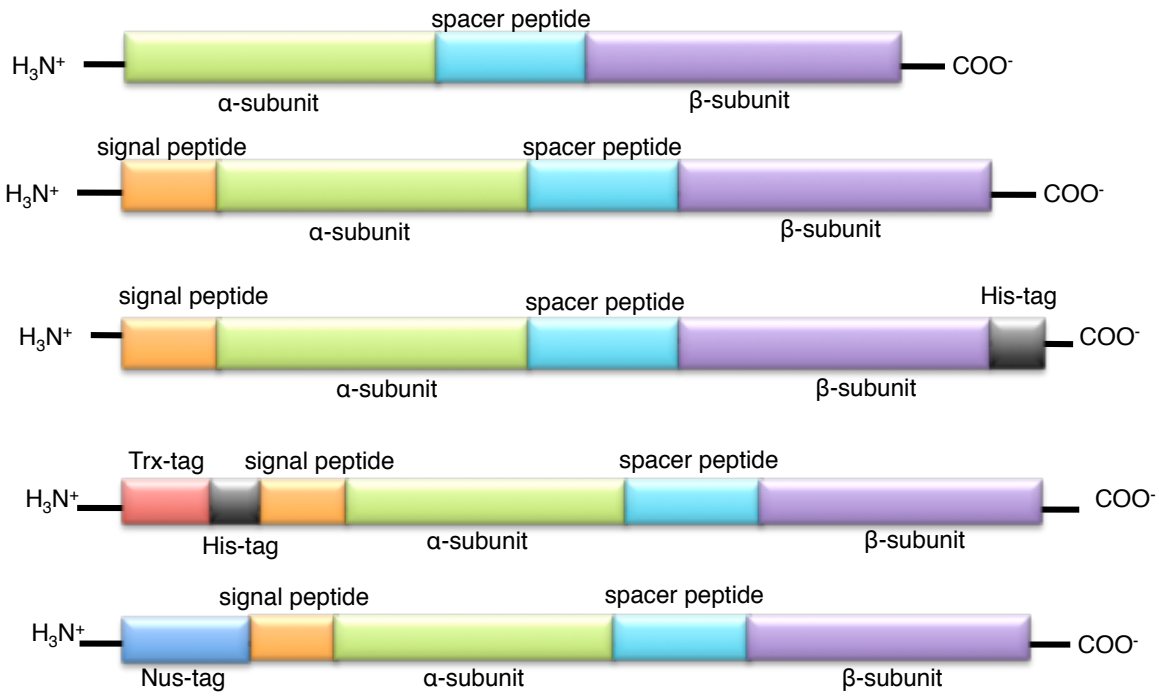

Figure 3.11. Cloned constructs of *bntA* for expression in *E. coli*.

3.3.7 Analysis of Δ*bntA Marinobacter* sp. DS40M6

A knockout mutant of *bntA* was analyzed for siderophore production and marinobactin headgroup formation under low-iron conditions. Wild-type *Marinobacter* sp. DS40M6 and Δ*bntA Marinobacter* sp. DS40M6 were grown in ASW media for 5 days under ambient temperature and siderophores were purified and analyzed by RP-HPLC at 215 nm. A distinct peak appears around 11 minutes in the HPLC trace for WT *Marinobacter* sp. DS40M6 that is not seen in Δ*bntA Marinobacter* sp. DS40M6 trace (**Figure 3.12**). Complementation of *bntA* restores production of M_{HG} when grown in iron-limited media resulting in almost the full conversion of the marinobactin suite to M_{HG} (**Figure 3.12**). Mass spectrometry analysis of the peak at 11 minutes showed a *m/z* value of 750 corresponding to the $[M+H]^+$ of apo-M_{HG}

(Figure 3.13) as has been previously reported.[3] This shows that the identified *bntA* gene is necessary for the hydrolysis of the marinobactin siderophores during bacterial growth.

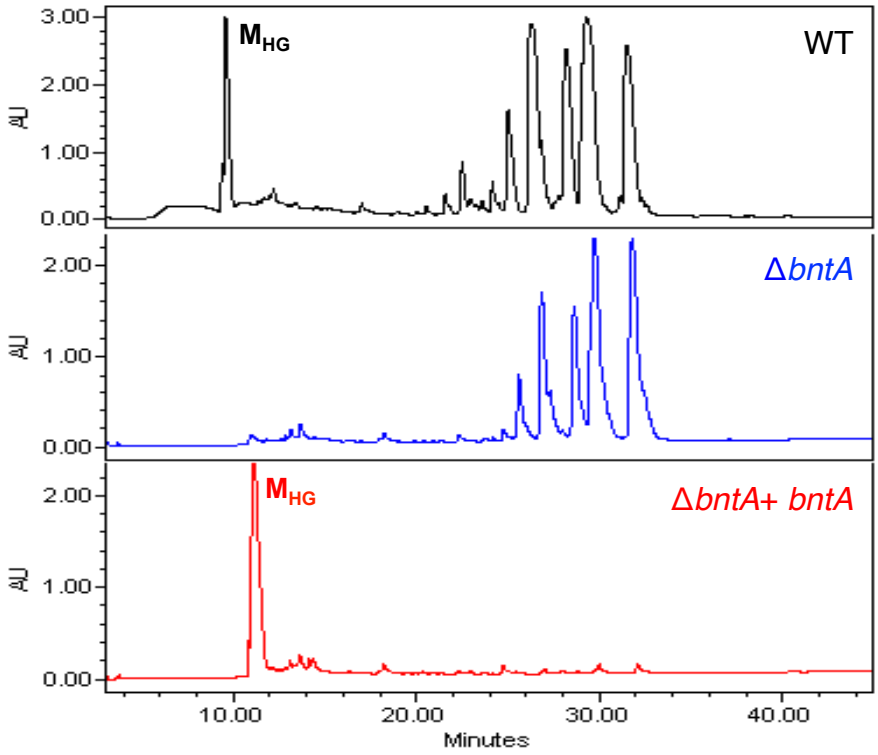

Figure 3.12. RP-HPLC trace of culture supernatants from WT *Marinobacter* sp. DS40M6 + empty pMMB208 (top, black), Δ*bntA Marinobacter* sp. DS40M6 + empty pMMB208 (middle, blue), and Δ*bntA Marinobacter* sp. DS40M6 + pMMB208-*bntA* (bottom, red).

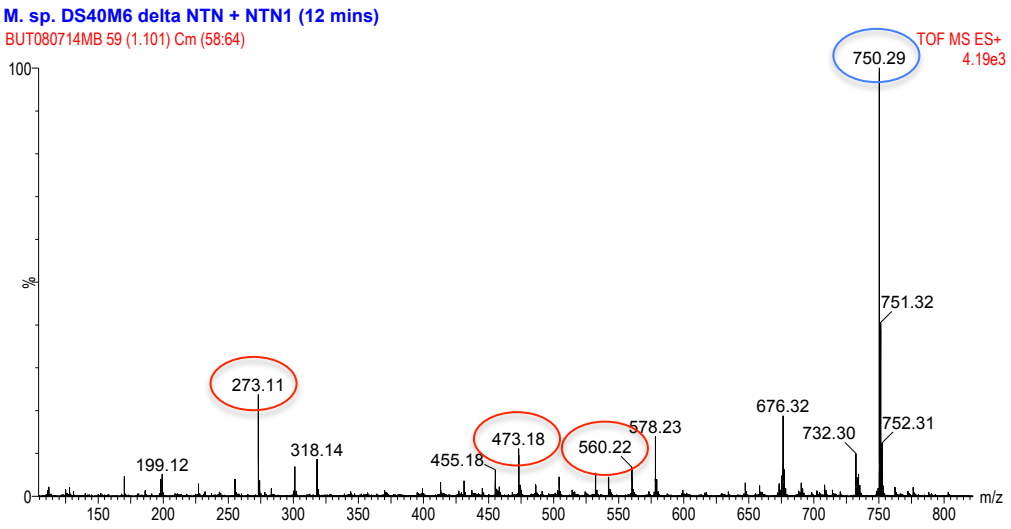

Figure 3.13. ESI-MS analysis of the compound eluting at 11 minutes from Δ*bntA* *Marinobacter* sp. DS40M6 + pMMB208-*bntA*.

3.3.8 Effect of M_{A-E} and M_{HG} on growth of *Marinobacter* sp. DS40M6 under low iron conditions

To investigate the ability of *Marinobacter* sp. DS40M6 to utilize Fe(III)-M_{HG} as a siderophore, the growth of *Marinobacter* sp. DS40M6 was monitored under low-iron conditions in the presence of either Fe(III)-M_{HG} or Fe(III)-marinobactins (Fe(III)-M_{A-E}). The bacteria grew to a significantly higher density in the presence of either Fe(III)-M_{HG} or Fe(III)-M_{A-E} when compared to the no added siderophore control (**Figure 3.14**). However, the growth curves of *Marinobacter* sp. DS40M6 with either Fe(III)-M_{HG} or Fe(III)-M_{A-E} grew to the same optical density over the same amount of time, suggesting M_{HG} can still be utilized for iron transport and uptake by *Marinobacter* sp. DS40M6.

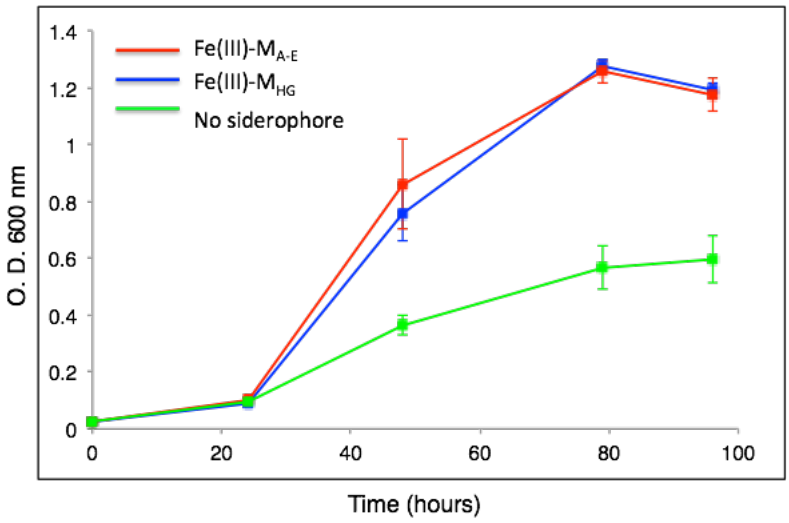

Figure 3.14. Growth curves of *Marinobacter* sp. DS40M6 in the presence of 1 μM Fe(III)-M_{HG} (blue), 1 μM Fe(III)-M_{A-E} (red) or no added siderophore (green).

3.4 Discussion

In this study, the putative Ntn-hydrolase, BntA, was shown to be necessary for removal of the fatty acid tails from the marinobactins in *Marinobacter* sp. DS40M6. BntA has a 32% sequence identity to the siderophore acylase, PvdQ, from *Pseudomonas aeruginosa* and 31-33% identity to the acyl-homoserine lactone acylases, Aac from *Ralstonia solanacearum* GM11000, AiiD from *Ralstonia* sp. XJ12B, and HacA from *Pseudomonas syringae*. To our knowledge, PvdQ is the only other known enzyme to remove a fatty acid tail from an acylated siderophore. PvdQ, however, hydrolyzes its substrate, acylated pyoverdine precursor, prior to excretion from the cell, whereas BntA is believed to hydrolyze the marinobactins after they are released into the extracellular medium.[3]

Previous studies have shown that some bacteria with acyl homoserine lactone acylases can use the fatty acid products as a sole carbon source as demonstrated by QuiP from *P. aeruginosa* and AiiD from *Ralstonia* sp. XJ12B.[21,19] *Marinobacter* species are well known for

their hydrocarbon degradation abilities and their importance in bioremediation of oil in the ocean.[22] It is possible that BntA is expressed under low nutrient conditions to release the more soluble marinobactin headgroup for iron uptake while utilizing the fatty acid product as a carbon source.

The enzymatic modification of siderophores has been seen previously with IroE from *E. coli*. IroE is an esterase that hydrolyzes the apo form of enterobactin and its glycosylated derivatives, the salmochelins. IroE hydrolyzes the trilactone backbone of enterobactin one time to form a linear trimer. The linearized siderophore chelates iron with only a slightly lower affinity than the cyclic form.[23] It is believed that IroE performs this hydrolysis on enterobactin prior to siderophore excretion from the cell since the linear trimer is more prevalent in the culture supernatant than the cyclic form.[24,25,26]

Similarly, the removal of the fatty acid tail from the amphiphilic marinobactins would produce a less hydrophobic siderophore without altering the iron chelating properties of the siderophore. The fatty acid tail provides a means for keeping the siderophore close for iron acquisition so it is not lost through diffusion. However, at high bacteria populations, the hydrolysis of the fatty acid tail would release the iron-chelating portion of the siderophore to be used among other nearby sister bacteria while providing a fatty acid hydrocarbon source for food.

3.5 References

1. Martinez, J.; Zhang, G.; Holt, P.; Jung, H.; Carrano, C.; Haygood, M.; Butler, A., Self-assembling amphiphilic siderophores from marine bacteria. *Science* **2000,** *287* (5456), 1245-1247.

2. Martinez, J.; Butler, A., Marine amphiphilic siderophores: Marinobactin structure, uptake, and microbial partitioning. *Journal of Inorganic Biochemistry* **2007,** *101* (11-12), 1692-1698.

3. Gauglitz, J. M.; Iinishi, A.; Ito, Y.; Butler, A., Microbial Tailoring of Acyl Peptidic Siderophores. Biochemistry: 2014; Vol. 53, pp 2624-2631.

4. Yeterian, E.; Martin, L.; Guillon, L.; Journet, L.; Lamont, I.; Schalk, I., Synthesis of the siderophore pyoverdine in Pseudomonas aeruginosa involves a periplasmic maturation. *Amino Acids* **2010,** *38* (5), 1447-1459.

5. Drake, E.; Gulick, A., Structural Characterization and High-Throughput Screening of Inhibitors of PvdQ, an NTN Hydrolase Involved in Pyoverdine Synthesis. *Acs Chemical Biology* **2011,** *6* (11), 1277-1286.

6. Bokhove, M.; Jimenez, P.; Quax, W.; Dijkstra, B., The quorum-quenching N-acyl homoserine lactone acylase PvdQ is an Ntn-hydrolase with an unusual substrate-binding pocket. *Proceedings of the National Academy of Sciences of the United States of America* **2010,** *107* (2), 686-691.

7. Koch, G.; Jimenez, P.; Muntendam, R.; Chen, Y.; Papaioannou, E.; Heeb, S.; Camara, M.; Williams, P.; Cool, R.; Quax, W., The acylase PvdQ has a conserved function among fluorescent Pseudomonas spp. *Environmental Microbiology Reports* **2010,** *2* (3), 433-439.

8. Simon, R.; Priefer, U.; Puhler, A., A broad host range mobilization system for *in vivo* genetic-engineering-transposon mutagenesis in gram-negative bacteria. *Bio-Technology* **1983,** *1* (9), 784-791.

9. Milton, D.; OToole, R.; Horstedt, P.; WolfWatz, H., Flagellin A is essential for the virulence of Vibrio anguillarum. *Journal of Bacteriology* **1996,** *178* (5), 1310-1319.

10. Steinmetz, M.; Richter, R., Plasmids designed to alter the antibiotic-resistance expressed by insertion mutations in *Bacillus subtilis*, through *in vivo* recombination. *Gene* **1994,** *142* (1), 79-83.

11. Morales, V.; Backman, A.; Bagdasarian, M., A series of wide-host-range low-copy-number vectors that allow direct screening for recombinants. *Gene* **1991,** *97* (1), 39-47.

12. Bachmann, B. O.; Ravel, J., Methods for In Silico Prediction of Microbial Polyketide and Nonribosomal Peptide Biosynthetic Pathways from DNA Sequence Data. Methods in Enzymology: 2009; Vol. 458, pp 181-217.

13. Korbie, D.; Mattick, J., Touchdown PCR for increased specificity and sensitivity in PCR amplification. *Nature Protocols* **2008,** *3* (9), 1452-1456.

14. Senanayake, S.; Brian, D., Precise large deletions by the PCR-based overlap extension method. *Molecular Biotechnology* **1995,** *4* (1), 13-15.

15. Zane, H.; Naka, H.; Rosconi, F.; Sandy, M.; Haygood, M.; Butler, A., Biosynthesis of Amphi-enterobactin Siderophores by Vibrio harveyi BAA-1116: Identification of a Bifunctional Nonribosomal Peptide Synthetase Condensation Domain. *Journal of the American Chemical Society* **2014,** *136* (15), 5615-5618.

16. Rose, T. M.; Henikoff, J. G.; Henikoff, S., CODEHOP (Consensus-Degenerate Hybrid Oligonucleotide Primer) PCR primer design. **2003,** *31* (13), 3763–3766.

17. Oinonen, C.; Rouvinen, J., Structural comparison of Ntn-hydrolases. *Protein Science* **2000,** *9* (12), 2329-2337.

18. Brannigan, J.; Dodson, G.; Duggleby, H.; Moody, P.; Smith, J.; Tomchick, D.; Murzin, A., A protein catalytic framework with an N-terminal nucleophile is capable of self-activation. *Nature* **1995,** *378* (6555), 416-419.

19. Lin, Y.; Xu, J.; Hu, J.; Wang, L.; Ong, S.; Leadbetter, J.; Zhang, L., Acyl-homoserine lactone acylase from Ralstonia strain XJ12B represents a novel and potent class of quorum-quenching enzymes. *Molecular Microbiology* **2003,** *47* (3), 849-860.

20. Shepherd, R.; Lindow, S., Two Dissimilar N-Acyl-Homoserine Lactone Acylases of Pseudomonas syringae Influence Colony and Biofilm Morphology. *Applied and Environmental Microbiology* **2009,** *75* (1), 45-53.

21. Huang, J.; Petersen, A.; Whiteley, M.; Leadbetter, J., Identification of QuiP, the product of gene PA1032, as the second acyl-homoserine lactone acylase of Pseudomonas aeruginosa PAO1. *Applied and Environmental Microbiology* **2006,** *72* (2), 1190-1197.

22. Duran, R., Marinobacter. Springer-Verlag, Berlin: In: Timmis KN (ed) Handbook of hydrocarbon and lipid microbiology, 2010; pp 1726–1735.

23. Lin, H.; Fiscchbach, M.; Liu, D.; Walsh, C., In vitro characterization of salmochelin and enterobactin trilactone hydrolases IroD, IroE, and Fes. *Journal of the American Chemical Society* **2005,** *127* (31), 11075-11084.

24. Larsen, N.; Lin, H.; Wei, R.; Fischbach, M.; Walsh, C., Structural characterization of enterobactin hydrolase IroE. *Biochemistry* **2006,** *45* (34), 10184-10190.

25. Hantke, K.; Nicholson, G.; Rabschs, W.; Winkelmann, G., Salmochelins, siderophores of Salmonella enterica and uropathogenic Escherichia coli strains, are recognized by the outer membrane receptor IroN. *Proceedings of the National Academy of Sciences of the United States of America* **2003,** *100* (7), 3677-3682.

26. Bister, B.; Bischoff, D.; Nicholson, G.; Valdebenito, M.; Schneider, K.; Winkelmann, G.; Hantke, K.; Sussmuth, R., The structure of salmochelins: C-glucosylated enterobactins of Salmonella enterica. *Biometals* **2004,** *17* (4), 471-481.

IV. Identification of an acylase involved in marinobactin fatty acid hydrolysis from *Marinobacter nanhaiticus* D15-8W

4.1. Introduction

The hydrolysis of the marinobactins by BntA from *Marinobacter* sp. DS40M6 led us to wonder whether or not this reaction was happening in other marinobactin-producing species. The genome of *Marinobacter* sp. DS40M6 is not sequenced, however, due to the presence of both proteogenic and non-proteogenic amino acids in the marinobactin headgroup, it is likely the marinobactins are synthesized non-ribosomally by non-ribosomal peptide synthetases (NRPS). The general biosynthetic machinery used in NRPS-mediated biosynthesis has been well-studied resulting in the creation of many publicly available software programs that can be used to predict the structure of natural products based on the sequences of the encoded NRPS proteins.[1-4] Therefore, genome mining has become a very advantageous tool to predict 1) if siderophores and other natural products are being produced and 2) what the structure of the natural product might be.

This process of genome mining was used to search the genomes of sequenced *Marinobacter* species for putative NRPSs biosynthetic genes related to the marinobactins. *Marinobacter nanhaiticus* D15-8W, whose genome was recently published due to the bacterium's ability to hydrolyze polyaromatic hydrocarbons,[5] was determined to have biosynthetic genes predicted to produce marinobactin-like siderophores. *M. nanhaiticus* D15-8W is also predicted to have two putative acylases related to BntA and PvdQ. One acylase,

MhtA, is predicted to be a periplasmic enzyme while the other, MhtB, is predicted to be membrane associated like BntA. Due to the difficulties with cloning and expressing BntA, the predicted periplasmic protein, MhtA, was cloned and expressed in *E. coli* to investigate its activity with the marinobactins *in vitro*.

4.2 Experimental

4.2.1 Bacterial strains and plasmids

Bacterial strains and plasmids used in this study are listed in Table 4.1. *M. nanhaiticus* D15-8W was a generous gift from Professor Li Zheng (First Institute of Oceanography, State Oceanic Administration, China).[5] *Eschericia coli* strains were cultured in Luria Bertani (LB) broth or LB agar plates at 30°C or 37°C with shaking at 225 rpm. When required, the LB broth was supplemented with 100 μg/mL ampicillin.

Table 4.1. Bacterial strains and plasmids used in this study.

Strain or Plasmid	Relevant characteristics	Source or reference
Marinobacter strain		
D15-8W	Wild-type, marine isolate	Ref. 5
E. coli strain		
Top10	F⁻ mcrA Δ(mrr-hsdRMS-mcrBC) φ80lacZΔM15 ΔlacX74 recA1 araD139 Δ(ara-leu) 7697 galU galK rpsL (StrR) endA1 nupG λ-	Invitrogen
BL21-CodonPlus(DE3)-RIPL	B F⁻ ompT hsdS($r_B^-m_B^-$) dcm$^+$Tet^r gal λ(DE3) endA Hte [argU proL Cam^r] [argU ileY leuW Strep/Spec^r]	Agilent
Lemo21(DE3)	*fhuA2 [lon] ompT gal (λ DE3) [dcm] ΔhsdS/ pLemo*(Cam^R) *λ DE3 = λ sBamHIo ΔEcoRI-B int::(lacI::PlacUV5::T7 gene1) i21 Δnin5* pLemo = pACYC184-*PrhaBAD-lysY*	NEB
Plasmid		
pET22-a(+)	Expression vector with a T7 promoter, Amp	Novagen
p22-*mhtA*-His$_6$	*mhtA* cloned into the NdeI and XhoI sites of pET22a(+) with a C-terminal His-tag	This study

4.2.2 Bioinformatic analysis of *M. nanhaiticus* D15-8W

The publicly available BLAST (Basic Local Alignment Search Tool) algorithm from the NCBI (National center for Biotechnology Information) website was used to search for putative siderophore biosynthesis genes involving ornithine and serine, based on the published structure of the marinobactins.[6] The publicly available NRPS/PKS predictor software (http://nrps.igs.umaryland.edu/nrps/)[3] was used to predict the amino acid specificity of the adenylation domains from putative NRPS proteins, as well as, module composition and domain organization.

4.2.3 Isolation of marinobactins from *M. nanhaiticus* D15-8W

M. nanhaiticus D15-8W was grown in 2L of artificial seawater (ASW) media (15.5 g/L NaCl, 0.75 g/L KCl, 0.2 g/L $MgSO_4 \cdot 7H_2O$, 0.1 g/L $CaCl_2 \cdot 2H_2O$, 1.0 g/L NH_4Cl, 5 g/L succinic acid, 3 g/L Na_2HPO_4, pH 7.0) at ambient temperature with shaking at 180 rpm. The bacterium was harvested at 6,000 rpm (SLA-3000 rotor) for 30 minutes after approximately three days of growth for isolation of the full-length marinobactins or after 10 days of growth for isolation of the marinobactin headgroup. Following centrifugation, the supernatant was adsorbed onto 1/10 the volume of Amberlite XAD-2 resin, washed with 2 column volumes of water and eluted in 2 column volumes of 100% methanol. The XAD-2 eluents were concentrated by rotary evaporation. Siderophores were further purified by RP-HPLC on a C4 prep column (Higgins) using methanol + 0.05% TFA (solvent A) and nanopure water + 0.05% TFA (solvent B). The samples were eluted in a gradient from 100% solvent A to 100% solvent B over 100 minutes. The isolated siderophores were identified by electrospray

ionization mass spectrometry (ESI-MS) in combination with tandem mass spectrometry (ESI-MS/MS) using a Micromass QTOF-2 tandem mass spectrometer.

4.2.4 Cloning *mhtA* from *M. nanhaiticus* D15-8W

Genomic DNA was isolated from a 5 mL culture of *M. nanhaiticus* D15-8W grown in 2216 media using Proteinase K to digest proteins and phenol:chloroform:isoamyl alcohol (25:25:1) extractions to isolate and purify the DNA. Genomic DNA was used as a template in PCR to amplify gene, *eno13542* (termed *mhtA*), from *M. nanhaitius* D15-8W with forward primer: 5'-AATCCTCATATGAAAAACTTCATATTGGGCTAT-3' and reverse primer: 5'-TAGTTCTCGAGGTCTTCGTCTGAAAGCAACCT-3' (restriction sites underlined). The restriction site for NdeI was included at the 5' end of the forward primer. The stop codon from *mhtA* was removed and the XhoI restriction site was included on the reverse primer to result in a C-terminal 6X-His-tag. The insert was digested with NdeI and XhoI then ligated into the NdeI and XhoI digested sites of the pET22b(+) vector. The ligated samples were heat inactivated then digested with BamHI for 10 minutes at 37°C to remove non-digested pET22b(+) prior to transformation into *E. coli* TOP10 cells. The presence of the desired insert was detected by band-stab PCR. The sequences of the plasmid inserts were analyzed at the UC Berkeley sequencing facility.

4.2.5 Expression of *mhtA* in *E. coli*

The plasmid p22-*mhtA*-His_6 was transformed into *E. coli* BL21-CodonPlus(DE3)-RIPL cells for protein production. The cells were grown in 700 mL of LB + amp at 30°C, 225 rpm. Upon reaching an O.D.600 of 0.4, the cultures were induced with 0.4 mM IPTG overnight at 16°C, 225 rpm. Cells were harvested at 6,000 rpm for 10 minutes and either used

immediately or flash frozen and stored at -80°C. The cell pellet was resuspended in 10 mL of lysis buffer (20 mM sodium phosphate pH 7.8, 0.1 M NaCl, 5 mM imidazole, and 1% triton x-100) per gram of cells. The resuspended pellet was lysed by sonication (output control 2, amplitude at 40%, 10 seconds on/50 seconds off, X 3) on ice with stirring. The crude lysate was clarified by centrifugation at 10,000 x g for 15 minutes and the resulting supernatant was filtered through a 0.45 µm sterile filter. The filtered supernatant was combined with Ni-NTA resin (1 mL per 700 mL culture) pre-rinsed with binding buffer (20 mM sodium phosphate pH 7.8, 0.1 M NaCl, 5 mM imidazole, 0.1% triton x-100) for 2 hours at 4°C with mild agitation. The resin was loaded onto a gravity column and washed with 5 column volumes of wash buffer (20 mM sodium phosphate pH 7.8, 0.1 M NaCl, 20 mM imidazole, 0.1% triton x-100) then eluted with 3 column volumes of elution buffer (20 mM sodium phosphate pH 7.8, 0.1 M NaCl, 500 mM imidazole, 0.1% triton x-100). The eluted fractions were concentrated and buffer exchanged into activity buffer (20 mM Tris pH 8, 50 mM NaCl, 2 mM CaCl2) using a 50 MWCO spin column (2 mL, Millipore). The concentrated and eluted protein was analyzed on a 12% SDS-page gel stained with coomassie brilliant blue.

4.2.6 Western blot analysis of MhtA-His_6 expressed in *E. coli* Lemo21(DE3)

The p22-*mhtA*-His_6 plasmid was transformed into *E. coli* Lemo21(DE3) cells for expression and purification as stated above with *E. coli* BL21-CodonPlus(DE3)-RIPL cells. The concentrated Ni-NTA eluent was loaded (20 µl) onto two 12% SDS-page gels. One gel was stained with coomassie blue and the other gel was transferred to a nitrocellulose membrane at 100 V on ice for 1 hour. The membranes were blocked with blocking buffer (5% w/v dried milk + 0.01% v/v tween 20) for 1 hour at 4°C. An anti-6X His-tag monoclonal

mouse antibody was used as the primary antibody and was incubated with the membrane overnight at 4°C. The Alexa Fluor 488 anti-mouse antibody was used as the secondary antibody and was incubated with the membrane for 3 hours at 4°C. Samples were washed with 1X PBS following incubation with primary and secondary antibody and analyzed on a GE Typhoon.

4.2.7 *In vitro* activity analysis of MhtA-His_6 with the marinobactins

Siderophores used as substrates were isolated and purified as described above. The concentration of apo-marinobactins was determined by spectroscopic titration in 25 mM sodium phosphate buffer pH 8 at 400 nm with a stock solution of Fe(III) standardized with 1,10-phenanthroline. Fe(III)-marinobactins were obtained by adding 1.5 equivalents of $FeCl_3$ (1.8 mM in 10 mM HCl) to the apo-marinobactins for 15 minutes at ambient temperature. *In vitro* activity analysis of MhtA-His_6 with the marinobactins was performed using 50 μM substrate in 20 mM tris pH 8, 50 mM NaCl, 2 mM $CaCl_2$. As a control, *E. coli* BL21-CodonPlus(DE3)-RIPL cells without plasmid were lysed and purified in tandem with *E. coli* BL21-CodonPlus(DE3)-RIPL cells containing the MhtA expression plasmid and used in equal volumes for activity analysis. The reactions were performed in the presence of 10% methanol to increase the solubility of apo- and Fe(III)-marinobactins and to prevent micelle formation. All reactions were performed in 200 μl volumes and incubated at 30°C for 72 hours. Reactions were quenched by the addition of 0.5 volume of 2.5 N HCl. Protein was precipitated out by adding 5 volumes ice cold ethanol and incubated at -20°C for 1 hour to overnight followed by centrifugation at 12,000 rpm, 4°C, for 15 minutes. The supernatant was removed, diluted 1:5 in water and lyophilized to dryness.

The samples were resuspended in 200 µl of water and analyzed on a C18 analytical column at a flow rate of 1 ml/min using nanopure water + 0.05% TFA (solvent A) and acetonitrile + 0.05% TFA (solvent B) as mobile solvents with detection at 215 nm. The samples were eluted in in a gradient going from 100% A (hold for 3 minutes) to 100% B over 50 minutes.

4.2.8 Activity analysis of MhtA-His_6 with C12-HSL and C8-HSL

The activity of MhtA-His_6 with C12-HSL and C8-HSL was monitored under the same conditions as the marinobactins with the exception that 1 mM substrate was used in a 300 µl reaction volume. A 50 µl aliquot of the reaction mixture was removed at various time points and quenched by the addition of 0.5 volume of 2.5 N HCl. Protein was removed and samples were prepared to dryness as described in the previous section. The reaction was monitored by following the formation of the hydrolysis product, homoserine lactone, which was detected by derivatization with DANSYL chloride (5-dimethylamino-1-naphthalenesulphonyl chloride). The dried sample was resuspended in 100 µl of 50 mM sodium bicarbonate and adjusted to pH 9-10 with 3M NaOH. DANSYL chloride (20 ml of 50 mM in acetonitrile) was added to the sample and incubated for 30 minutes in the dark. Reactions were quenched by the addition of HCl, filtered through a 0.22 µM spin filters and analyzed by RP-HPLC at 254 nm using ddH_2O + 0.05% TFA and acetonitrile + 0.05% TFA as mobile solvents with detection at 254 nm. Samples were eluted starting in 100% solvent and holding for 3 minutes then moving to 50% solvent B over 30 minutes.

4.2.9 Activity analysis of MhtA-His_6 with C12-HSL in the presence of Fe(III)-M_A

It was investigated whether or not the Fe(III)-marinobactins have an inhibitory affect on MhtA-His_6 activity by monitoring the hydrolysis of C12-HSL following incubation of MhtA-His_6 with Fe(III)-M_A. MhtA-His_6 was incubated with either 10 μM Fe(III)-M_A or 10 μM apo-M_A in activity buffer (20 mM tris pH 8, 0.1 M NaCl, 2mM $CaCl_2$) to a total volume of 500 μL overnight at 30°C. An aliquot of C12-HSL in methanol was placed into a fresh eppendorf tube and dried overnight at 30°C to remove the solvent. The sample was prepared so the C12-HSL would have a final concentration of 1 mM in a 500 μL reaction volume. The MhtA-His_6 solution with either Fe(III)-M_A or apo-M_A was added to the dried C12-HSL and incubated for an additional 7 hours at 30°C. Aliquots of 200 μL were removed after 1 hour and 7 hours and quenched by the addition of 5 volumes of methanol followed by incubation for 1 hour at -20°C. The samples were prepared by reaction with DANSYL chloride and analyzed by RP-HPLC as previously described.

4.3 Results

4.3.1 Marinobactins produced by *M. nanhaiticus* D15-8W

To determine if other bacterial species produce the marinobactins and a marinobactin acylase, the genomes of sequenced *Marinobacter* species were screened for putative non-ribosomal peptide synthetases (NRPS) involved in siderophore biosynthesis and a *bntA*-like gene. NRPSs are large multi-modular synthetases comprised, at a minimum, of a condensation, adenylation, and thioesterase domain to incorporate amino acids into a growing peptide chain in an assembly line fashion.[2] *M. nanhaiticus* D15-8W contains two

genes, ENO16762 and ENO16763, annotated as putative NRPSs. Genes surrounding ENO16762 and ENO16763 encode for putative siderophore uptake, transport and tailoring enzymes suggesting these NRPSs are involved in siderophore biosynthesis (**Table 4.2**). Publicly available software (http://nrps.igs.umaryland.edu/nrps/) was used to predict the amino acid specificity of each adenylation domain.[4]

Table 4.2. Putative marinobactin biosynthesis and transport genes in the genome of *M. nanhaiticus* D15-8W.

Gene locus	Protein accession no. (GenBank)	Size (aa)	Predicted function
J057_03590	ENO16756	339	N-hydroxylornithine o-acetyltransferase
J057_03595	ENO16757	334	Taurine catabolism dioxygenase TauD/TfdA, aspartyl hydroxylase
J057_03600	ENO16758	68	MbtH domain-containing protein
J057_03605	ENO16759	304	ABC-type Fe3+-hydroxamate transport system
J057_03610	ENO16760	671	iron-hydroxamate transporter
J057_03615	ENO16761	753	TonB-dependent siderophore receptor
J057_03620	ENO16762	5348	NRPS
J057_03625	ENO16763	3219	NRPS
J057_03630	ENO16764	437	ornithine N-monooxygenase

The predicted biosynthetic scheme for marinobactin biosynthesis in *M. nanhaiticus* D15-8W is shown in Figure 4.1. The first module of gene ENO16763 has high similarity to acyl coenzyme A ligases as predicted by BLASTp analysis. Acyl coenzyme A ligases activate fatty acids by coupling coenzyme A with the fatty acid using ATP. Similar NRPS domains are present in the first module of other lipopeptide-producing NRPSs, such as, PvdL from *Pseudomonas aeruginosa,* which starts the biosynthesis of pyoverdine.[7] The adenylation (A) domain in module 2 (M2) is predicted to load L-aspartic acid, which might be epimerized to D-aspartic acid due to the presence of the epimerization domain. The hydroxylation of aspartic acid may be accomplished by gene ENO16757, which encodes a taurine catabolism

dioxygenase/aspartyl hydroxylase, based on homology. The third amino acid in the marinobactins is L-diaminobutyric acid, however, no prediction was made for the A domain of module 3 (M3). BLASTp analysis shows M3 to have homology to the pyoverdine biosynthetic protein, PvdL, which has an A domain specific for diaminobutyric acid. The A domain specific for diaminobutyric acid in PvdL has an 8 letter code of DIWELTXX similar to the 8 letter code of the A domain in M3 of *M. nanhaiticus* D15-8W, DIWELTA-, suggesting this domain could be specific for diaminobutyric acid.[7,4] It is not known what enzyme might be responsible for the cyclization of aspartic acid and diaminobutryic acid, however, condensation and condensation-like cyclization (cyc) domains are known to catalyze cyclization of cysteine, serine, and threonine residues forming heterocyclic ring moieties.[8]

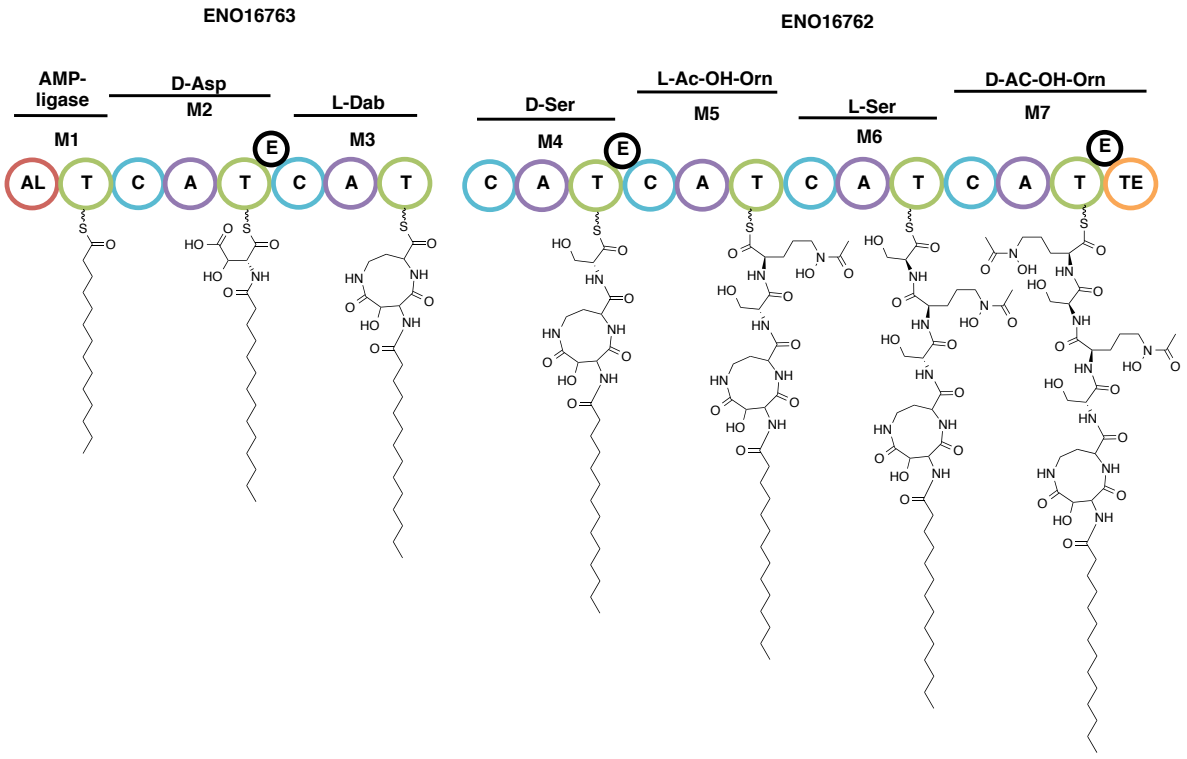

Figure 4.1. Predicted biosynthetic scheme for marinobactins in *M. nanhaiticus* D15-8W (the FA tail can be C12:0, C14:0, C16:1 or C16:0). Biosynthesis is predicted to begin with acetylation by the AL (Acyl-CoA ligase) domain. Biosynthesis is predicted to occur in a linear fashion using traditional NRPS logic (T = thiolation domain, C = condensation domain, A = adenylation domain, E = epimerase domain, TE = thioesterase domain).

NRPS protein ENO16762 was predicted to have adenylation domains specific for L-serine, L-N^5-acetyl-N^5-hydroxyornithine, L-serine, and L-N^5-acetyl-N^5-hydroxyornithine followed by a thioesterase domain. Two epimerases are predicted to convert the first added serine and last L-N^5-acetyl-N^5-hydroxyornithine to the D-configuration. These predictions correspond to the amino acids present in the marinobactin headgroup attached to a N-terminal fatty acid appendage.

4.3.2 Isolation of marinobactins from *M. nanhaiticus* D15-8W

To determine whether *M. nanhaiticus* D15-8W produced the marinobactin siderophores as predicted, siderophores were isolated from a culture of *M. nanhaiticus* D15-8W grown in iron-limited ASW media. Five major peaks were seen in the RP-HPLC profile and subjected to mass spectrometry analysis (Figure 4.2). The compounds in peaks 1-5 were identified by comparing the masses and ESI-MS/MS fragmentation patterns to the published structure of the marinobactins.[6,9] Peak 1 was identified as M_{HG} (*m/z* 750) suggesting *M. nanhaiticus* D15-8W produces the marinobactins and a BntA-like acylase able to catalyze the hydrolysis of the fatty acid appendage from the marinobactin headgroup (Figure 4.3). Peak 2 was identified as marinobactin A (M_A; *m/z* 932 $[M+H]^+$) with a C12:0 fatty acid (Figure 4.4). Peaks 3, 4 and 5 were identified as M_C (C14:0; *m/z* 960 $[M+H]^+$, Figure 4.5), M_D (C16:1; *m/z* 986 $[M+H]^+$, **Figure 4.6**), and M_E (C16:0; *m/z* 988 $[M+H]^+$, Figure 4.7), respectively. Production of marinobactin B (C14:1) was not observed in the cultures of *M. nanhaiticus* D15-8W, although the other members of the suite of acyl marinobactins are produced by *M. nanhaiticus* D15-8W, as well as the marinobactin headgroup, consistent with what has been previously seen with *Marinobacter* sp. DS40M6.[9]

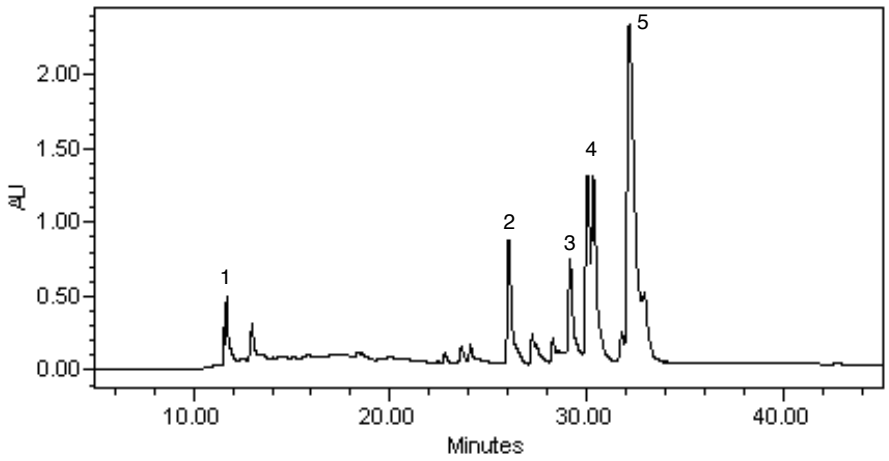

Figure 4.2. Analysis of siderophores isolated from the supernatant of *M. nanhaiticus* D15-8W when grown in iron-limited media by RP-HPLC monitored at 215 nm. Peak 1 corresponds to M_{HG}, peak 2 is M_A, peak 3 is M_C, peak 4 is M_D and peak 5 is M_E.

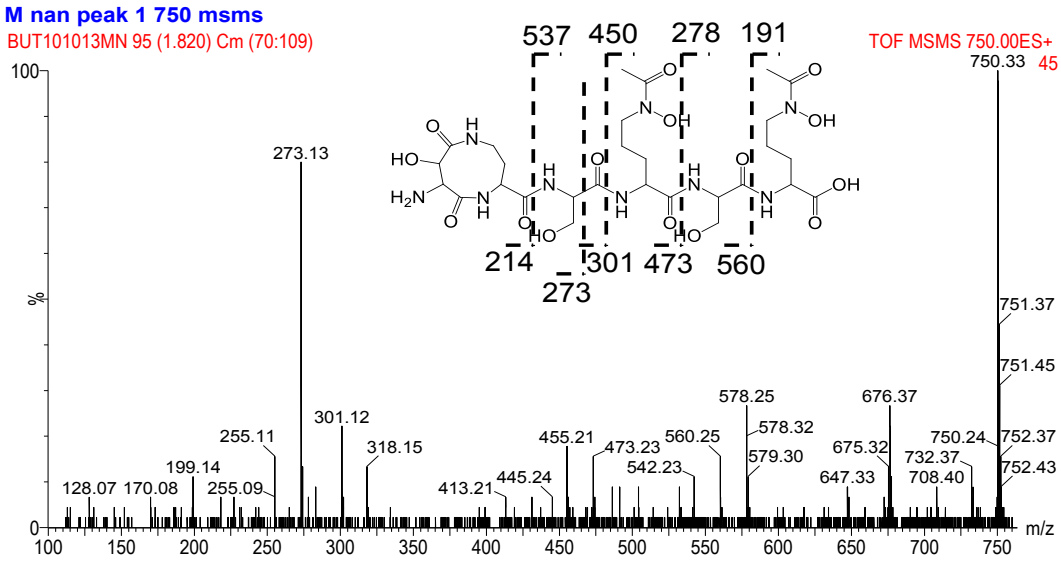

Figure 4.3. ESI-MS/MS analysis of peak 1 corresponding to M_{HG} from the RP-HPLC analysis of siderophores isolated from the supernatant of *M. nanhaiticus* D15-8W when grown in iron-limited media.

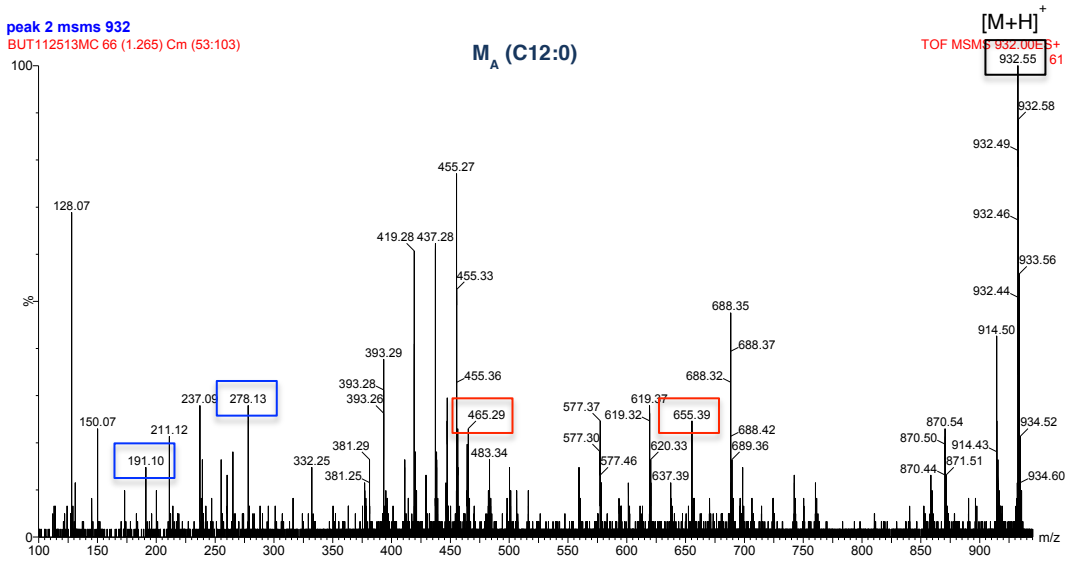

Figure 4.4. ESI-MS/MS analysis of peak 2 from the RP-HPLC analysis of siderophores isolated from the supernatant of *M. nanhaiticus* D15-8W when grown in iron-limited media.

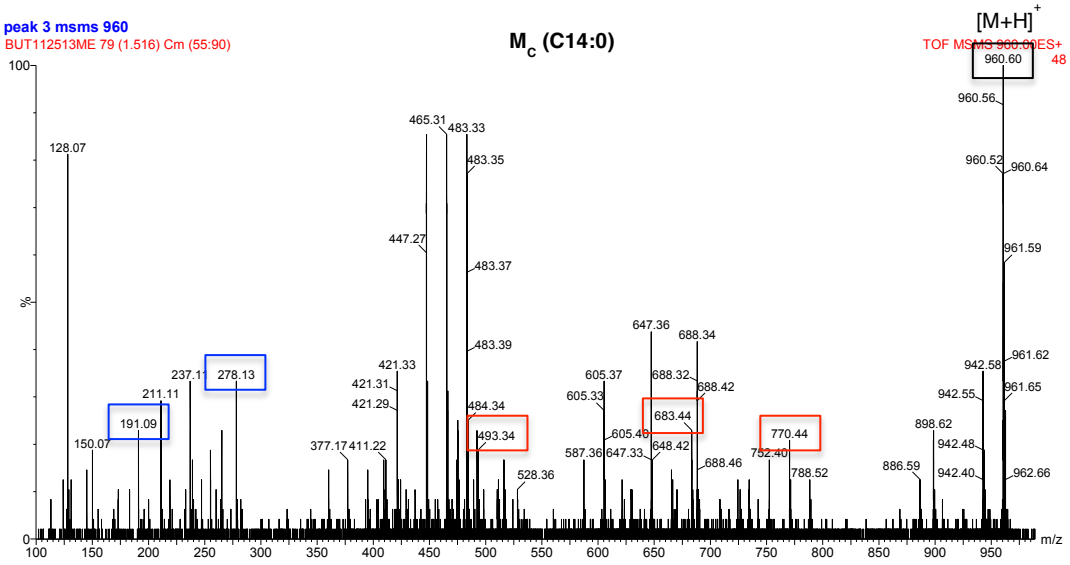

Figure 4.5. ESI-MS/MS analysis of peak 3 from the RP-HPLC analysis of siderophores isolated from the supernatant of *M. nanhaiticus* D15-8W when grown in iron-limited media.

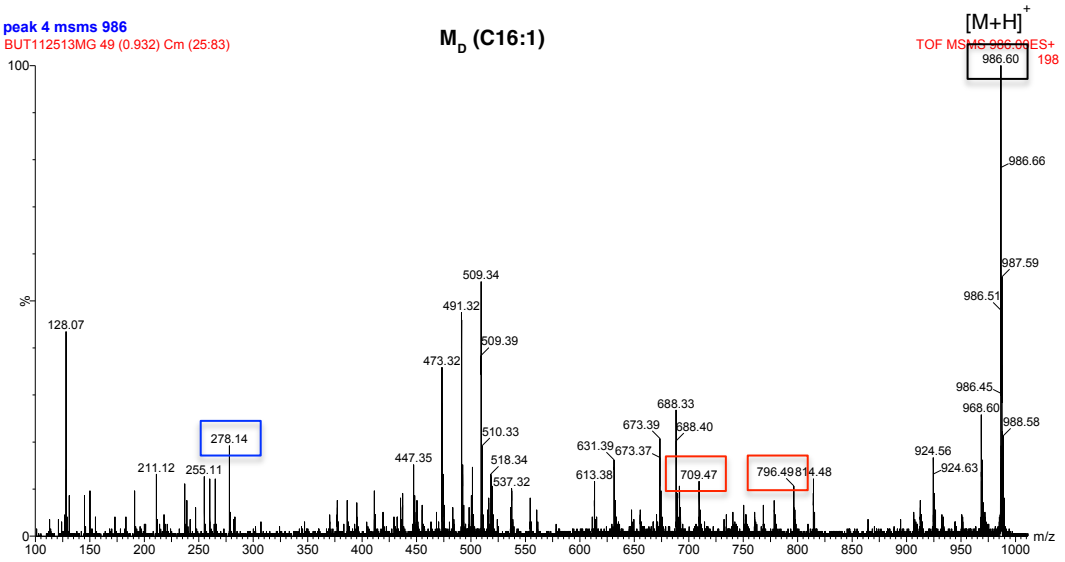

Figure 4.6. ESI-MS/MS analysis of peak 4 from the RP-HPLC analysis of siderophores isolated from the supernatant of *M. nanhaiticus* D15-8W when grown in iron-limited media.

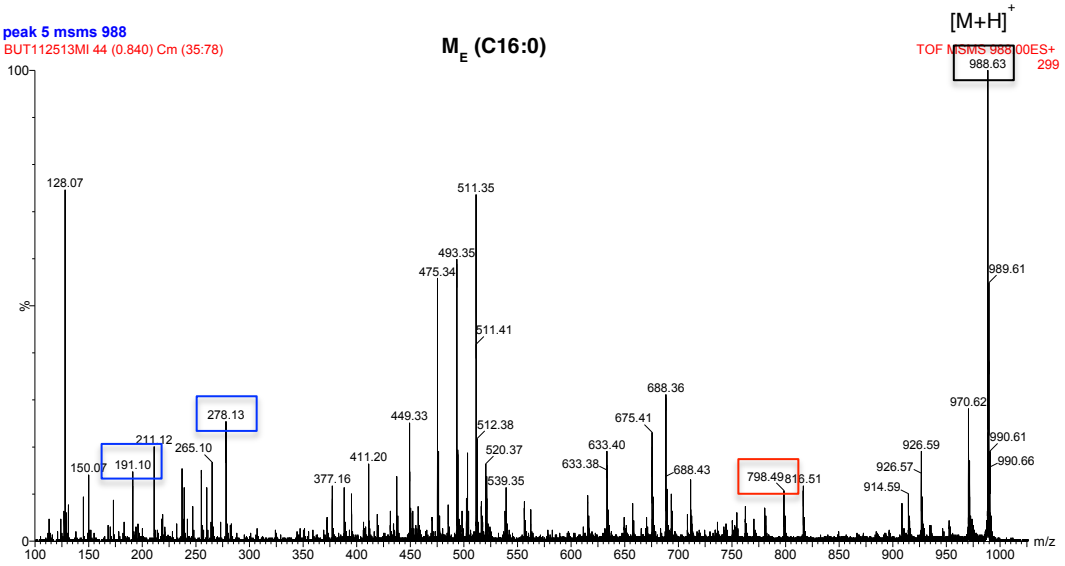

Figure 4.7. ESI-MS/MS analysis of peak 5 from the RP-HPLC analysis of siderophores isolated from the supernatant of *M. nanhaiticus* D15-8W when grown in iron-limited media.

4.3.3 Screening the *M. nanhaiticus* D15-8W genome for potential marinobactin acylases

The *M. nanhaiticus* D15-8W genome was screened for homologues of *bntA* from *Marinobacter* sp. DS40M6 and *pvdQ* from *P. aeruginosa* PAO1 using BLASTp analysis. Two genes, ENO13542 (named *mhtA*) and ENO13543 (named *mhtB*), were annotated as acyl-homoserine lactone acylases and have a 30% and 31% identity to PvdQ from *P. aeruginosa*, respectively, and a 67% identity to each other. The BLASTp analysis of MhtA and MhtB predict both proteins to be part of the Ntn-hydrolase family, like PvdQ. Publicly available software (http://www.psort.org/psortb/index.html) was used to predict the cellular location of each protein with MhtB predicted to be an outer membrane-associated protein and MhtA predicted to be a periplasmic protein. Using the same software program, BntA, from *Marinobacter* sp. DS40M6 was also predicted to be membrane-associated and has a slightly higher percent identity to the predicted outer membrane protein, MhtB, at 63% versus 58% with MhtA. Therefore, due to solubility issues with the recombinant expression of BntA, the predicted periplasmic protein, MhtA, from *M. nanhaiticus* D15-8W was selected for our initial investigation. We cloned and overexpressed the *mhtA* gene to investigate fatty acid hydrolysis with the marinobactins and acyl-homoserine lactones.

4.3.4 Cloning and expression of *mhtA* in *E. coli*

Gene, *mhtA*, was amplified by PCR from the genomic DNA of *M. nanhaiticus* D15-8W. An analysis of the PCR reaction on a 1% agarose gel resulted in the appearance of a band between 2.5 kb and 3.0 kb (Figure 4.8), which is around the size of the expected 2682 bp

mhtA gene. The *mhtA* gene was ligated into the NdeI and XhoI sites of the pET22b(+) expression vector resulting in the 6X C-terminal His-tagged plasmid, p22-*mhtA*-His_6.

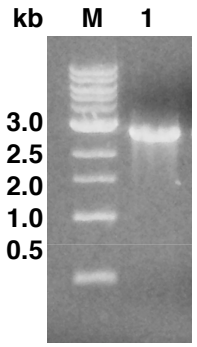

Figure 4.8. Agarose gel analysis of PCR amplified *mhtA* gene from *M. nanhaiticus* D15-8W genomic DNA. M = molecular weight marker, 1 = amplified *mhtA* gene.

For expression of MhtA-His_6 in *E. coli*, p22-*mhtA*-His_6 was transformed into *E. coli* BL21-CodonPlus(DE3)-RIPL cells. As a control, *E. coli* BL21-CodonPlus(DE3)-RIPL cells without the p22-*mhtA*-His_6 plasmid were grown and isolated in tandem. An SDS-page analysis of induced *E. coli* BL21-CodonPlus(DE3)-RIPL + p22-*mhtA*-His_6 cultures resulted in the appearance of a 100 kDa band when compared to the *E. coli* without plasmid control (Figure 4.9). By comparison to other Ntn-hydrolases (e.g. PvdQ), this is the correct mass for the unprocessed polypeptide prior to the self-activation that all Ntn-hydrolases undergo,[10] and the same was observed with overexpression of BntA-His_6 from *Marinobacter* sp. DS40M6. An SDS-page gel analysis of Ni-NTA enriched extracts from p22-*mhtA*-His_6 in *E. coli* BL21-CodonPlus(DE3)-RIPL cells resulted in the same protein band pattern as the *E. coli* BL21-CodonPlus(DE3)-RIPL cells only control (Figure 4.9). This suggests that the majority of the protein is being expressed in the insoluble fraction.

While the expression level of MhtA-His_6 was too low to identify an α-subunit (~25 kDa) and a β-subunit (~70 kDa) of the active form of the enzyme unambiguously on a gel, active enzyme was found to be present through an activity assay, namely, the hydrolysis of octanoyl-*p*-nitroaniline, which produces the yellow *p*-nitroanaline product (Figure 4.10).[11] Sequencing of the p22-*mhtA*-His_6 plasmid insert revealed one mutation, S474G, however, this mutation did not appear to affect the enzyme activity. This preparation of MhtA-His_6 was used to investigate hydrolysis of the acyl marinobactins *in vitro*.

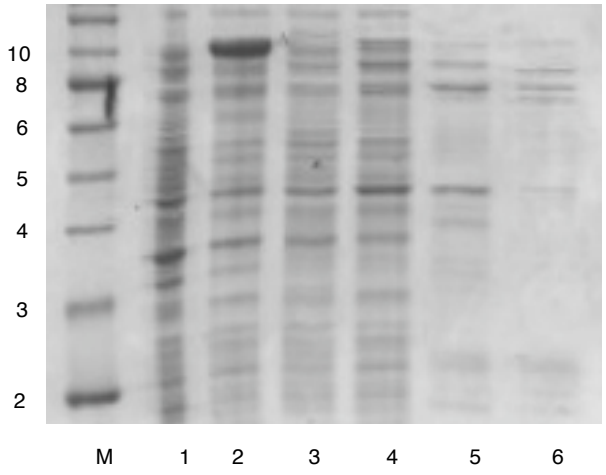

Figure 4.9 SDS-page analysis of MhtA-His_6 in *E. coli* compared to *E. coli* cells alone. (M) Molecular weight marker (1) Induced lysate *E. coli* only (2) induced lysate p22-*mhtA*-His_6 in *E. coli* (3) soluble fraction *E. coli* only (4) soluble fraction p22-*mhtA*-His_6 in *E. coli* (5) Ni-NTA eluent *E. coli* only (6) Ni-NTA eluent p22-*mhtA*-His_6 in *E. coli*.

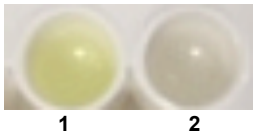

Figure 4.10. The presence of active MhtA-His_6 following expression in *E. coli* and purification using Ni-NTA resin was determined by incubation with the colorimetric substrate octanoyl-pNA. (1) octanoyl-pNA incubated with purified MhtA-His_6; (2) octanoyl-pNA incubated with the *E. coli* only control.

4.3.5 Western blot analysis of MhtA expressed in *E. coli* Lemo21(DE3)

A Western blot analysis was performed on MhtA-His_6 expressed in *E. coli* Lemo21(DE3) cells to identify the His-tagged β-subunit of MhtA. Due to the lack of affinity tag on the α-subunit of MhtA, only the β-subunit could be detected by this method. Two 12% SDS-page gels were loaded with 20 μL of MhtA-His_6, which was purified by Ni-NTA resin then stored at 4°C for a month and a half. The SDS-page gel analysis of the sample looks much different than what has been previously seen with the expression of the enzyme (Figure 4.11). Two very distinct bands around 75 kDa and 23 kDa appear on the coomassie stained gel that are not normally seen following MhtA-His_6 purification. The identity of the band around 75 kDa was confirmed as the β-subunit of MhtA by Western blot analysis (Figure 4.11). The increase in production of fully processed MhtA-His_6 is possibly due to the long incubation time at 4°C, which might be necessary to let the auto-processing of the enzyme occur.

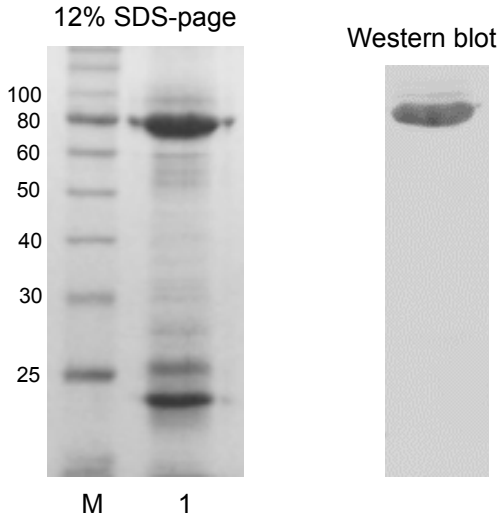

Figure 4.11. (Left) 12% SDS-page analysis of MhtA-His_6 expressed in Lemo21(DE3) and purified using Ni-NTA resin. (Right) Western blot analysis of the SDS-page gel.

4.3.6 Reactivity of MhtA-His$_6$ with the marinobactins

Hydrolysis of the marinobactins by the putative periplasmic *M. nanhaiticus* D15-8W Ntn-hydrolase, MhtA, was monitored *in vitro*. Incubation of MhtA-His$_6$ with 50 μM apo-M_A resulted in the appearance of a peak around 11 minutes (Figure 4.12). ESI-MS analysis of this peak showed a parent ion of *m/z* 750 ($[M+H]^+$) with fragmentation ions of *m/z* 560, *m/z* 473, and *m/z* 273 as previously reported for M_{HG} (Figure 4.13).[12] Incubation of MhtA-His$_6$ with 50 μM apo-M_E also produced M_{HG}; however, M_E with a C16:0 fatty acid tail appears to be hydrolyzed at a slower rate than M_A with a C12:0 fatty acid tail (Figure 4.14); however, it is possible that the lower solubility and CMC (critical micelle concentration) of M_E is prohibiting the enzyme from hydrolyzing this substrate under the experimental conditions used. This preference of substrate based on the length of the fatty acid was also seen with PvdQ and other quorum quenching acylases.[13,14,15,16]

To explore the activity of MhtA-His$_6$ with the Fe(III)-bound marinobactins, recombinant MhtA-His$_6$ was incubated with 50 μM Fe(III)-M_A under the same conditions as the apo-marinobactins. After 72 hours of incubation no hydrolysis of the iron bound siderophore was observed (Figure 4.12). Likewise, Fe(III)-M_E was not hydrolyzed (Data not shown). The geometry and conformation of the apo-marinobactins change when bound to Fe(III), possibly blocking access of the amide bond to the serine nucleophile.[17] A change in marinobactin conformation could also prevent access of the substrate at the active site all-together. The inability of MhtA to hydrolyze ferric marinobactins is of interest due to the potential regulatory role it might serve with respect to marinobactin hydrolysis and iron uptake.

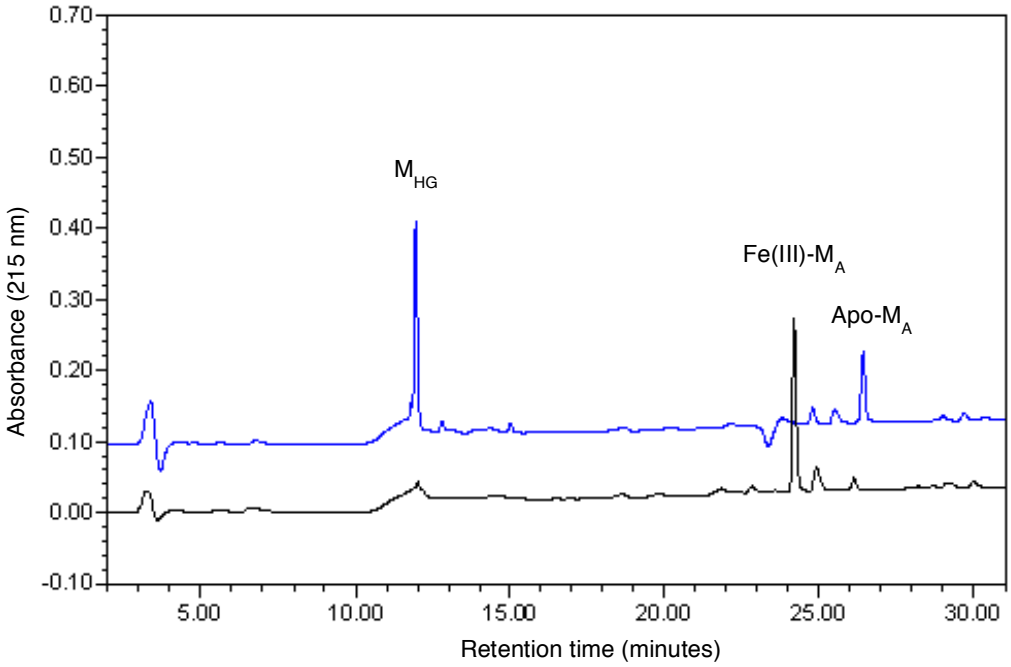

Figure 4.12. RP-HPLC of MhtA-His_6 with apo-M_A (blue) and Fe(III)-M_A (black) monitored at 215 nm.

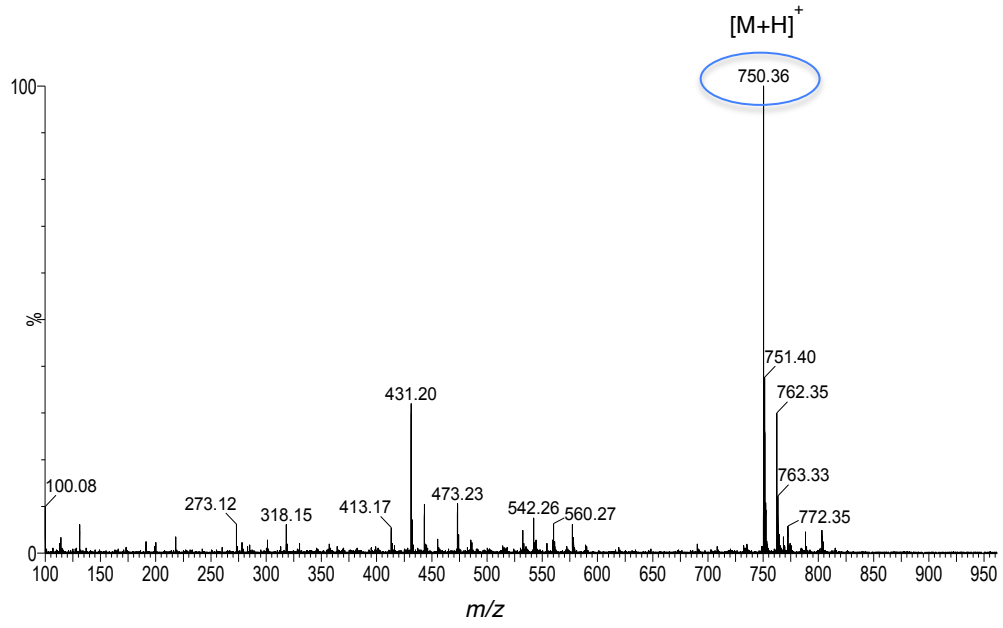

Figure 4.13. ESI-MS analysis of RP-HPLC peak at 11 minutes from the catalyzed hydrolysis of apo-M_A with MhtA-His_6.

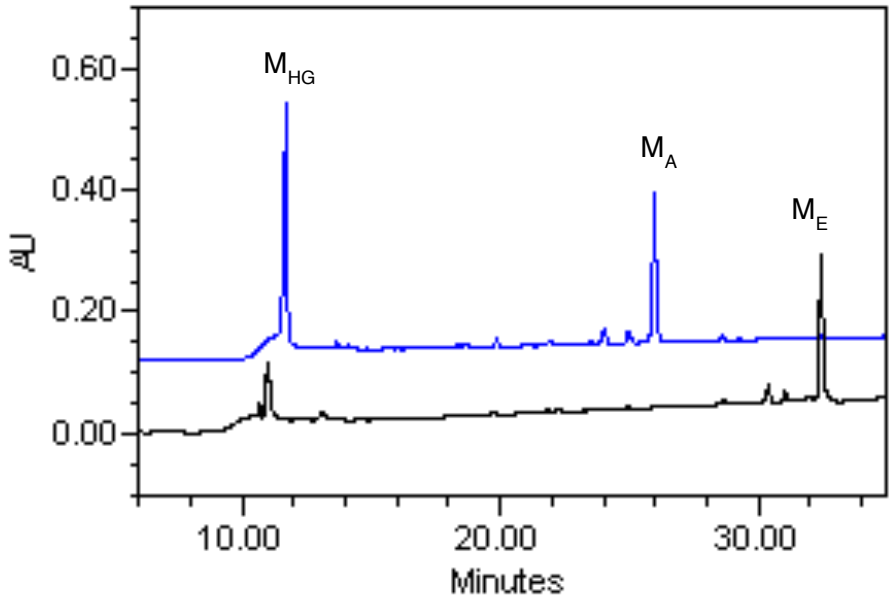

Figure 4.14. RP-HPLC of MhtA-His_6 with apo-M_A (blue) and apo-M_E (black) monitored at 215 nm.

4.3.7 Reactivity of MhtA-His_6 with C8-HSL and C12-HSL

PvdQ and other quorum quenching Ntn-hydrolases have been shown to hydrolyze the quorum sensing molecules, acyl-homoserine lactones; therefore, the activity of MhtA-His_6 with C12-HSL was also monitored using *E. coli* BL21-CodonPlus(DE3)-RIPL cells only as a control. The acyl homoserine lactone with a C12 fatty acid was used since M_A also has a C12 fatty acid. The formation of the hydrolysis product, homoserine lactone, was monitored by derivatization with 5-dimethylamino-1-naphthalenesulphonyl chloride (DANSYL chloride) to increase the hydrophobicity of the homoserine lactone product for analysis by RP-HPLC at 254 nm as shown in Figure 4.15. A peak around 17 minutes is observed when the hydrolysis product of MhtA-His_6 and C12-HSL is reacted with DANSYL chloride. This same peak does not appear in the control after 7 hours of incubation. ESI-MS analysis of this

peak showed an m/z value of 353 corresponding to DANSYL homoserine (Figure 4.16). The high pH for the derivatization reaction with DANSYL chloride hydrolyzes the ester bond in the lactone ring resulting in the formation of DANSYL homoserine instead of DANSYL homoserine lactone.

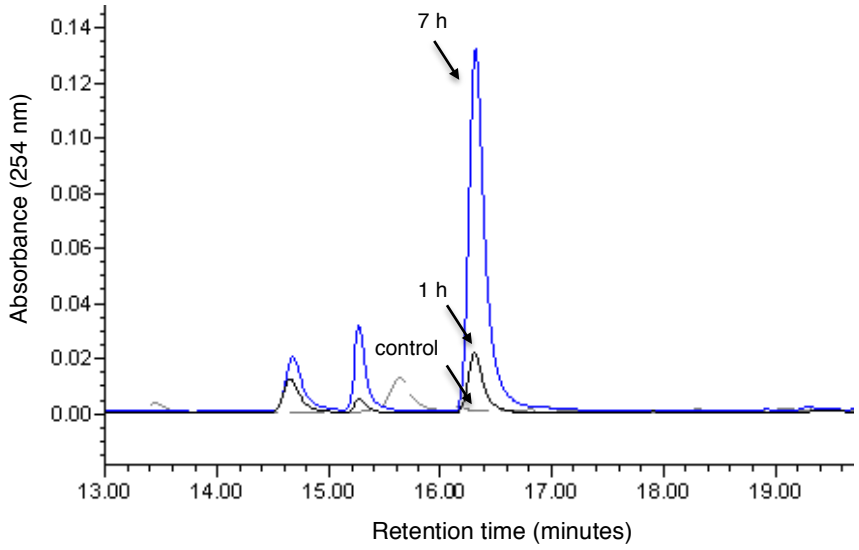

Figure 4.15. RP-HPLC of the C12-HSL hydrolysis product derivatized with DANSYL chloride following incubation with MhtA-His_6 from 1-7 hours.

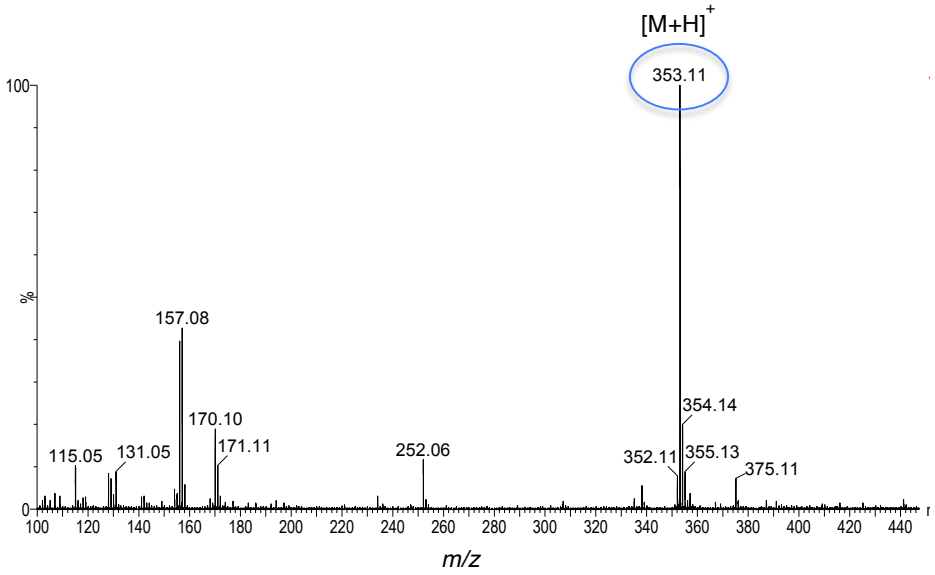

Figure 4.16. ESI-MS analysis of the peak eluting at 17 minutes corresponding to the $[M+H]^+$ of DANSYL homoserine.

The hydrolysis of C8-HSL was also monitored with MhtA-His_6 to see if MhtA could hydrolyze shorter acyl homoserine lactones as well. The reaction was run under the same conditions as performed with C12-HSL and the hydrolysis product was detected by derivatization with DANSYL chloride. After 5 minutes of reaction time, the hydrolysis product could already be detected and the concentration increased over the course of seven hours (Figure 4.17). Cell-free extracts of *Marinobacter* sp. DS40M6 were shown to catalyze the hydrolysis of C8-HSL suggesting BntA could possibly catalyze this reaction too.[9]

The majority of sequenced *Marinobacter* species are predicted to have acylases similar to BntA and MhtA, however, most of these species do not have the biosynthetic genes for marinobactin production and it is not known if the *Marinobacter* species produce or respond to acyl-homoserine lactones as quorum sensing signaling molecules. Previous studies, however, have shown that some bacteria with acyl homoserine lactone acylases can use the

fatty acid products as sole carbon sources during growth, as in the case of QuiP from *P. aeruginosa* and AiiD from *Ralstonia* sp. XJ12B.[14,18]

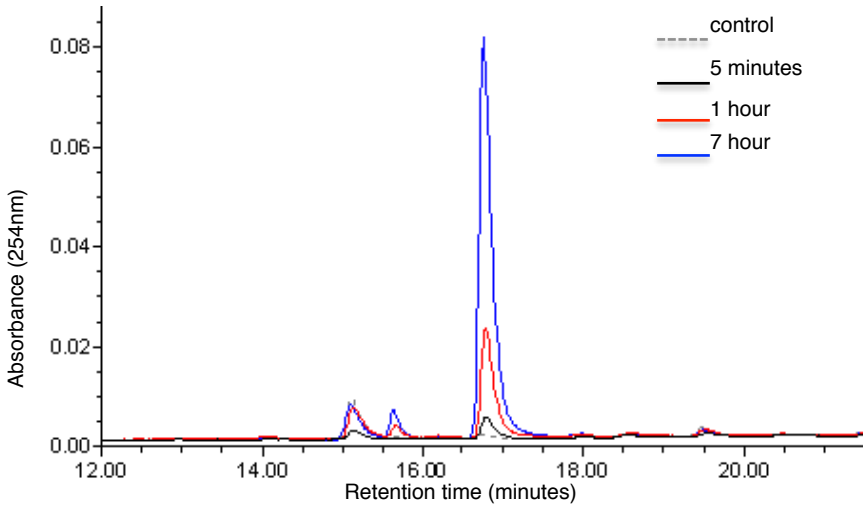

Figure 4.17. RP-HPLC showing DANSYL homoserine formation following the catalyzed hydrolysis of C8-HSL by MhtA-His_6 over time.

4.3.8 Inhibition analysis of MhtA-His_6 by Fe(III)-M_A

A preliminary analysis on the potential inhibition of MhtA-His_6 by the Fe(III)-marinobactins was performed by monitoring the hydrolysis of C12-HSL by MhtA following overnight incubation with Fe(III)-M_A. MhtA was incubated with equal amounts of apo-M_A as a control. The hydrolysis product, homoserine lactone, was derivatized with DANSYL chloride for analysis by RP-HPLC at 254 nm. After 1 hour of incubation with C12-HSL, a small peak around 17 minutes appears in both samples (Figure 4.18A). After 7 hours of incubation, the peak around 17 minutes increases equally for each sample (Figure 4.18B) suggesting that Fe(III)-M_A does not inhibit MhtA-His_6 under the experimental conditions used. Prior inhibition of marinobactin hydrolysis was seen in crude enzyme preps from

Marinobacter sp. DS40M6 when Fe(III)-marinobactins were added to the reaction;[20] however, the iron bound marinobactins do not appear to inhibit MhtA under the experimental conditions used.

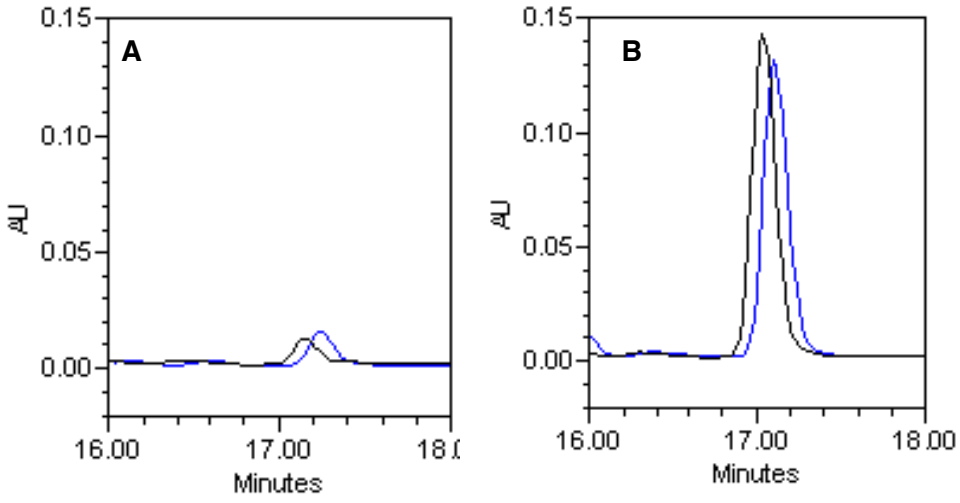

Figure 4.18. RP-HPLC analysis of DANSYL homoserine lactone formation following incubation of MhtA-His_6 with C12-HSL after overnight incubation with apo-M_A (blue) or Fe(III)-M_A (black) after 1 hour (A) and 7 hours (B).

4.4 Discussion

Marinobacter nanhaiticus D15-8W was shown to produce the marinobactin siderophores, which are also converted into M_{HG} during bacterial growth. *M. nanhaiticus* D15-8W has two BntA-like acylases, MhtA and MhtB, with MhtA predicted to be periplasmic and MhtB membrane associated. To avoid the insolubility of the membrane-associated BntA, the predicted periplasmic MhtA was used for an *in vitro* activity analysis with the marinobactins. Incubation of MhtA-His_6 with the marinobactins produced M_{HG} as detected by RP-HPLC and ESI-MS/MS, where the hydrolysis of M_A appeared to be favored over M_E under the

experimental conditions used. Interestingly, however, the hydrolysis of the Fe(III)-bound marinobactins to produce Fe(III)-M_{HG} did not occur.

It is not known if the biological substrates of MhtA are the marinobactins even though they have the capability to degrade them or how MhtB might be involved in this process. The predicted outer membrane association of MhtB corresponds to the hypothesis that the marinobactins are hydrolyzed following excretion into the extracellular milieu; however, it is unclear how the predicted periplasmic localization of MhtA allows access to excreted marinobactins. It is possible that MhtA can process acyl marinobactins taken up by the cell as a form of siderophore recycling. Hydrolysis of the fatty acid from the amphiphilic marinobactins would produce a more hydrophilic siderophore without altering the iron chelating properties. The fatty acid tail provides a way to keep the siderophore close to the bacterial membrane so it is not lost through diffusion. However, at high bacterial populations, a more hydrophilic siderophore could be released and used by nearby bacteria while providing a fatty acid hydrocarbon source. In sum, we propose that the putative Ntn-hydrolases, MhtA from *M. nanhaiticus* D15-8w, is able to hydrolyze the fatty acid appendage from the marinobactins during bacterial growth, releasing the marinobactin head group.

4.5 References

1. Challis, G.; Ravel, J.; Townsend, C., Predictive, structure-based model of amino acid recognition by nonribosomal peptide synthetase adenylation domains. *Chemistry & Biology* **2000,** *7* (3), 211-224.

2. Crosa, J.; Walsh, C., Genetics and assembly line enzymology of siderophore biosynthesis in bacteria. *Microbiology and Molecular Biology Reviews* **2002,** *66* (2), 223-+.

3. Stachelhaus, T.; Mootz, H.; Marahiel, M., The specificity-conferring code of adenylation domains in nonribosomal peptide synthetases. *Chemistry & Biology* **1999,** *6* (8), 493-505.

4. Bachmann, B. O.; Ravel, J., Methods for In Silico Prediction of Microbial Polyketide and Nonribosomal Peptide Biosynthetic Pathways from DNA Sequence Data. Methods in Enzymology: 2009; Vol. 458, pp 181-217.

5. Gao, W.; Cui, Z.; Li, Q.; Xu, G.; Jia, X.; Zheng, L., Marinobacter nanhaiticus sp nov., polycyclic aromatic hydrocarbon-degrading bacterium isolated from the sediment of the South China Sea. *Antonie Van Leeuwenhoek International Journal of General and Molecular Microbiology* **2013,** *103* (3), 485-491.

6. Martinez, J.; Zhang, G.; Holt, P.; Jung, H.; Carrano, C.; Haygood, M.; Butler, A., Self-assembling amphiphilic siderophores from marine bacteria. *Science* **2000,** *287* (5456), 1245-1247.

7. Schalk, I.; Guillon, L., Pyoverdine biosynthesis and secretion in Pseudomonas aeruginosa: implications for metal homeostasis. *Environmental Microbiology* **2013,** *15* (6), 1661-1673.

8. Rausch, C.; Hoof, I.; Weber, T.; Wohlleben, W.; Huson, D., Phylogenetic analysis of condensation domains in NRPS sheds light on their functional evolution. *Bmc Evolutionary Biology* **2007,** *7*.

9. Gauglitz, J.; Inishi, A.; Ito, Y.; Butler, A., Microbial Tailoring of Acyl Peptidic Siderophores. *Biochemistry* **2014,** *53* (16), 2624-2631.

10. Oinonen, C.; Rouvinen, J., Structural comparison of Ntn-hydrolases. *Protein Science* **2000,** *9* (12), 2329-2337.

11. Patricelli, M.; Cravatt, B., Characterization and manipulation of the acyl chain selectivity of fatty acid amide hydrolase. *Biochemistry* **2001,** *40* (20), 6107-6115.

12. Gauglitz, J. M.; Iinishi, A.; Ito, Y.; Butler, A., Microbial Tailoring of Acyl Peptidic Siderophores. Biochemistry: 2014; Vol. 53, pp 2624-2631.

13. Drake, E.; Gulick, A., Structural Characterization and High-Throughput Screening of Inhibitors of PvdQ, an NTN Hydrolase Involved in Pyoverdine Synthesis. *Acs Chemical Biology* **2011,** *6* (11), 1277-1286.

14. Huang, J.; Petersen, A.; Whiteley, M.; Leadbetter, J., Identification of QuiP, the product of gene PA1032, as the second acyl-homoserine lactone acylase of Pseudomonas aeruginosa PAO1. *Applied and Environmental Microbiology* **2006,** *72* (2), 1190-1197.

15. Chen, C.; Chen, C.; Liao, C.; Lee, C., A probable aculeacin A acylase from the Ralstonia solanacearum GMI1000 is N-acyl-homoserine lactone acylase with quorum-quenching activity. *Bmc Microbiology* **2009,** *9*.

16. Shepherd, R.; Lindow, S., Two Dissimilar N-Acyl-Homoserine Lactone Acylases of Pseudomonas syringae Influence Colony and Biofilm Morphology. *Applied and Environmental Microbiology* **2009,** *75* (1), 45-53.

17. Xu, G.; Martinez, J.; Groves, J.; Butler, A., Membrane affinity of the amphiphilic marinobactin siderophores. *Journal of the American Chemical Society* **2002,** *124* (45), 13408-13415.

18. Lin, Y.; Xu, J.; Hu, J.; Wang, L.; Ong, S.; Leadbetter, J.; Zhang, L., Acyl-homoserine lactone acylase from Ralstonia strain XJ12B represents a novel and potent class of quorum-quenching enzymes. *Molecular Microbiology* **2003,** *47* (3), 849-860.

19. Duran, R., Marinobacter. In: Timmis KN (ed) Handbook of hydrocarbon and lipid microbiology, 2010; pp 1726–1735.

20. Iinishi, A. Microbial Hydrolysis of Fatty Acid Amides of Amphiphilic Marine Siderophores. University of California, Santa Barbara, Santa Barbara, 2008.

V. Enzymatic hydrolysis of the amphi-enterobactins produced by *Vibrio harveyi* BAA-1116

5.1 Introduction

The amphi-enterobatins are produced by the bioluminescent marine bacterium, *Vibrio harveyi* BAA-1116 (recently classified as *Vibrio campbellii*).[1] The amphi-enterobactins are an acylated form of the prototypic siderophore, enterobactin. Unlike enterobactin, the amphi-enterobactins have an additional serine residue to form a tetralactone backbone, which is acylated with a C10-C14 fatty acid (Figure 5.1).[1] The fatty acids are found in hydroxylated, saturated, and unsaturated forms. The amphi-enterobactins are very hydrophobic and are isolated from the cell membrane following centrifugation.

A compound capable of chelating Fe(III) was also isolated from the cell-free supernatant of *V. Harveyi* BAA-1116 when grown in a low-iron media.[2] The compound is a dimer of 2,3-dihydroxybenzoyl-L-Serine (2,3-DHBA-L-Ser) as determined by ESI-MS and ESI-MS/MS. This dimer corresponds to the amphi-enterobactins minus one 2,3-DHBA-L-Ser and one L-Ser-FA. No biosynthetic genes for 2,3-DHBA-L-Ser are present beyond the amphi-enterobactin biosynthetic gene cluster suggesting the dimer is formed from an enzyme catalyzed hydrolysis of the amphi-enterobactins (Figure 5.1).[2]

The *V. Harveyi* BAA-1116 genome was analyzed to discover an esterase that could selectively hydrolyze the amphi-enterobactins to produce the 2,3-DHBA-L-Ser dimer.

Eighteen putative esterases are encoded in the genome of *V. harveyi* BAA-1116. We cloned potential amphi-enterobactin esterases and monitored their esterase activity using amph-enterobactin C12-OH as a substrate. An amphi-enterobactin esterase would provide another example of how bacteria can modify the structure of their siderophores following biosynthesis to change their physical properties.

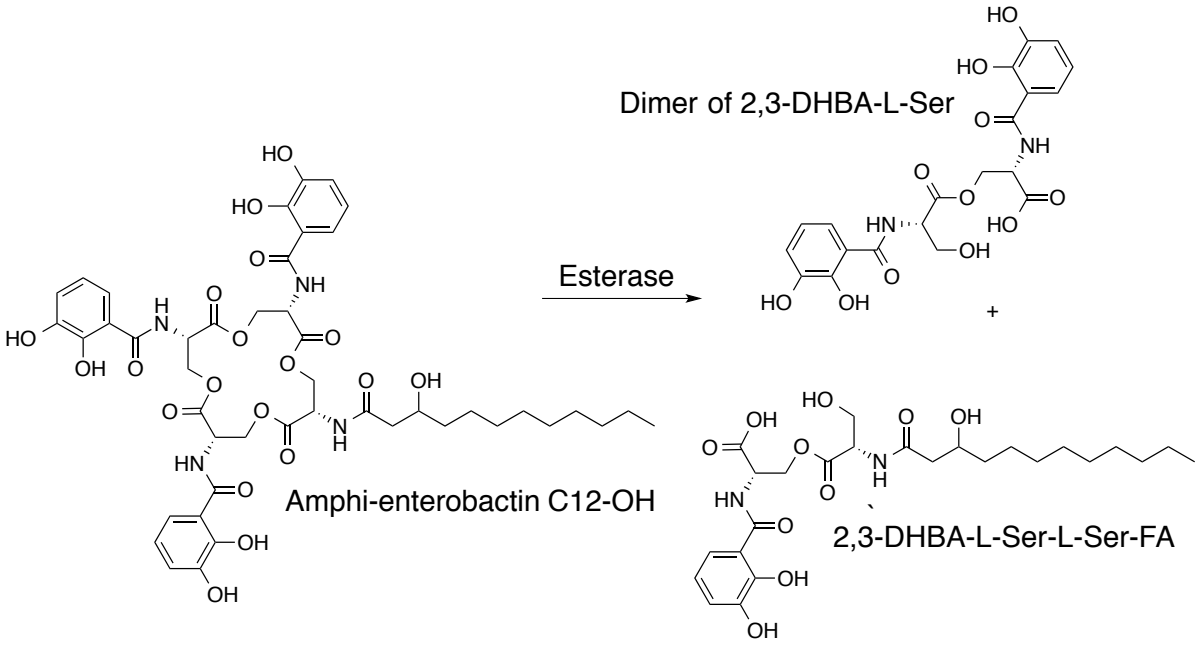

Figure 5.1. The amphi-enterobactins are produced by *Vibrio harveyi* BAA-1116, which also produces the dimer of 2,3-DHBA-L-Ser. Due to the lack of biosynthetic genes for 2,3-DHBA-L-Ser, the formation of the dimer is hypothesized to be a product of amphi-enterobactin hydrolysis by an esterase.

5.2 Experimental

5.2.1 Bioinformatic analysis of potential amphi-enterobactin esterases

The national center for biotechnology information website (NCBI) was used to search the genome of *V. harveyi* BAA-1116 for putative amphi-enterobactin esterases. The basic local

alignment search tool (BLAST) was used to determine homology between the predicted esterases and the characterized proteins of known function.

5.2.2 Cloning and expression of *VIBHAR_06926*

V. harveyi BAA-1116 genomic DNA was isolated using Proteinase K and phenol:chloroform:isoamyl extractions to remove unwanted protein. The genomic DNA was used as a template for PCR with primers F-VH06926-NheI (5'-ACCTGGGCTAGCATGACCATTGAAAGCCTAAGCCAAGC-3') and R- VH06926-NotI (5'-GTTTAAGCGGCCGCGGCAAATAAGTACTTAGCGTGGAAG-3'). The amplified gene was digested with NheI and NotI to produce sticky ends for ligation into the pET24a(+) vector, which was pre-digested with NheI and NotI. Ligated samples were transformed into *E. coli* TOP10 cells for sequencing at the UC Berkeley sequencing facility.

For protein expression, the plasmid was transformed into *E. coli* BL21-CodonPlus(DE3)-RIPL cells. Cells were grown in 500 mL of LB-Kan at 225 rpm at room temperature. When the O.D. at 600 nm reached 0.89, the culture was induced with 0.4 mM IPTG overnight at 16°C. The cells were harvested with an SLA-3000 rotor at 6,000 rpm for 10 minutes at 4°C. The pellet was resuspended in 20 mL binding buffer (20 mM NaPhosphate pH 7.8 + 0.1 M NaCl + 5 mM imidazole) and lysed by sonication (output ctrl. 2, 40% amplitude, 20 s on/60 s off, X 3) on ice with stirring. The crude lysate was clarified by centrifugation at 10,000 x g at 4°C for 15 minutes. The clarified supernatant was filtered through a 0.22 μm syringe filter and added to 2 mL of Ni-NTA resin pre-rinsed with binding buffer. The sample was gently agitated at 4°C for 1-3 hours then loaded onto a gravity column and washed with 10 mL binding buffer. The resin was washed with 5 mL of wash buffer 1 (20 mM NaPhosphate pH

7.8, 0.1 M NaCl, 20 mM imidazole) followed by 5 mL of wash buffer 2 (20 mM NaPhosphate pH 7.8, 0.1 M NaCl, 50 mM imidazole) and then 5 mL of wash buffer 3 (20 mM NaPhosphate pH 7.8, 0.1 M NaCl, 100 mM imidazole). The resin was eluted with three 1.5 mL fractions of elution buffer (20 mM NaPhosphate pH 7.8, 0.1 M NaCl, 500 mM imidazole) and analyzed by SDS-page analysis.

The enzyme was further purified by gel filtration chromatography using the S200 HR 10/30 HR column on an ATKA FPLC system. Fractions from the 100 mM Ni-NTA wash and eluent #1 were combined and concentrated in a 2 ml 10 kDa MWCO Centricon filter at 7,500 x g and 4°C to a final volume of ~150 µl prior to loading the sample onto the column. The sample was eluted with 1.5 column volumes of gel filtration buffer (50 mM tris pH 8, 50 mM NaCl) at a flow rate of 0.5 ml/min.

5.2.3 Knockout mutant of *VIBHAR_06926*

The knockout mutant of VIBHAR_06926 was kindly constructed and sent to us by our collaborators Dr. Hiroaki Naka and Professor Margo Haygood at OHSU.

5.2.4 Activity analysis of VIBHAR_06926-His_6 with the amphi-enterobactins

The concentration of apo-amphi-enterobactin C12-OH was determined by monitoring the absorbance at 310 nm (ε = 7080 $M^{-1}cm^{-1}$) in methanol. Fe(III)-amphi-enterobactin was prepared by adding 1.2 volumes of Fe(III) in 10 mM HCl. Protein concentration was determined by monitoring the absorbance at 280 nm (ε = 46,995 $M^{-1}cm^{-1}$). For an *in vitro* analysis of VH_06926-His_6 activity, 35 µM of apo-amphi-enterobactin C12-OH or 35 µM Fe(III)-amphi-enterobactin C12-OH was combined with 500 nM purified protein in 20 mM HEPES pH 7, 100 mM NaCl, 1 mM DTT and incubated at room temperature for 2 hours.

The reactions were quenched by the addition of 0.5 volumes 2.5 N HCl and analyzed by RP-HPLC on a C4 analytical column moving from 90% water/10% acetonitrile + 0.05% TFA to 100% acetonitrile over 50 minutes.

A general esterase activity assay was used to determine if the expressed esterase was active.[3] The assay combined 1 μL of purified enzyme with 20 μL substrate (2 μL ethyl acetate/mL acetone) in 100 μL 0.2 mM sodium phosphate buffer pH 7.8. The pH indicator, bromothymol blue (6 μL) was added to the reaction and the reactions were incubated overnight. Acetic acid was added in place of ethyl acetate as a positive control.

5.2.5 Cloning and expression of *VIBHAR_01343*

Gene *VIBHAR*_01343 was cloned form *V. harveyi* BAA-1116 genomic DNA using forward primer 5'-ACCTGGCATATGTCAGCATTACTCAACTATAAGCAGG-3' (Nde1 restriction site underlined) and reverse primer 5'-ACCTGGCTCGAGACTCGAAATATATTTCCTGATCACACGC-3' (XhoI restriction site underlined). The stop codon was removed from the reverse primer to attach a C-terminal 6X His-tag. The amplified insert was purified by band stab PCR and digested with NdeI and XhoI. The pET22b(+) vector was digested with NdeI and XhoI in tandem to linearize the vector. The digested vector and insert were ligated at 16°C overnight and transformed into *E. coli* TOP10 cells to form the plasmid, p22-*VH01343*-His_6. Colonies containing the p22-*VH01343*-His_6 plasmid were identified by colony PCR using the primers constructed for gene amplification.

For protein production, the p22-*VH01343*-His_6 plasmid was transformed into *E. coli* BL21-CodonPlus(DE3)-RIPL cells and grown in LB + 100 μg/μL ampicillin at 37°C until

the O.D. at 600 nm reached 0.55. The culture was induced with 1 mM IPTG and grown for an additional 3 hours at 37°C. Cells were harvested at 6,000 rpm for 10 minutes at 4°C. Bacterial pellets were flash frozen and stored at -80°C.

5.2.6 Activity analysis of VH01343-His_6 with apo- and Fe(III)- amphi-enterobactin

The concentration of apo-amphi-enterobactin C12-OH and the preparation of Fe(III)-amphi-enterobactin was performed as described above. Protein concentration was determined by monitoring the absorbance at 280 nm (ε = 28,420 $M^{-1}cm^{-1}$). To monitor activity, 50 nM VH01343-His_6 was incubated with 100 μM apo- or Fe(III)-amphi-enterobactin C12-OH in 100 μL reaction volumes. The reactions were performed in 20 mM Tris pH 7.25, 50 mM NaCl, 2 mM NaCl and incubated at 30°C for 2 hours. Reactions were quenched by adding 0.5 volumes of 2.5 N HCl in methanol followed by RP-HPLC analysis as described above.

5.2.7 Apo- and Fe(III)- amphi-Enterobactin hydrolysis *in vivo*

For an *in vivo* analysis, wild type *V. harveyi* BAA-1116 and Δ*VH06926 V. harveyi* BAA-1116 were grown in 1L of iron-limited ASG media as previously described.[1] The bacteria was harvested by centrifugation at 4°C and 6,000 rpm (SLA-3000) for 30 minutes. The pellet was resuspended in 10 mL of 20 mM sodium phosphate pH 8.0, 100 mM NaCl, 2 mM EDTA, and 1% triton x-100. Lysozyme (1 mg/ml) and benzonase (200-500 units/g cells) were added to the resuspend pellet with 1 mM $MgCl_2$ on ice for 1 hour to lyse the cells. The lysate was clarified by centrifugation at 10,000 x g for 10 minutes followed by filtration through a 0.22 μm filter. The lysate (100 μL/sample) was incubated with 30 μM apo-amphi-

enterobactin, 30 μM Fe(III)-amphi-enterobactin or 30 μM apo-linear-amphi-enterobactin for 1 hour at room temperature. As a control, 30 μM of each siderophore sample was incubated with buffer to check for random hydrolysis. The reaction was quenched by precipitating the protein with 700 μL of ice-cold methanol and incubating at -20°C for 1 hour followed by centrifugation at 10,000 x g for 15 minutes. The supernatants were diluted with water and lyophilized to dryness. Reaction products were monitored by RP-HPLC on an analytical C18 column as described above.

5.3 Results

5.3.1 Bioinformatic analysis of putative amphi-enterobactin esterases

The genome of *V. harveyi* BAA-1116 was screened for putative amphi-enterobactin esterases. The *V. harveyi* BAA-1116 genome contains eighteen genes that encode for putative esterases (Table 5.1). One predicted esterase, *VIBHAR_06926*, is located in close proximity to *VIBHAR_06920*, which encodes for a putative siderophore-interacting protein. VIBHAR_06920 is similar to the siderophore-interacting protein, ViuB, from *Vibrio cholerae*. ViuB and its homologues catalyze the release of Fe(III) from iron-siderophore complexes including tris-catecholate-containing siderophores by reducing Fe(III) to Fe(II).[4,5]

VIBHAR_01343, is also of interest due to its annotation as an esterase/lipase suggesting the protein product might work on a fatty acid substrate like the amphi-enterobactins. The *VIBHAR_01343* gene is downstream of genes necessary for the biosynthesis of 2,3-dihydroxybenzoic acid (*VIBHAR_01396-VIBHAR_01400*) and the fatty acyl coA ligase, *aebG*, which are essential for amphi-enterobactin biosynthesis. The putative esterases encoded by genes *VIBHAR_05814* and *VIBHAR_00873* are also amphi-enterobactin

hydrolase candidates due to their homology to broad specificity esterases and palmitoyl-CoA esterases, respectively.

Table 5.1. Genes annotated as putative esterases in the genome of *V. harveyi* BAA-1116

Accession #	GENE	Size (AA)	BLAST
ABU69618.1	VIBHAR_00616	254	Biotin biosynthesis protein (BioH), pimelyl-ACP methyl ester esterase
ABU69873.1	VIBHAR_00873	175	Esterase YqiA
ABU70150.1	VIBHAR_01160	415	Fermentation/respiration switch protein, Esterase FrsA
ABU70320.1	VIBHAR_01343	255	Acyl-CoA esterase, esterase/lipase YbfF
ABU70494.1	VIBHAR_01524	179	Esterase
ABU71147.1	VIBHAR_02182	104	GDXG family lipase
ABU71149.1	VIBHAR_02184	161	GDXG family lipase
ABU71832.1	VIBHAR_02879	549	Vest, para-nirobenzyl esterase
ABU71845.1	VIBHAR_02892	381	esterase
ABU72387.1	VIBHAR_03442	771	Serine protease
ABU72541.1	VIBHAR_03626	427	Dehydrogenase, deacetylase
ABU73695.1	VIBHAR_05801	200	Arylesterase, acyl-CoA thioesterase
ABU73708.1	VIBHAR_05814	145	Esterase
ABU74306.1	VIBHAR_06415	305	phospholipase
ABU74549.1	VIBHAR_06662	290	phospholipase
ABU74800.1	VIBHAR_06926	279	Esterase, S-formylgutathione hydrolase
ABU74831.1	VIBHAR_06957	284	esterase

5.3.2 Cloning and expression of *VIBHAR_06926*

Amplification of *VIBHAR_06926* from *V. harveyi* genomic DNA resulted in the appearance of a band around 800 bp's when analyzed on an agarose gel (Figure 5.2). This corresponds to the correct length of the expected *VIBHAR_06926* gene. Ligation of the amplified gene into the pET22b(+) vector resulted in the formation of the p22-*VH06926*-His_6 plasmid.

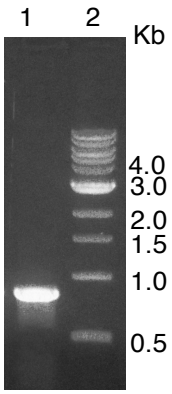

Figure 5.2. 0.8% Agarose gel of the amplified *VIBHAR_06926* gene by PCR. (1) amplified *VIBHAR_06926* gene (2) molecular weight marker.

Expression of p22-*VH06926*-His_6 in *E. coli* BL21-CodonPlus(DE3)-RIPL cells resulted in the appearance of a band around 30 kDa that was not seen in the uninduced control (Figure 5.3, lane 3). Following clarification of the crude lysate by centrifugation, VH06926-His_6 remained in the soluble fraction (Figure 5.3, lane 4). Purification of VH06926-His_6 using Ni-NTA resin resulted in purified protein as determined by SDS-page analysis (Figure 5.3). A large amount of expressed protein, however, was eluted from the Ni-NTA resin during the 100 mM imidazole wash; therefore, the 100 mM imidazole wash was combined with the eluted fractions for further purification by gel filtration chromatography. The gel filtration chromatogram shows a sharp peak eluting around 12 mL (Figure 5.4). This peak was collected and concentrated for analysis on a SDS-page gel, which showed a distinct, large band representing purified VH06926-His_6 (Figure 5.5). The protein concentration was determined by monitoring the absorbance at 280 nm using the extinction coefficient 46,995 $M^{-1}cm^{-1}$ calculated from ProtPram (Expasy).

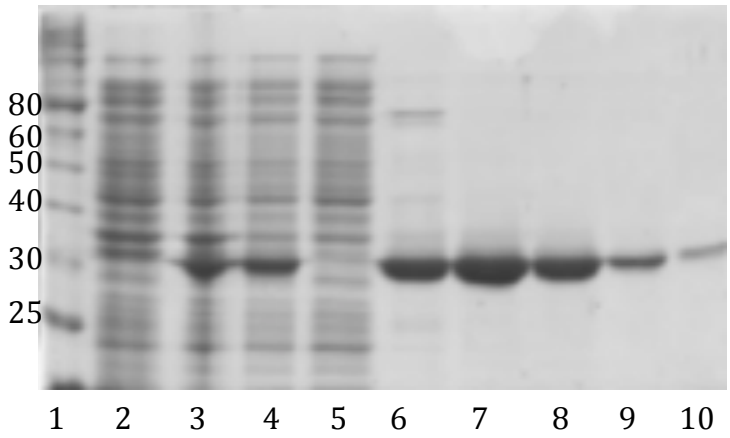

Figure 5.3. 12% SDS-page gel showing the purification of VH06926-His_6. Lane 1: MW marker, Lane 2: uninduced crude lysate, Lane 3: Induced crude lysate, Lane 4: Induced clarified lysate, Lane 5: Ni-NTA flow through, Lane 6: 50 mM imidazole wash, Lane 7: 100 mM imidazole wash, Lane 8: Elution #1, Lane 9: Elution #2, Lane 10: elution #3.

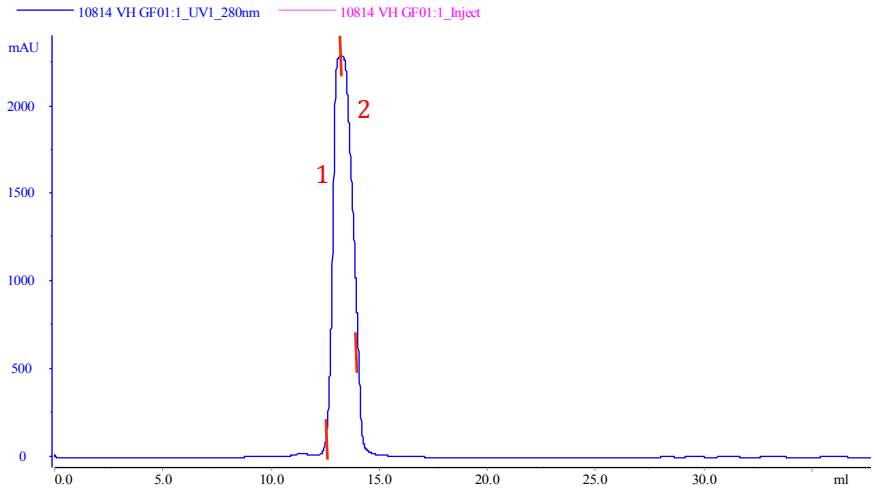

Figure 5.4. Gel filtration chromatography of VH_06926-His_6 eluted from the Ni-NTA resin. An S200 HR 10/30 column was used on an ATKA FPLC.

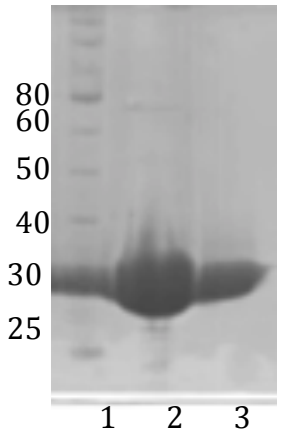

Figure 5.5. 12% SDS-page gel showing purified VH_06926-His_6 eluted from an S200 HR 10/30 gel filtration column.

5.3.3 Knockout mutant of *VIBHAR_06926*

Our collaborators Dr. Hiroaki Naka and Professor Margo Haygood at OHSU constructed a knockout mutant of the *VIBHAR_06926* gene to determine if the gene is necessary for amphi-enterobactin hydrolysis. Wild type *V. harveyi* BAA-1116, Δ*VIBHAR_06926 V. harveyi* BAA-1116 and Δ*VIBHAR_06926 V. harveyi* BAA-1116 + Δ*VIBHAR_06926* were grown in iron-limited synthetic seawater media to evaluate siderophore production. Since we are interested in the formation of the 2,3-DHBA-L-Ser dimer, only the cell-free supernatant was analyzed for siderophore production by RP-HPLC. The RP-HPLC chromatogram of siderophores produced by wild type *V. harveyi* BAA-1116 shows a peak around 29.5 minutes (Figure 5.6). ESI-MS analysis of this peak corresponds to the $[M+H]^+$ of the dimer (*m/z* 465) (Figure 5.7), which fragments into the 2,3-DHBA-L-Ser monomer (*m/z* 224) as seen in the tandem mass spectrum (Figure 5.8).

The knockout mutant, Δ*VIBHAR_06926* #2 *V. harveyi* BAA-1116, also produces the 2,3-DHBA-L-Ser dimer as seen by the appearance of a peak around 29.5 minutes (Figure 5.6). ESI-MS analysis verified the identity of this peak (*m/z* 465) indicating that the 2,3-DHBA-L-Ser dimer is still being formed when VH_06926 is no longer present (Figure 5.9). The *VIBHAR_06926* knockout mutant was complemented with the *VIBHAR_06926* gene to see how dimer formation would be affected when the gene was added back. Two different complement strains, *V. harveyi* BAA-1116 + pMMB208-*VIBHAR_06926*-1 and *V. harveyi* BAA-1116 + pMMB208-*VIBHAR_06926*-6, were constructed and analyzed by RP-HPLC. *V. harveyi* BAA-1116 + pMMB208-*VIBHAR_06926*-1 produced the dimer as seen by the appearance of a peak around 29.5 minutes (Figure 5.6) and verified by ESI-MS (Figure 5.10). Interestingly, there appears to be more dimer formed in the *V. harveyi* BAA-1116 + pMMB208-*VIBHAR_06926*-1 complement strain than in wild type *V. harveyi* BAA-1116 suggesting that a high concentration of VIBHAR_06926 may be able to catalyze amphi-enterobactin hydrolysis. The second complement strain, *V. harveyi* BAA-1116 + pMMB208-*VIBHAR_06926*-6, results in the complete abolishment of dimer formation (Figure 5.6), which is what would have been expected for the knockout mutant. The complementation of the *VIBHAR_06926* gene might have somehow interrupted siderophore production, preventing dimer formation.

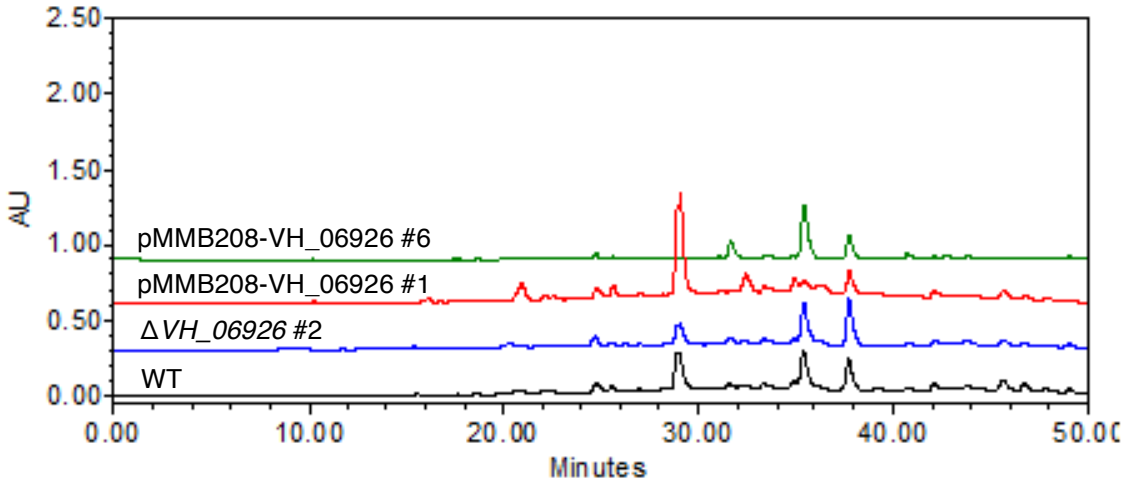

Figure 5.6. RP-HPLC analysis of siderophores released into the supernatant of wild type *V. harveyi* (black), Δ*VIBHAR_06926 V. harveyi* (blue), Δ*VIBHAR_06926* + pMMB208-*VIBHAR_06926*-1 (red), and Δ*VH_06926* + pMMB208-*VIBHAR_06926*-6 (green).

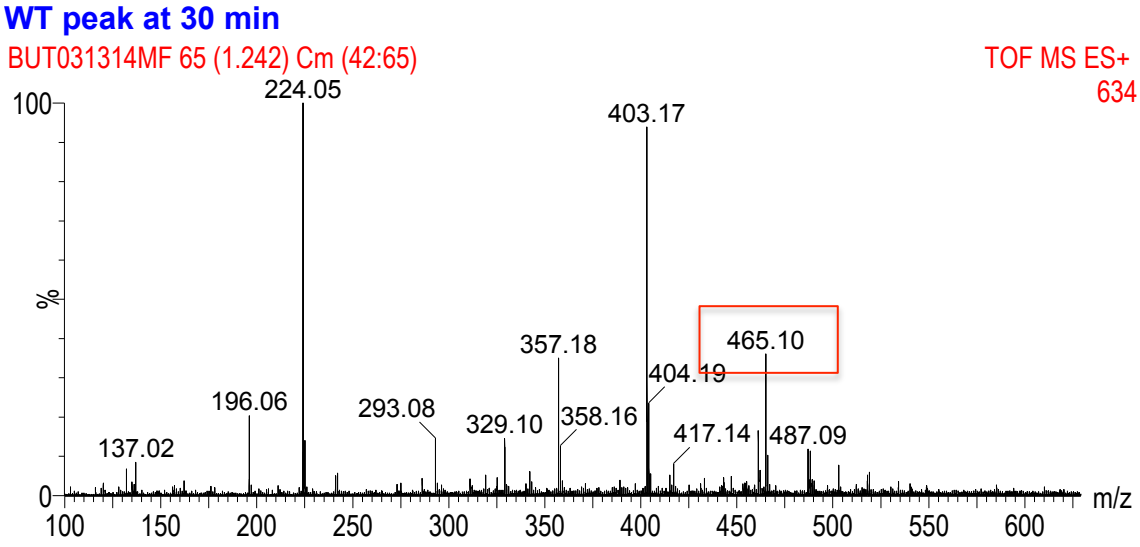

Figure 5.7. ESI-MS analysis of the peak eluting at 29.5 minutes from wild type *V. harveyi* BAA-1116.

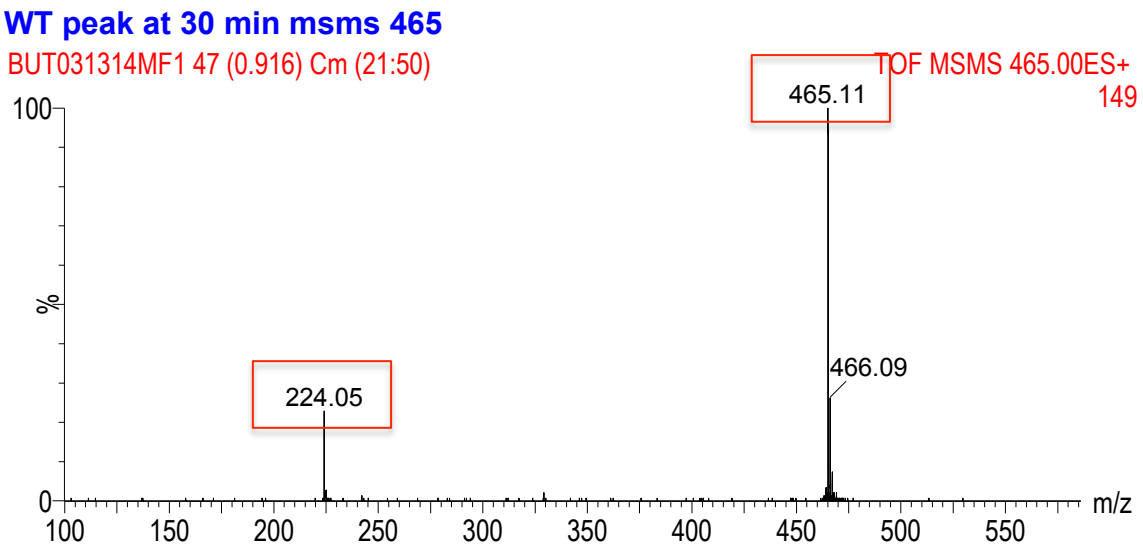

Figure 5.8. ESI-MS/MS analysis of the dimer produced by wild type *V. harveyi* BAA-1116.

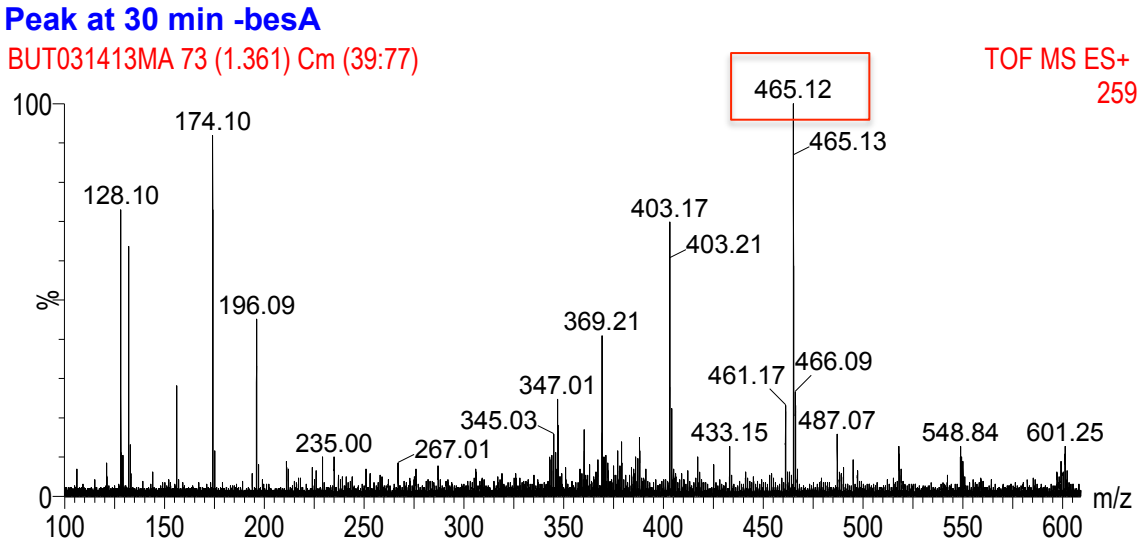

Figure 5.9. ESI-MS analysis of the peak eluting at 29.5 minutes from Δ*VIBHAR_06926 V. harveyi* BAA-1116.

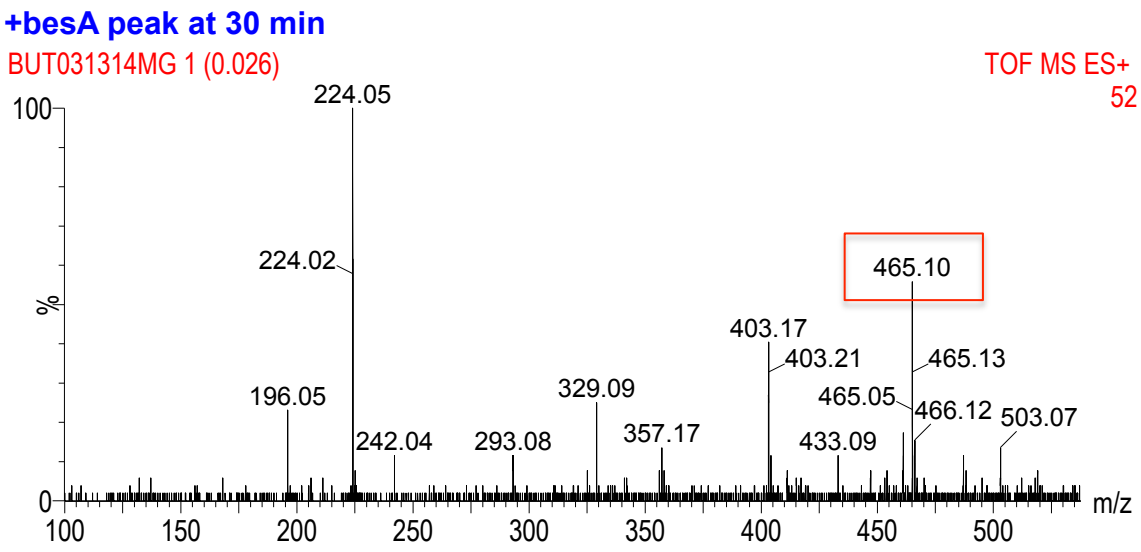

Figure 5.10. ESI-MS analysis of the peak eluting at 29.5 minutes from Δ*VIBHAR_06926* + pMMB208-*VIBHAR_06926*-1.

5.3.4 Activity analysis of VIBHAR_06926-His_6 with the amphi-enterobactins

To determine if VH06926-His_6 could hydrolyze the amphi-enterobactins into 2,3-DHBA-L-Ser and L-Ser-FA, apo- and Fe(III)-amphi-enterobactin C12-OH were incubated with VH06926-His_6 and the reaction products were analyzed by RP-HPLC. As a control, the siderophores were incubated in buffer to check for random hydrolysis. VH06926-His_6 does not appear to hydrolyze the apo-amphi-enterobactins since the sample looks the same as the buffer only control (Figure 5.11). The Fe(III)-amphi-enterobactins were also incubated with VH06926-His_6 and again, there did not appear to be any difference in reaction products between the sample and control (Figure 5.12).

To determine if the enzyme was in its active form, a general colorimetric esterase activity assay was used.[3] Ethyl acetate was used as an ester substrate for VH06926-His_6 in the presence of the pH indicator bromothymol blue. If esterase activity is present, the indicator

will change from blue to yellow as the ethyl acetate hydrolyzes into acetic acid, thereby lowering the reaction pH. Incubation of purified VH06926-His_6 with ethyl acetate resulted in a color change from blue to green after 24 hours of incubation suggesting that the enzyme was in its active form. Therefore, it can be concluded that the amphi-enterobactins are not the substrate for VH06926-His_6.

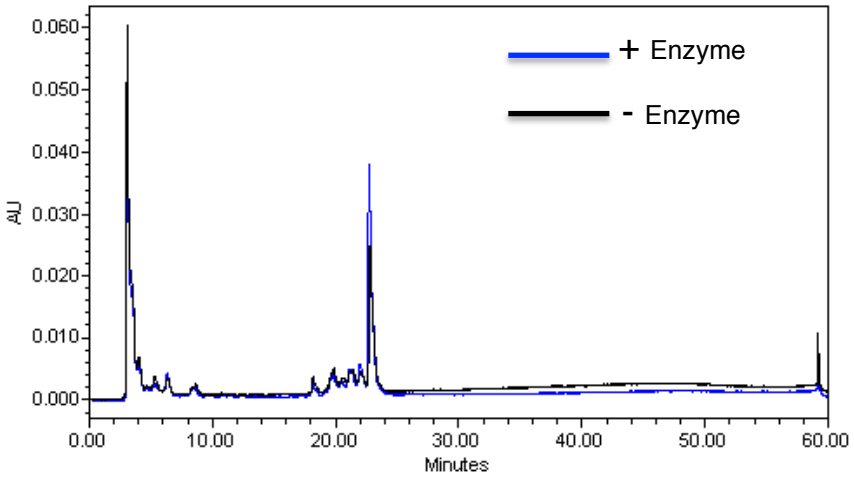

Figure 5.11. RP-HPLC analysis of apo-amphi-enterobactin C12-OH incubated with VH06926-His_6 (blue) and without enzyme (black).

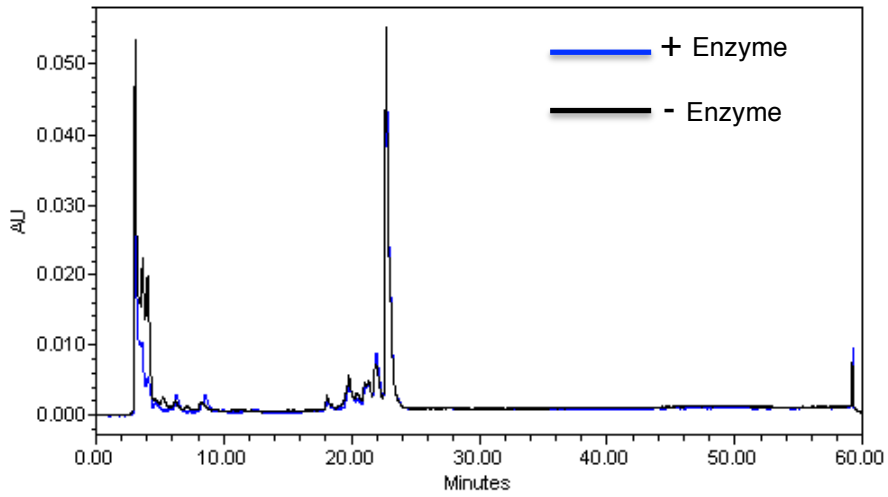

Figure 5.12. RP-HPLC analysis of Fe(III)-amphi-enterobactin C12-OH incubated with VH06926-His_6 (blue) and without enzyme (black).

5.3.5 Cloning and expression of *VIBHAR_01343*

Amplification of *VIBHAR_01343* from *V. harveyi* genomic DNA resulted in a band around 800 bp's when analyzed on an agarose gel (Figure 5.13). This corresponds to the correct length of the *VIBHAR_01343* gene. Ligation of *VIBHAR_01343* into the pET22b(+) vector resulted in the plasmid p22-*VH01343*-His_6.

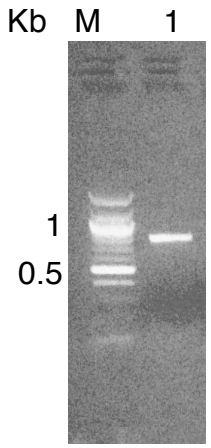

Figure 5.13. 0.8% agarose gel analysis of the PCR amplified *VIBHAR_01343* gene from *V. harveyi* genomic DNA (lane 1). M = molecular weight marker.

The plasmid, p22-*VH01343*-His_6, was expressed in *E. coli* BL21-CodonPlus(DE3)-RIPL cells and analyzed by SDS-page analysis. A large band is present in the induced crude lysate (Figure 5.14, lane 1), which corresponds to the expected mass of 28 kDa's for VH01343-His_6. This large band, however, disappears in the clarified lysate (Figure 5.14, lane 2) suggesting the majority of the protein is being expressed in the insoluble fraction. Concentration and purification of soluble VH01343-His_6 using Ni-NTA resin resulted in a small amount of soluble, purified VH01343-His_6 (Figure 5.14, lane 5).

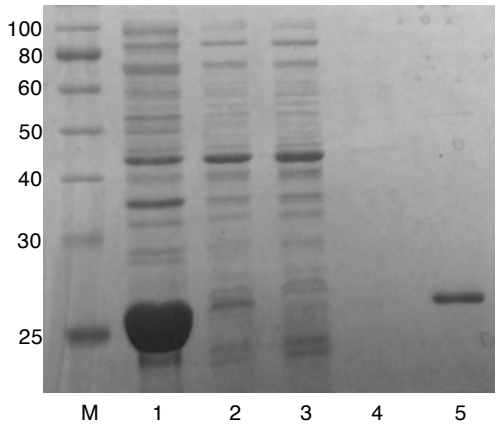

Figure 5.14. 12% SDS-page gel of VH01343-His_6 expressed in *E. coli* BL21-CodonPlus(DE3)-RIPL cells. M, molecular weight marker; Lane 1: induced crude lysate; Lane 2: induced clarified lysate; Lane 3: Ni-NTA flow through; Lane 4: Ni-NTA wash; Lane 5: Ni-NTA eluent.

5.3.6 Activity analysis of VH01343-His_6 with apo- and Fe(III)- amphi-enterobactin

To determine if VH01343-His_6 can convert the apo-amphi-enterobactins to the 2,3-DHBA-L-Ser dimer, purified VH01343-His_6 was incubated with apo-amphi-enterobactin C12-OH at 30°C for 2 hours and the reaction products were analyzed by RP-HPLC at 310 nm. Again, no difference is seen between the sample with enzyme (blue) and the control without enzyme (black) (Figure 5.15). VH01343-His_6 was also incubated with Fe(III)-amphi-enterobactin C12-OH at 30°C for 2 hours to determine if the enzyme would hydrolyze the iron-bound form. As seen with the apo-form, no hydrolysis of the Fe(III)-amphi-enterobactins appeared to occur (Figure 5.16).

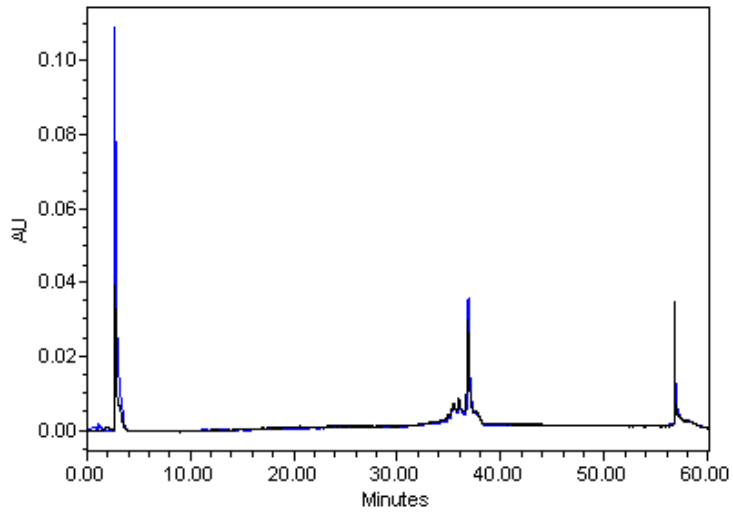

Figure 5.15 Hydrolysis of apo-amphi-enterobactin by VH01343-His_6 (Blue). Black = no enzyme control.

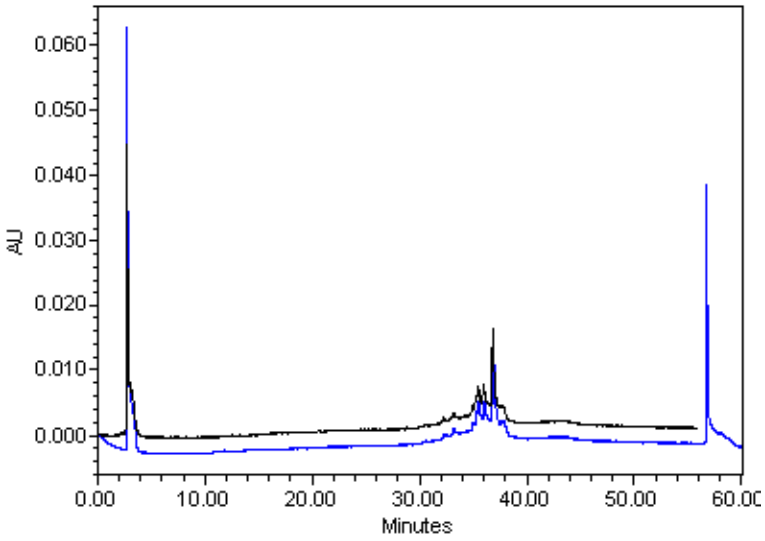

Figure 5.16 Hydrolysis of Fe(III)-amphi-enterobactin by VH01343-His_6 (Blue). Black = no enzyme control.

5.3.7 *In vivo* hydrolysis analysis of apo- and Fe(III)- amphi-enterobactin

Since neither *VIBHAR_06926* nor *VIBHAR_01343* appeared to hydrolyze the amphi-enterobactins, hydrolysis of the amphi-enterobactins was analyzed *in vivo* to verify that the reaction was occurring enzymatically. Apo- and Fe(III)- amphi-enterobactin C12-OH were incubated with cell-free lysates of wild type *V. harveyi* BAA-1116 and compared to a buffer only control. Cell-free lysates of the *VIBHAR_06926* knockout mutant were also incubated with the amphi-enterobactins to monitor hydrolysis. No 2,3-DHBA-L-Ser dimer is formed when apo-amphi-enterobactin C12-OH is incubated in the buffer only control (Figure 5.17, black); however, small amounts of dimer are present after incubation of apo-amphi-enterobactin C12-OH with the cell-free extracts of wild type *V. harveyi* BAA-1116 as shown by the appearance of a small peak around 16 minutes (Figure 5.17, blue). The cell-free lysate from Δ*VIBHAR_06926 V. harveyi* BAA-1116 also produced some dimer following incubation with apo-amphi-enterobactin C12-OH (Figure 5.17, red) further confirming that *VIBHAR_06926* is not involved in dimer formation.

When the cell-free lysate from wild type *V. harveyi* BAA-1116 was incubated with Fe(III)-amphi-enterobactin C12-OH, a large portion of the Fe(III)-amphi-enterobactins was converted to the 2,3-DHBA-L-Ser dimer as seen by the appearance of a peak around 16 minutes in conjunction with the disappearance of the Fe(III)-amphi-enterobactin peak around 33 minutes (Figure 5.18, blue). Small amounts of dimer formed in the buffer only control suggesting that some random hydrolysis of the substrate was also occurring (Figure 5.18, black). When Fe(III)-amphi-enterobactin was incubated with cell-free lysates of Δ*VIBHAR_06926 V. harveyi* BAA-1116, dimer formation occurred similarly to what was

seen in the wild type sample further confirming that *VIBHAR_06926* is not involved with Fe(III)-amphi-enterobactin hydrolysis.

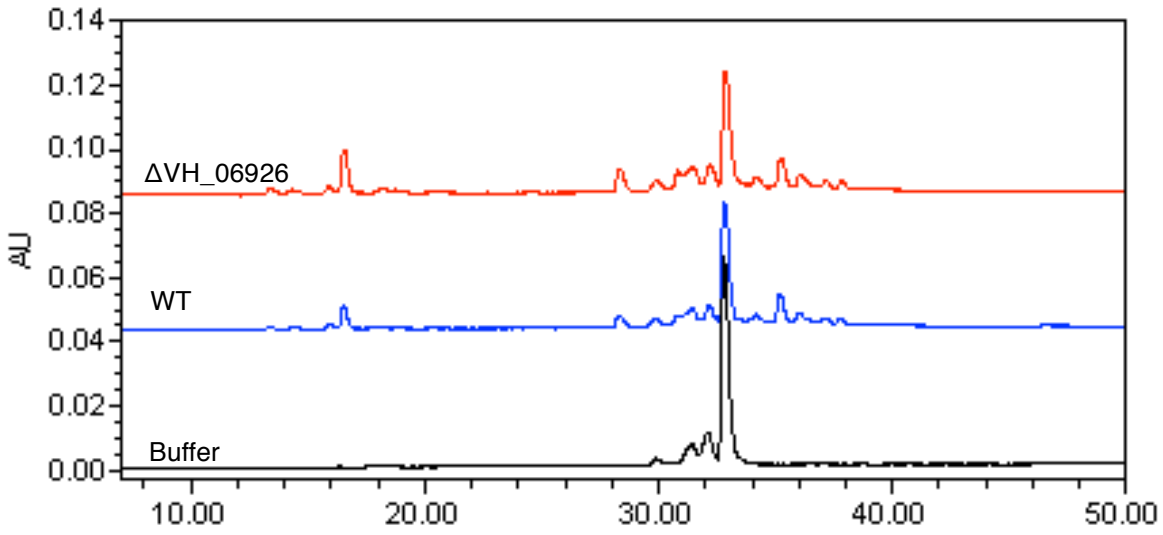

Figure 5.17 RP-HPLC analysis of apo-amphi-enterobactin C12-OH following incubation with cell-free lysates of wild type *V. harveyi* BAA-1116 (blue), Δ*VIBHAR_06926 V. harveyi* (red) and the buffer only control (black).

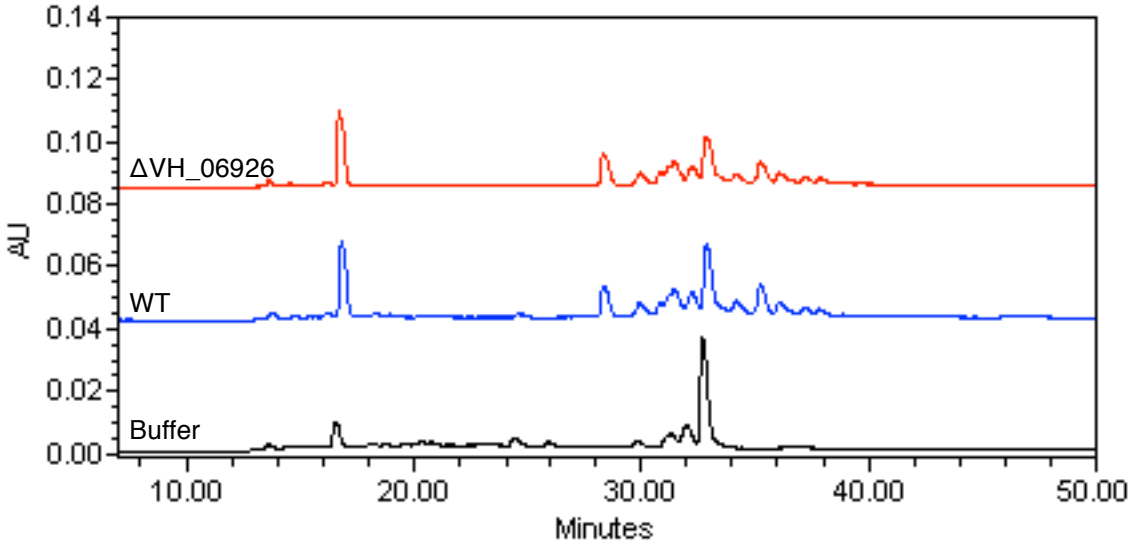

Figure 5.18 RP-HPLC analysis of Fe(III)-amphi-enterobactin C12-OH following incubation with cell-free lysates of wild type *V. harveyi* BAA-1116 (blue), Δ*VIBHAR_06926 V. harveyi* (red) and the buffer only control (black).

5.4 Discussion

The amphi-enterobactins are produced by the marine bacterium, *V. harveyi* BAA-1116 and are isolated from the bacterial pellet following centrifugation.[1] The same bacterium produces a dimer of 2,3-DHBA-L-Ser, which is isolated from the cell-free supernatant following centrifugation (Figure 5.1).[2] No biosynthetic genes for the 2,3-DHBA-L-Ser dimer are present in the genome of *V. harveyi* BAA-1116 suggesting that the dimer is a hydrolysis product of the amphi-enterobactins. Since no 2,3-DHBA-L-Ser monomers are isolated from the culture supernatant, it is hypothesized that the 2,3-DHBA-L-Ser dimer is forming enzymatically. Incubation of cell-free lysates from *V. harveyi* BAA-1116 with Fe(III)-amphi-enterobactin results in the conversion of Fe(III)-amphi-enterobactin to the 2,3-DHBA-L-Ser

dimer (Figure 5.18) verifying that this reaction is occurring enzymatically and is not a random hydrolysis product. It also appears that the enzyme prefers the Fe(III)-amphi-enterobactins over the apo form.

The Fes esterase found in certain pathogenic enterobactin-producing species catalyzes the hydrolysis of iron-bound enterobactin as a way to release the iron from the tightly bound catechol ligands.[6] *V. harveyi* BAA-1116 likely uses a similar mechanism for iron release from the amphi-enterobactins. Fes, however, hydrolyzes enterobactin at all ester bonds of the triserine lactone to form the corresponding 2,3-DHBA-L-Ser monomers.[6] The putative amphi-enterobactin esterase from *V. harveyi* BAA-1116 appears to selectively hydrolyze the amphi-enterobactins at two ester bonds of the tetra-serine lactone. Another esterase found in certain pathogenic enterobactin-producing species, termed IroE, selectively catalyzes the hydrolysis of one ester bond of the triserine lactone to form the corresponding linear trimer.[7,6] This linear trimer is believed to be utilized as a more hydrophilic siderophore in membrane-rich environments since enterobactin is quite hydrophobic and partitions into lipid bilayers.[8,9] It is likely that the Fe(III)-amphi-enterobactins are hydrolyzed to remove iron; however, the bacteria may only selectively hydrolyze the Fe(III)-amphi-enterobactins into the 2,3-DHBA-L-Ser dimer and L-Ser-FA as a way of recycling the siderophore into a more hydrophilic form to scavenge iron in membrane-rich environments.

5.5 References

1. Zane, H.; Naka, H.; Rosconi, F.; Sandy, M.; Haygood, M.; Butler, A., Biosynthesis of Amphi-enterobactin Siderophores by Vibrio harveyi BAA-1116: Identifi*cation of a Bi*functional Nonribosomal Peptide Synthetase Condensation Domain. *Journal of the American Chemical Society* **2014,** *136* (15), 5615-5618.

2. Zane, H. K. Marine Siderophores: Structure and Biosynthesis. University of California, Santa Barbara, 2014.

3. Lisboa, H.; Biasetto, C.; de Medeiros, J.; Araujo, A.; Silva, D.; Teles, H.; Trevisan, H., Endophytic fungi producing of esterases: Evaluation in vitro of the enzymatic activity using pH indicator. *Brazilian Journal of Microbiology* **2013,** *44* (3), 923-926.

4. Miethke, M.; Hou, J.; Marahiel, M., The Siderophore-Interacting Protein YqjH Acts as a Ferric Reductase in Different Iron Assimilation Pathways of Escherichia coli. *Biochemistry* **2011,** *50* (50), 10951-10964.

5. Butterton, J.; Calderwood, S., Identification, Cloning, and Sequencing of a Gene Required For Ferric Vibriobactin Utilization by *Vibrio cholerae*. *Journal of Bacteriology* **1994,** *176* (18), 5631-5638.

6. Lin, H.; Fischbach, M.; Liu, D.; Walsh, C., In vitro characterization of salmochelin and enterobactin trilactone hydrolases IroD, IroE, and Fes. *Journal of the American Chemical Society* **2005,** *127* (31), 11075-11084.

7. Larsen, N.; Lin, H.; Wei, R.; Fischbach, M.; Walsh, C., Structural characterization of enterobactin hydrolase IroE. *Biochemistry* **2006,** *45* (34), 10184-10190.

8. Luo, M.; Lin, H.; Fischbach, M.; Liu, D.; Walsh, C.; Groves, J., Enzymatic tailoring of enterobactin alters membrane partitioning and iron acquisition. *Acs Chemical Biology* **2006,** *1* (1), 29-32.

9. Fischbach, M.; Lin, H.; Liu, D.; Walsh, C., How pathogenic bacteria evade mammalian sabotage in the battle for iron. *Nature Chemical Biology* **2006,** *2* (3), 132-138.